(Part 2 of 2 Parts)

SEMINAR ON UNDERSTANDING DIGITAL CONTROL AND ANALYSIS IN VIBRATION TEST SYSTEMS

Jointly Sponsored By

GODDARD SPACE FLIGHT CENTER
Greenbelt, Maryland

JET PROPULSION LABORATORY
Pasadena, California

THE SHOCK AND VIBRATION INFORMATION CENTER
Naval Research Laboratory, Washington, D.C.

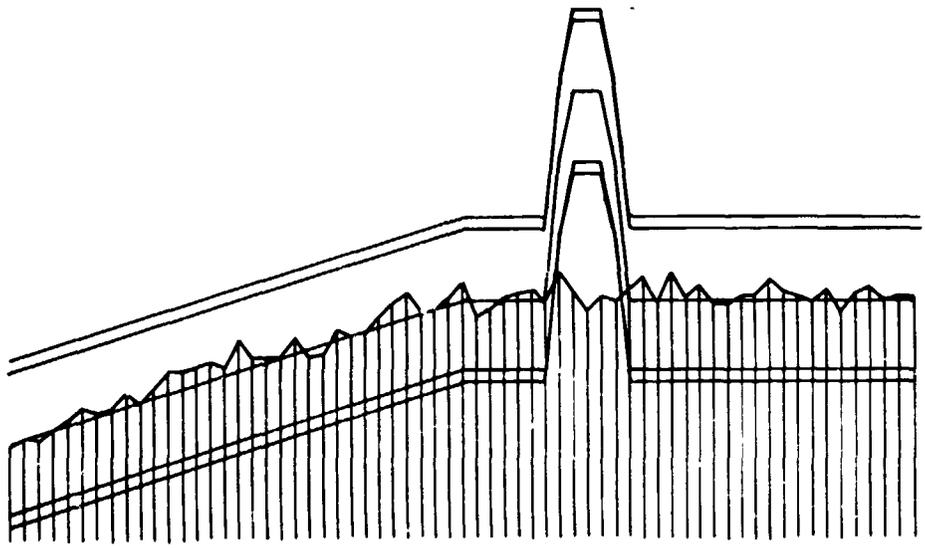

A Publication of
THE SHOCK AND VIBRATION
INFORMATION CENTER
Naval Research Laboratory, Washington, D.C.

SEMINAR ON UNDERSTANDING DIGITAL CONTROL AND ANALYSIS IN VIBRATION TEST SYSTEMS

MAY 1975

A Publication of
THE SHOCK AND VIBRATION
INFORMATION CENTER
Naval Research Laboratory, Washington, D.C.

The Seminar was held at the Goddard Space Flight Center, Greenbelt, Maryland, on 17-18 June 1975 and at the Jet Propulsion Laboratory, Pasadena, California, on 22-23 July 1975.

CONTENTS

PAPERS APPEARING IN PART 2

Detailed Topics

PSEUDO-RANDOM AND RANDOM TESTING 1
Robert S. Norin

SINE-SWEEP TESTING USING DIGITAL CONTROL 11
Alfred G. Ratz

TIME HISTORY SYNTHESIS FOR SHOCK TESTING ON SHAKERS 23
David O. Smallwood

MODAL ANALYSIS USING DIGITAL TEST SYSTEMS 43
Mark Richardson

HARDWARE/SOFTWARE DEVELOPMENT TECHNIQUES TO SUPPORT COMPUTER CONTROLLED TEST SYSTEMS 65
Laurie R. Burrow, Jr.

TECHNIQUES FOR NARROWBAND RANDOM OR SINE ON WIDEBAND RANDOM VIBRATION TESTING WITH A DIGITAL CONTROL SYSTEM 83
Michael K. Stauffer

A REVIEW OF ENVIRONMENTAL TEST INNOVATIONS PERMITTED BY DIGITAL CONTROL SYSTEMS 95
W. Brian Keegan

SAFETY PROTECTION OF TEST ARTICLES USING DIGITAL CONTROL SYSTEMS 107
Robert A. Dorian

PSEUDO-RANDOM AND RANDOM TESTING

Robert S. Norin
Time/Data Corporation
Palo Alto, California

This paper describes control techniques, hardware implementation, and operational aspects of current digital control systems used for pseudo-random and random vibration testing.

INTRODUCTION

The advantages of digital random vibration control systems, when compared with analog systems, have been well established since the first digital systems were introduced in the late 1960's and early 1970's (1, 2, 3, 4). Since this time, digital random control systems have evolved in their sophistication and performance. This is a trend primarily due to the increasing awareness of the potentialities of digital systems on the part of environmental testing personnel and manufacturers of digital systems, as well as the rapid evolution of higher performance processing hardware. The impact of increasing integration and decreasing size and price of key electronic modules has enabled manufacturers to offer basic digital vibration systems which are more than competitive with analog control units on the basis of cost alone.

The purpose of this paper is to describe the control techniques, hardware implementation, and operational aspects of a typical state-of-the-art digital random vibration control system. The first portion of the paper discusses a number of techniques for dealing with important technical aspects of the random vibration control problem. These include the generation of pseudo-random and true random noise, the control spectrum estimation problem, the accuracy/speed tradeoff, and control correction strategies. The second half of the paper deals with system hardware, the operator-system interface, safety features, and operational capabilities of sophisticated digital random vibration control systems.

BASIC CONSIDERATIONS

The goal of any random vibration control system is to excite a shaker system with a continuous random drive signal whose power spectrum is adjusted in such a way that the power spectral density (PSD) of a response accelerometer signal (or averaged spectrum of a number of signals) conforms exactly to a specified reference spectrum.

The basic function requirements for digital random control operation are:

1. Random noise generation.
2. Response (control) spectrum estimation.
3. Spectrum modification.

Figure 1 shows a functional block diagram for a typical digital random vibration control system.

The timing flow for a typical implementation of these functional tasks in a digital system is illustrated in Fig. 2.

We now proceed to examine in detail the three basic functional requirements as they apply to a digital control system.

GENERATION OF RANDOM AND PSEUDO RANDOM SIGNALS

If we are given a particular drive spectrum defined by a certain finite bandwidth and number of spectral lines, then by adding a random phase angle to each of the spectral lines to produce a complex Fourier spectrum, and taking the inverse Fourier transform, a frame of a time-domain signal with the required spectral characteristics is produced. Repeating this operation continuously and concatenating the resulting frames, as shown in Fig. 3, produces a continuous random signal (1, 3). In order to prevent discontinuities and to

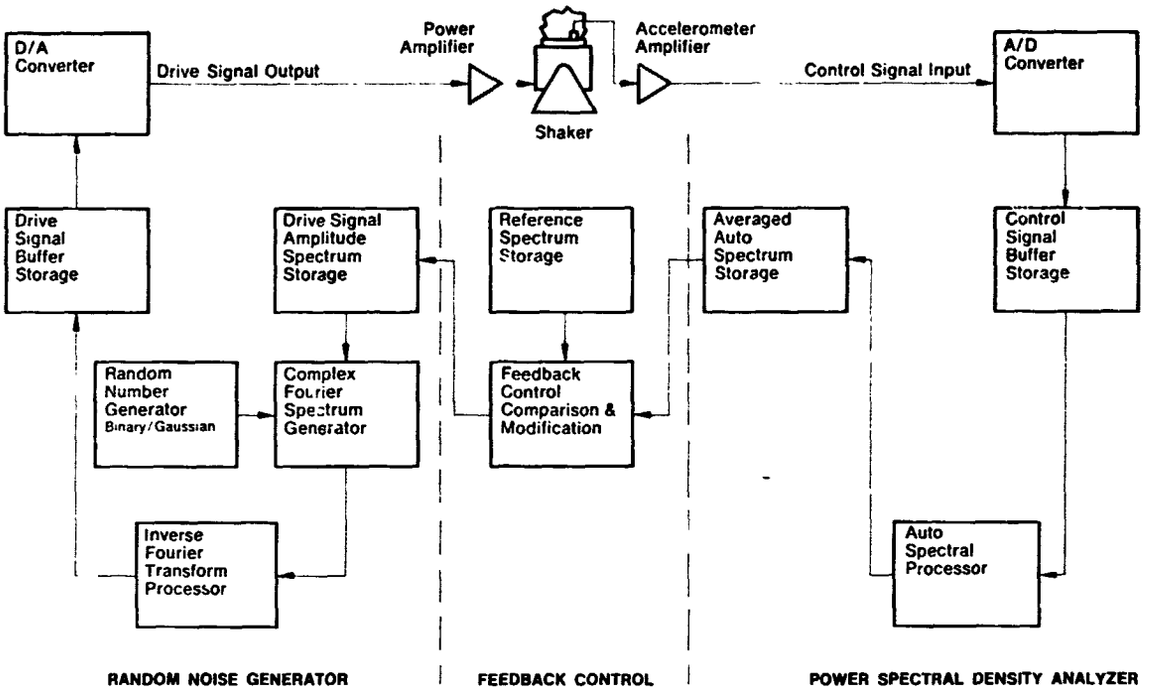

Fig. 1. Functional Block Diagram for Digital Random Vibration Control System

maintain the proper correlation between frames, it is necessary to use a smoothing or windowing operation at the boundary between adjacent frames. By accounting for these and other subtleties, the random noise produced by this system is indistinguishable from the noise produced by a natural Gaussian Random noise source, but has the advantage that its spectrum can be rapidly changed to any arbitrary shape with a frequency resolution of 0.1% or less.

The normalized amplitude distribution of a random noise signal generated by this digital process is shown in Fig. 4. This distribution, as a function of standard deviation units, is displayed both logarithmically and linearly. The Gaussian distribution curves are superimposed on the experimental results.

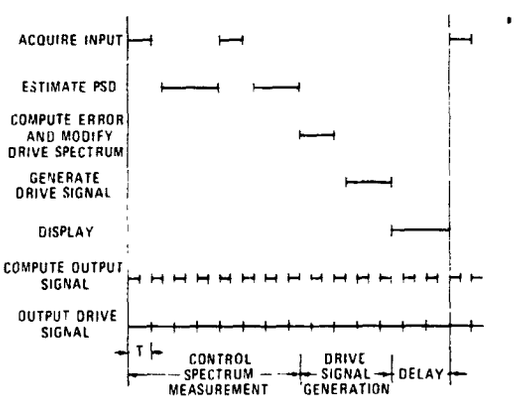

Fig. 2. Typical Random Control Loop Timing

Although the original spectrum from which the digital random signal was derived had only a finite number of spectral lines, the spectrum of the random signal, when analyzed with finer resolution and averaged over a large number of frames, is seen in Fig. 5 to approach the continuous spectrum expected from a Gaussian random signal.

A large number of frames of data are required to obtain a meaningful spectrum because of the statistical uncertainty or variance associated with any measurement of a random signal. The variance problem can be circumvented by generating a "pseudo-random" or "zero variance" signal. Basically this is accomplished by initially randomizing the phases of the spectral components of the drive signal and maintaining them constant throughout the test, while adjusting the magnitudes every L frames. Thus, the same frame is repeated L times. L is usually chosen to be large enough that a steady state condition is reached prior to analysis. If the analysis frame period T is the same as the output frame period, then a single analysis frame is sufficient to determine the spectrum.

Because of the periodicity of the waveform, energy will be produced only at those frequencies defined in the drive spectrum, i.e., the spectrum is "leakage free" and contains "holes" as illustrated in Fig. 6.

Similarly, the amplitude histogram of a pseudo-random signal (shown in Fig. 7), while Gaussian-like,

contains structure not seen in the random case.

While pseudo-random noise can be used in principle to meet many random test specifications, it has not found wide acceptance in vibration laboratories because of its peculiar "sound", discrete spectrum, discrete amplitude structure, and historical lack of precedence in analog random equipment.

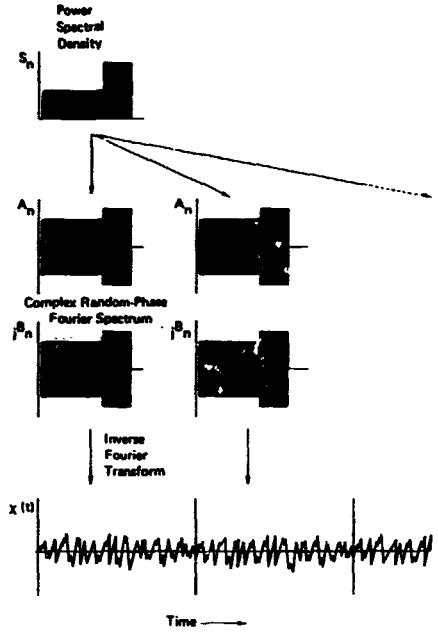

Fig. 3. Generation of Continuous Random Noise Signal

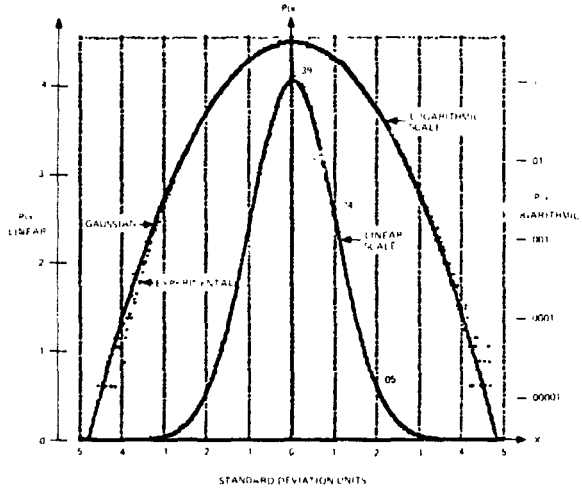

Fig. 4. Theoretical vs Experimental Normalized Amplitude Distribution Curves for Digital Random Noise Signal

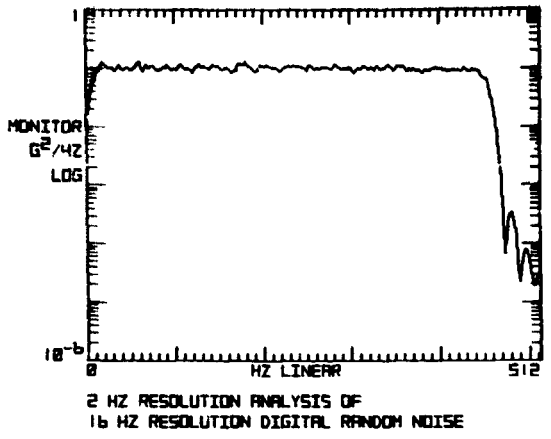

Fig. 5. Spectrum of Digital Random Noise.

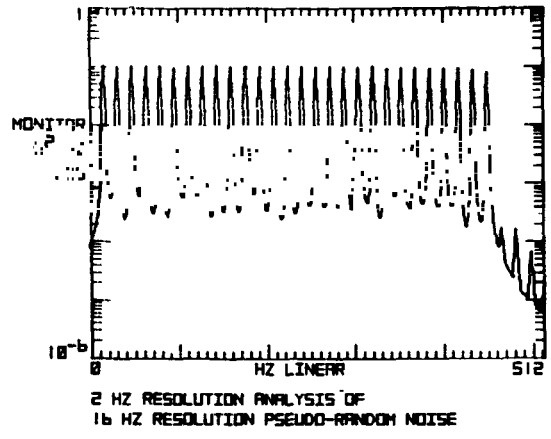

Fig. 6. Spectrum of Digital Pseudo-Random Noise

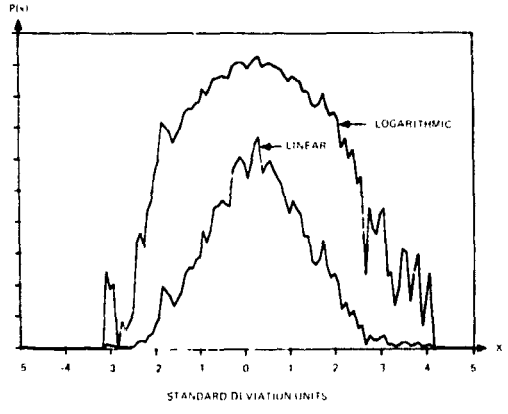

Fig. 7. Typical Amplitude Distribution Curves for Pseudo-Random Noise Signal

PSD ESTIMATION

If random noise is to be used for testing, then because of the statistical uncertainty of the spectral measurements one is faced with a tradeoff between control accuracy and system response time. At the heart of the control problem is the task of estimating the spectrum (PSD) of the response signal we are trying to control.

A convenient measure of the statistical reliability of a spectral estimate is its "equivalent number of degrees of freedom (k)", defined as:

$$k = \frac{2\,(\text{average value})^2}{\text{variance}} \qquad (1)$$

It can be shown that for linear spectral averaging, k = 2 for each frame of Gaussian distributed random data (5). By way of illustration, after an estimate with 16 degrees of freedom (d.o.f.) there is 90% confidence that a particular spectral value is within an interval of about 5 dB around its correct value; for 64 d.o.f. the interval is about 2.5 dB; for 256 d.o.f. the interval is about 1.25 dB.

The response PSD can be estimated using either of two methods; direct and indirect. Both methods are described in the following paragraphs.

The Direct PSD Estimate

The traditional method of estimating the response PSD, illustrated in Fig. 2, is to acquire a frame of data and then directly compute the PSD from the sampled data by Fast Fourier Transform (FFT) techniques (2, 3). As PSD's are accumulated, they are averaged. If the averaging is linear, a drive spectrum correction is made after N PSD's are averaged, and then a new average is accumulated. If exponential averaging is used, a running average with a time constant of N frames is maintained, and a drive correction is made after each frame.

The variance in the direct PSD estimate is inversely proportional to N for both linear and exponential averaging (6).

The Indirect PSD Estimate

A new algorithm has recently been introduced (7) which significantly improves the speed and accuracy with which an estimate of the response PSD is made. This algorithm is based on a combination of time-domain and frequency-domain techniques.

Basically, the procedure used is to first separately sum the drive signal, x(t), and the response signal, y(t), in the time-domain for M consecutive frames of uniform length T. The PSD of each of the two summed data frames is then computed. The above process is repeated N times with the autospectra being linearly averaged. Finally the estimate $|\hat{Y}|^2$ of the response spectrum $|Y|^2$ is given by:

$$|\hat{Y}|^2 = \frac{\sum_{j=1}^{N} |Y_{Mj}|^2}{\sum_{j=1}^{N} |X_{Mj}|^2} |X|^2 \qquad (2)$$

where $|Y_{Mj}|^2$ is the PSD resulting from the j^{th} sum of M frames of the response signal y(t),

$|X_{Mj}|^2$ is the PSD resulting from the j^{th} sum of M frames of the drive signal x(t),

and $|X|^2$ is simply the drive spectrum used when Y_{Mj} and X_{Mj} were obtained.

It can be shown (7) that the variance in the PSD estimate using equation (2) is inversely proportional to MN, while for a fixed M and N, the variance tends to be greatest around resonances.

The timing flow for a typical implementation of this indirect PSD estimation method with M = 4 and N = 2 is shown in Fig. 8.

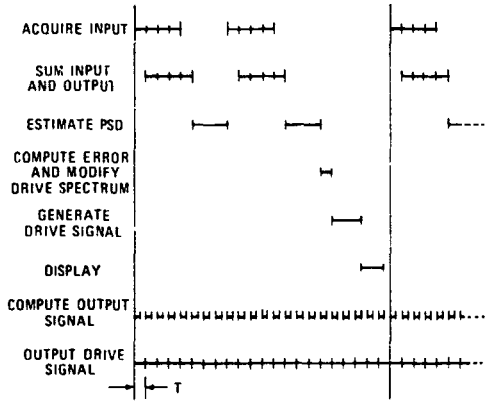

Fig. 8. Indirect Method Random Control Timing, N=2, M=4.

There is a twofold advantage to the indirect method. First, since a time-domain summation calculation is faster than a PSD calculation, and only two PSD calculations are needed for each M data frames, more input (response) data can be processed per unit of time using the indirect method than with the direct method. Table 1 summarizes the percentage of time

Table 1. Percentage of Time Devoted to Input Data Acquisition for Different Parameters and Hardware Configuration

CONTROL BANDWIDTH HZ	PROCESSING HARDWARE (Note)	INDIRECT			DIRECT		
		N=2 M=2	N=2 M=4	N=2 M=8	N=2	N=4	N=8
1024	1	22	37	55	18	19	20
1024	2	30	42	66	27	35	42
1024	3	33	52	69	28	36	43
2048	1	13	22	35	10	11	11
2048	2	20	36	52	18	23	29
2048	3	25	41	59	21	27	30
3072	1	7	13	16	5	6	6
3072	2	12	24	37	10	15	16
3072	3	20	34	51	16	25	29

Note: 1 = CPU (PDP11/35) only
2 = CPU + Hardware FFT Processor
3 = CPU + Hardware FFT Processor + Output Processor

that is spent acquiring input data for both methods as a function of M and N, control bandwidth, and typical processing hardware. Input acquisition is discontinuous, i.e., occurs less than 100% of the time, due to the additional processing functions required during the control loop operations including random drive signal generation, drive spectrum correction, PSD estimation, displays, safety checks, and miscellaneous bookkeeping. It is observed from Table 1 that by adding hardware to perform tasks such as Fourier computations and output signal generation in parallel with other functions, input data can be processed more than 50% of the time for control bandwidths up to 3000 Hz using the indirect method with N = 2 and M = 8.

The second advantage is that for a given number of input data frames the statistical variance of the indirect method estimate is significantly lower than the corresponding direct method estimate. It has been observed empirically that the variance of a indirect PSD estimate, although somewhat dependent on the characteristics of the load being driven, is typically less than the variance obtained with a direct PSD estimate using four times as many data frames. In terms of statistical degrees of freedom using linear PSD averaging this means that for the indirect method, k 8MN, while for the direct method, k = 2N.

Figures 9 through 12 illustrate the reduction in variance using the direct method. Figures 9 and 10 show direct and indirect PSD estimates, respectively, of a nominally flat 2000 Hz spectrum, each using 8 input data frames. A tolerance interval of 4 dB (± 2 dB) is superimposed on the estimates. Figures 11 and 12

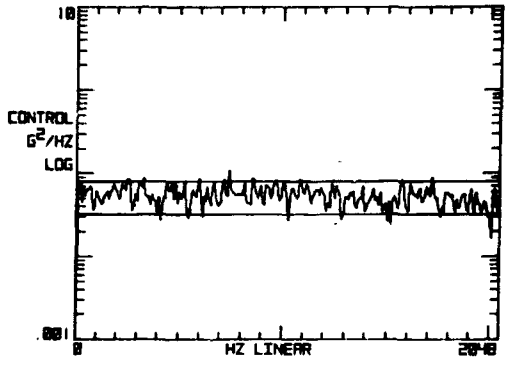

Fig. 9. Direct Estimate of Flat Spectrum 8 Frames

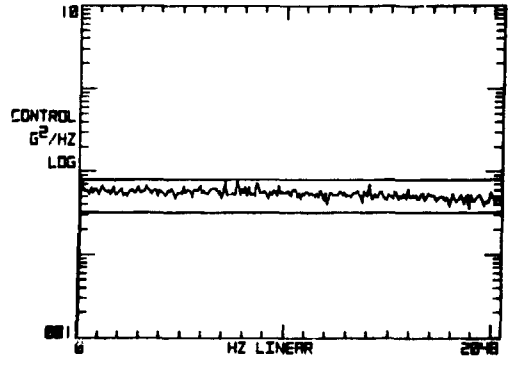

Fig. 10. Indirect Estimate of Flat Spectrum, 8 Frames

illustrate corresponding results with 32 data frames. Comparing Figures 10 and 11 it is seen that the indirect estimate with 8 frames is at least as good as the 32 frame direct estimate. Similarly, the variance in the 32 frame indirect estimate (Fig. 12), ±1 dB, is comparable to that expected from a 256 degree of freedom estimate, requiring 128 frames using the direct method.

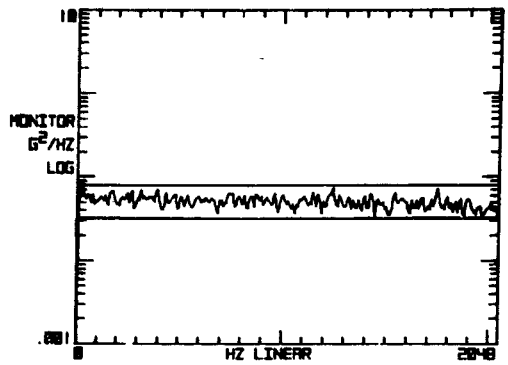

Fig. 11. Direct Estimate of Flat Spectrum, 32 Frames

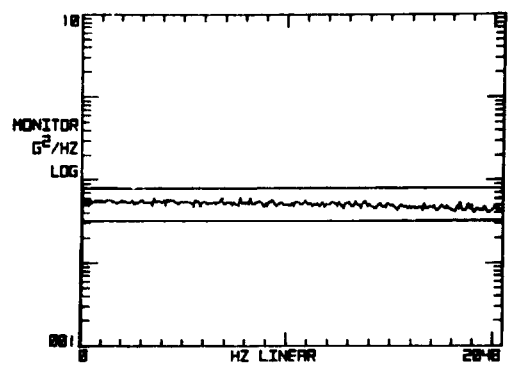

Fig. 12. Indirect Estimate of Flat Spectrum, 32 Frames

THE COMPLETE CONTROL LOOP

Overall random vibration control is achieved by combining a rapid, accurate PSD estimation technique with a bold, yet stable, drive spectrum modification strategy. A typical strategy for drive spectrum modification is the following (3): For each spectral component, determine the error as the ratio of reference to control PSD estimate. Convert the ratio to a logarithm and correct the drive by one-third of the logarithmic value, e.g., a 3 dB error produces a 1 dB correction, a 6 dB error produces a 2 dB correction, etc.

Figure 13 illustrates a typical control point PSD estimate using the indirect method while controlling through a peak-notch transfer function with a 36 dB dynamic range. The control strategy implemented is based on the method outlined above. Tolerance bands of ± 2 dB are superimposed on the plot. The corresponding drive spectrum is shown in Fig. 14. Note that the variance in the PSD estimate tends to be greatest at the 500 Hz resonance and 1000 Hz antiresonance. Figures 15 and 16 show corresponding control and drive spectra using the same control strategy and the direct PSD estimation method with N = 4. Notice that the variance using the indirect method is significantly less than using the direct estimate, even though the total acquisition and processing time was only 20 to 40% longer, depending on system hardware, for the indirect method (both estimates required 4 PSD calculations). The cumulative effect of a good PSD estimate and control strategy is illustrated by comparing the drive spectra, Figures 14 and 16. A smoother drive spectrum could be obtained in the direct case by adopting a more conservative correction strategy, but at the expense of overall correction time.

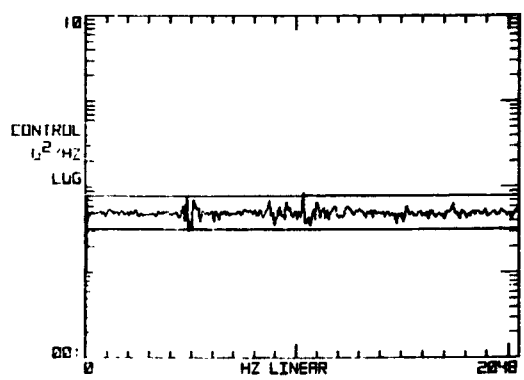

Fig. 13. Typical Control Point PSD Estimate, Indirect Method, N = 2, M = 8

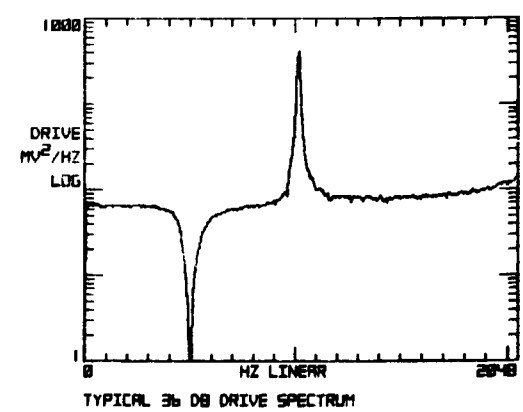

Fig. 14. Typical Drive Spectrum, Indirect Method, N=2, M=8

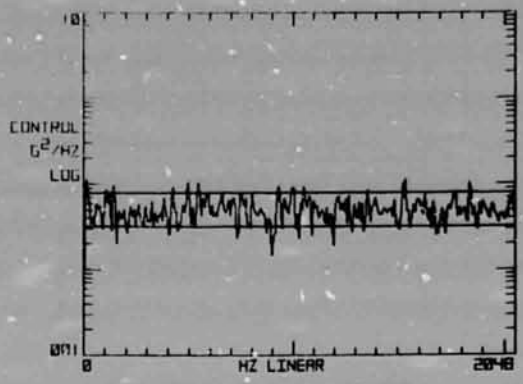

Fig. 15. Typical Control Point PSD Estimate, Direct Method, N=4

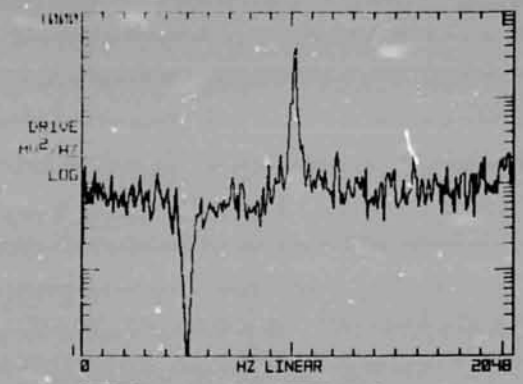

Fig. 16. Typical Drive Spectrum, Direct Method, N=4

DIGITAL SYSTEM HARDWARE

Basic hardware requirements for a digital random vibration control system include a central processing unit (typically a 16-bit minicomputer) with associated memory (16 to 32 thousand words), programmable analog-to-digital and digital-to-analog converter systems (10 or 12-bits, 1 to 8 input channels, with a maximum sampling rate at least 20 kHz), programmable filters for input and output (low-pass, minimum 48 dB/octave rolloff), a display device (typically 4" x 5" CRT), a program loading device (typically a high-speed paper tape reader), and a system control panel and/or an alphanumeric keyboard. A variety of peripheral devices such as parallel processing units, mass storage devices (magnetic tape units, disks, or cassettes), large screen displays, and hard-copy devices (X-Y plotters, electrostatic copiers, etc.) enhance both the performance and convenience of a basic digital control system.

A representative digital random vibration control system is shown in Fig. 17. A block diagram of the basic system components and options is shown in Fig. 18, while Fig. 19 shows a close-up of the control panel as used for random vibration control operation. A unique advantage of many digital systems is that the same system hardware can be used for other control and analysis applications simply by loading different operating programs. The system shown here, for example, uses the same control panel and system hardware for random acoustic control, swept narrowband random on wideband random vibration control, and swept sine on random vibration control operation (8). By replacing the overlay on the right half of the control panel and loading appropriate software the system becomes a sinusoidal (9) or transient (10) control system.

Fig. 17. Typical Digital Random Vibration Control System

SYSTEM OPERATION

Operator interaction with the system described here is through the control panel (Fig. 19) and alphanumeric keyboard terminal. Test parameters are initially entered by the operator from the keyboard. A typical dialog between the operator and the system is

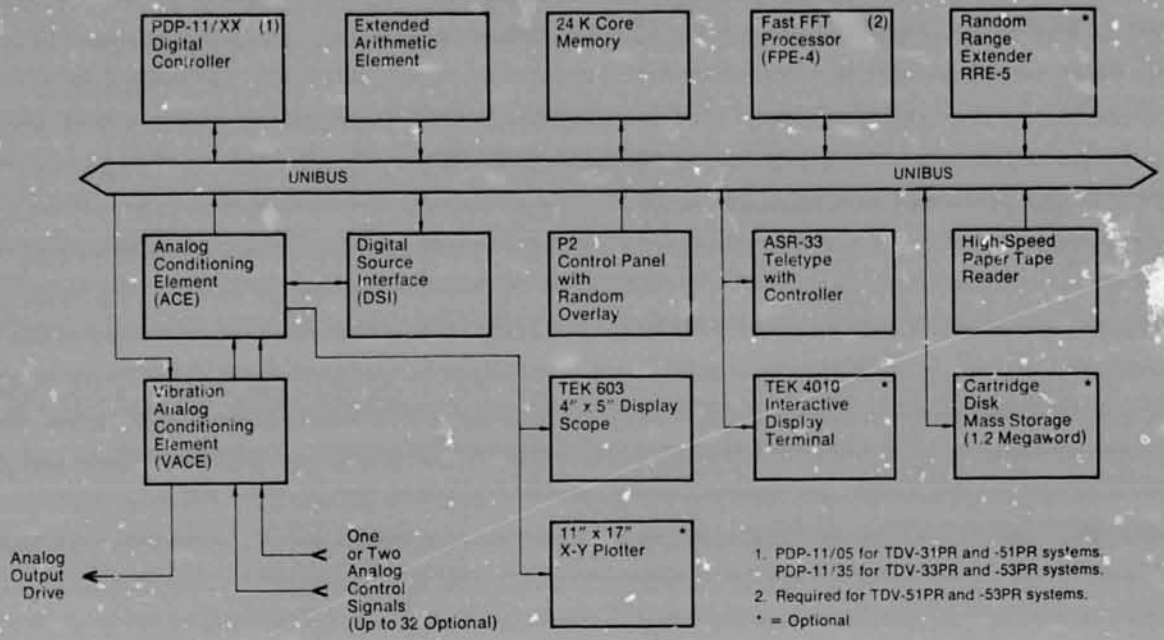

Fig. 18. Block Diagram of Principal Components of Typical Digital Random Vibration Control System

illustrated in Fig. 20. Operator responses are underlined. The total bandwidth to be controlled, filter spacing, and the GRMS value of the reference spectrum are computer-calculated responses. Once test parameters have been entered, they can be edited through a corrections routine, listed for a printed record, and saved on disk or punched paper tape to allow for fast, accurate setup of future tests.

If more than one control channel is specified, then the average of the estimated PSD's of each selected channel is used as the spectrum to be controlled. Additionally, the spectrum of any channel ("auxiliary" channel) can be independently displayed during and after test operations. The auxiliary channel definition can be changed during test operations. Control panel switches also permit the operator to arbitrarily modify the reference spectrum, even while the test is continuing. If desired, the drive signal can be clipped to any arbitrary voltage or sigma level.

With test parameters entered, the operator can initiate the test at any time from the control panel by selecting the TEST function and pressing the START switch. Before the test begins, a very low level, short duration check is made to confirm that a proper response signal is being received by each channel specified in the setup. If the "loop-check" is unsatisfactory (e.g., faulty charge amplifier, improper signal connections, etc.) a diagnostic message is printed for the operator and the test is not permitted to start. Upon completion of a satisfactory loop-check, the test begins upon receipt of a c[illegible]nd from the operator.

Fig. 19. Digital Random Vibration Control Panel

```
ENTER PARAMETERS 1=YES 0=NO: 1
INPUT 2=DISK, 1=KYBD, 0=RDR: 1

1 TEST ID: T2123
2 HEADING: T-2123 Z-AXIS

3 BANDWIDTH: 2000
 BANDWIDTH: 2048.

4 RESOLUTION 64/128/256/512: 256
FREQUENCY INCREMENT: 8.000

REFERENCE SPECTRUM:
5 INITIAL SLOPE, DB/OCT: 12
   ALARM LIMIT DB : 3
   ABORT LIMIT DB : 6

6 FREQUENCY    HZ.: 50
   LEVEL  GSQR/HZ.: .01
   ALARM LIMIT DB : 3
   ABORT LIMIT DB : 6

7 FREQUENCY    HZ.: 200
   LEVEL  GSQR/HZ.: .01
   ALARM LIMIT DB : 3
   ABORT LIMIT DB : 6

8 FREQUENCY    HZ.: 400
   LEVEL  GSQR/HZ.: .1
   ALARM LIMIT DB : 6
   ABORT LIMIT DB : 9

9 FREQUENCY    HZ.: 600
   LEVEL  GSQR/HZ.: .1
   ALARM LIMIT DB : 6
   ABORT LIMIT DB : 9

10 FREQUENCY    HZ.: 0

10 FINAL SLOPE, DB/OCT: -18

GRMS : 6.511

11 LOW LEVEL, -DB: -20
12 LEVEL INCREMENT, DB: 3
13 START-UP TIME SEC: 10
14 SHUT-DOWN TIME SEC: 1
15 TEST TIME HRS, MIN, SEC: 0,5,0
16 AUTOMATIC INCREASE, 1=YES 0=NO: 0
17 CONTROL CHANNELS: 1
18 AUXILIARY CHANNEL: 2
19 ACCEL SENS MV/G:
   CH 1: 10
   CH 2: 10
20 DRIVE CLIPPING  1=YES, 0=NO: 0
21 ALARM LEVEL GRMS: 8
   ABORT LEVEL GRMS: 10
22 LOOP-CHECK MAX DRIVE(VOLTS): .1

CORRECTIONS 1=YES 0=NO: 0
```

Fig. 20. Dialog for Entry of Typical Test Parameters

Initial equalization to the reference spectrum takes place at the low level specified during setup, e.g., in Fig. 20, -20 dB with respect to the full GRMS level. When the test has equalized at low level, it may be increased to the full GRMS level either manually, in steps specified during setup (e.g., 3 dB) or automatically, either after a specified time at low level or by pressing the INCREASE switch The test shuts down automatically if permitted to run for the specified duration at full level. The test also shuts down automatically if an abort condition occurs, and may be shut down manually at any time. Whenever a test is shut down, the test level is decreased smoothly in the specified shut down time and a post test message is printed, providing a record of the test duration at full level and of why it shut down, as shown in Fig. 21.

Conditions which cause an automatic abort include:

1. Initial open loop condition on any selected channel.
2. Loss of signal on any selected channel.
3. Control signal exceeding the GRMS limit specified.
4. G^2/Hz level of any line of the control spectrum deviating from its corresponding reference spectrum line by more than the specified abort limit.
5. An operator abort command.
6. Closure of any of 16 external contacts.

```
Z-AXIS RANDOM ON T1012

ABORTED
CTL SIGNAL LOSS!

 TEST TIME HRS, MIN, SEC: 0,0,22

MONITOR FRAMES: 5

-------------------------------

T-2123 Z-AXIS

ABORTED
OPERATOR HALT!

 TEST TIME HRS, MIN, SEC: 0,0,58

-------------------------------

Z-AXIS RANDOM ON T1012

COMPLETED

 TEST TIME HRS, MIN, SEC: 0,2,0

MONITOR FRAMES: 25
```

Fig. 21. Examples of Post Test Documentation

During and after a test, calibrated and annotated displays (see Figures 5, 6, and 9 through 16) of the control, monitor (averaged control), reference, error, and auxiliary spectrums are available for test analysis and documentation.

CONCLUSIONS

The control techniques, hardware implementation, and operation aspects of digital random vibration control systems have been discussed. When compared to analog systems, today's digital random control systems offer faster test setup, more resolution, wider dynamic range, more flexible frequency coverage, repeatable test execution, more complete test documentation, and easy, economical conversion to other control and anlysis tasks.

REFERENCES

1. Chapman, C. P., Shipley, J., and Heizman, C. L, "A Digitally Controlled Vibration or Acoustics Testing System: Parts I, II, III," Institute of Environmental Sciences, 1969 Proceedings, pp. 387-409

2. Heizman, C. L., "A High Performance Digital Vibration Control and Analysis System," Institute of Environmental Sciences, 1972 Proceedings, pp. 309-315.

3. Nelson, D. B., "Performance and Methodology of a Digital Random Vibration Control System," Institute of Environmental Sciences, 1973 Proceedings, pp. 187-192.

4. Chapman, C. P., Kim, B. K., and Boctor, W., "Digital Vibration Control Techniques," International Instrumentation Automation Conference and Exhibit, New York City, October, 1974. ISA Paper No. 74-631.

5. Blackman, R. B. and Tukey, J. W., "The Measurement of Power Spectra," Dover Publications, Inc., New York, pp. 21-25.

6. Bendat, J. S. and Piersol, A. G., "Random Data: Analysis and Measurement Procedures," Wiley Interscience, New York, pp. 189-193.

7. Norin, R. S. and Sloane, E. A., "A New Algorithm for Improving Digital Random Control System Speed and Accuracy," Institute of Environmental Sciences, 1975 Proceedings. pp. 46-52.

8. Stauffer, M. K., "Techniques for Narrowband Random or Sine on Wideband Random Vibration Testing with a Digital Control System," Seminar on Understanding Digital Control and Analysis in Vibration Test Systems, 1975 Proceedings.

9. Norin, R. S., "A Multi-Channel, Multi-Strategy Sinusoidal Vibration Control System," Institute of Environmental Sciences, 1974 Proceedings.

10. Barthmaier, J. P., "Shock Testing Under Minicomputer Control," Institute of Environmental Sciences, 1974 Proceedings.

SINE-SWEEP TESTING USING DIGITAL CONTROL

Dr. Alfred G. Ratz
Ling Electronics
Anaheim, California

A review is given of the theory of swept-sine vibration testing using an electrodynamic shaker. The objective is to show how the control requirements can be fully satisfied with a digital system, based on the use of a minicomputer. The only equipment needed over that for control of either random or pulse testing is a digitally-controlled sine oscillator. Automatic compression speed, specimen Q, sweep rate, tracking filter feedback, control to the average or the maximum of a number of simultaneous acceleration signals, specimen protection, are among the topics covered. Finally, examples are given showing the performance of a practical system with single and multiple return accelerometers.

INTRODUCTION

The purpose of this paper is to describe the theory and practice of putting together an automatic sine-test control system for an electrodynamic exciter, based on the use of a minicomputer. The discussion centers around a particular embodiment for reference and example; however, the emphasis of the discussion is on fundamental techniques. Some of the techniques are basic to swept-sine testing for any type of control; other techniques are truly unique to digital systems.

There are a number of important advantages in using a digital system for sine control. The system permits test parameters to be automatically set up ahead of time without tying up the exciter and associated equipment. There are no switches or potentiometers to be adjusted by the operator, as compared with the considerable number of critical controls that must be tuned in a sophisticated analog system. System setup errors and debugging times are eliminated. The level of operator skill is considerably reduced. Automatic monitoring of pertinent test results is easily arranged. It is also easy to expand a system to meet new needs by simply modifying the software programming.

In summary, then, the advantages possible with digital control are: increased productivity (that is, we can quickly go from one type of test to another), operational cost savings (due to the increased productivity, as well as the ability to use operators with less skill), repeatability (the identical program held in paper tape, on disc, or using some other digital storage medium, can be used over and over so that the identical test is called out), test integrity (no human error in setting up the test, no controls to be inadvertently manipulated during a test), and safety and protection. In the latter case, the computer can watch over a variety of parameters with an unflagging attention, a reaction speed, and a sensitivity impossible with a practical analog system.

Sine control using a digital computer has tended to take second place to the random control or the shock pulse control of an electrodynamic exciter. There are several reasons for this, some quite valid. Accurate shock control, for example, has always proven very difficult to achieve, prior to the introduction of the digital control system. And, the cost and complexity of analog random systems have made them a target for newer technology. But, in terms of the performance requirements and the design problems to be handled, the control of sine testing presents a level of technical difficulty that is in many ways more severe than that experienced with random control. For example, if one examines the various digital random control systems presently described in the literature, one finds that, in dynamic range of equalization, hardly any match the performance of high-quality analog systems. The degradation in performance becomes glossed over by digital considerations; but with swept-sine control, it is difficult to achieve a similar camouflage. as the sinewave sweeps over the frequency band, as each specimen resonance is dealt with in its turn, the quality of control remains at all times clear,

discernible, and disguised.

Sine control capability of a digital control system is usually added as an adjunct to random control; and the system serving as the basis of the present discussion is indeed obtained by the simple expansion of an automatic random control system. The only ancillary equipment added to give the system sine-control capability is a digitally-controlled oscillator.

THE ELECTRODYNAMIC EXCITER

Electrodynamic vibration exciters are important features of the environmental test facilities associated with the design, development, and proof-testing of aircraft, missiles, and satellites. The principle of the electrodynamic exciter follows that of the permanent-magnet loudspeaker. But, the emphasis of design is quite different. Frequency response is secondary. Considerations of force, power, length of stroke, etc., are much more important. Consequently, the transfer characteristic of the exciter is far from flat.

Interactions between load and exciter can modify the frequency response, introducing sharp peaks and notches across the spectrum. Resonances are often introduced by the properties of any fixture used to mount the specimen to the exciter, as well as by the transfer function of the specimen itself.

Thus, the unpredictable properties of the frequency characteristic of the exciter and its load make mandatory the use of closed-loop control. Otherwise, it is not possible to carry out representative testing. Any attempts simply to drive the exciter open loop can only lead to chaotic and indeterminate results. For efficient operation, feedback is needed.

Swept-sine is the basic sine-test mode. With swept-sine testing, the electrodynamic vibration exciter is driven by a sinusoidal signal, whose frequency is slowly swept back and forth between two limits, at a predetermined (usually logarithmic) sweep rate. At each frequency, the vibration level must adhere precisely to a value established by a programmed input curve (level versus frequency).

Other forms of sine tests: dwell, phase control, multiple-accelerometer control, etc., are simply modifications and adaptations of swept-sine, and are best discussed as such.

BASIC THEORY OF SINE CONTROL

We now discuss the parameters needed for a successful sine vibration system. The object is to apply a sweeping sinewave with a specified amplitude profile to the test object.

Compression Control. A real-time amplitude feedback control cannot be used for several reasons. The complex nature of the response of the test item would require a specific complex equalizer in order to achieve a stable closed loop. Test objects vary tremendously in their response. A different specific equalizer would be required for each test package. Most important is the fact that there is insufficient bandwidth through the control system (exciter, driving amplifier, accelerometer electronics, etc.) to permit a stable reliable closed-loop instantaneous-signal control system.

Amplitude control is achieved by applying the technique often called compressor control, or AVC. The essence of the method is to obtain a measure of the vibration level (rms or peak) at the exciter, and then to attenuate or amplify the amplitude of the sine drive to eliminate any discrepancy between the measured and the required level.

The required attenuation gain range over which the sine level must be adjustable is of importance. A typical test object can be expected to have resonances in its transfer-function response with values of Q up to and exceeding 60 dB. Even so, the typical required accuracy is 2% of specified level. The control must thus cover over a 1000:1 range with 2% accuracy of point at every attenuation level in the active dynamic range.

Compression With Random Control. The range of amplitude control required to handle spectral fluctuations in the response of the specimen is demonstrably much greater with sine testing than for random. With wide-band random, resonances with extremely sharp values of Q become invisible to the control system, and do not need to be dealt with at all. Also, one finds the limitations of control performance obscured behind such factors as the statistical jitter on the output spectral plot.

With random control, the numbers representing the spectrum deal with it basically as a set of linear quantities. One finds little awareness of how seriously the spectral dynamic range is limited in practice by the significant figures actually available to represent the individual spectral lines. Even so, marginally successful random control systems are reported. But, there is no such lucky situation for the designer of the sine system. The sinewave stands out clear and naked. If its amplitude were represented linearly, three decimal digits would be needed to express accuracy and three to handle ranging, for a total of six decimal digits. The excessive number of

decimal digits causes the designer to search for an alternate method of representing signal strength, to the linear method that passes as acceptable for random control.

A logarithmic format can handle a large dynamic range with constant percentage accuracy. Hence, a log control scheme is the one used in all successful sine-control systems. A logarithm control schere is also essential to solve the problems inherent with compressor control stability, as it turns out.

Servo Control Loop. Figure 1 shows the basic elements of a compressor control loop, whether digital or analog. In Figure 1, the reference (ref) is the required vibration amplitude on the test package at the present value of frequency. The difference is obtained between the reference (ref) and the level at the test object. It is used to generate an error signal. The integrator smooths out the error signal and applies a gain command to the attenuation amplifier. The amplifier adjusts the level of the drive signal and then applies it to the test package. The detector rectifies the sinewave representing the resultant acceleration, and generates the new control signal, thereby closing the feedback loop.

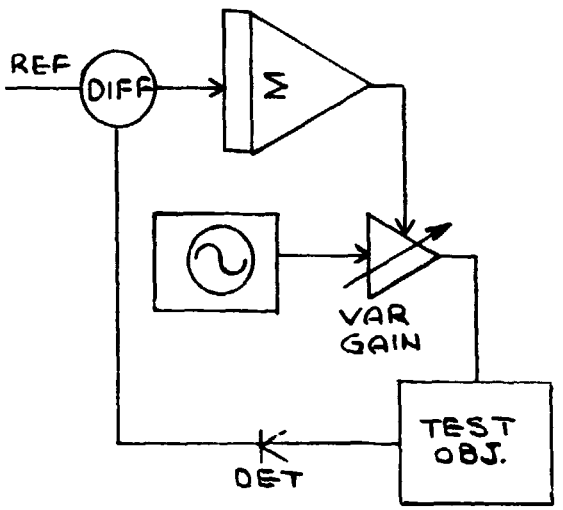

Figure 1 - Basic Servo Loop

Compressor Speed. An important parameter of the compressor control loop is its speed of response. The requirements for wide dynamic range and high accuracy force the feedback loop gain to be high. The complexity of the test specimen requires that the compressor-loop time constant be the predominant time constant in the servo.

The speed of response of the control loop is set by two considerations. The control loop must be fast enough to satisfactorily hold the desired acceleration level as the drive frequency is swept through the test resonances. The control loop must be slow enough to permit smoothing of the ripple from the rms detector, thereby permitting the control to accurately follow the average level of the sinewave. (If the control tends to follow some instantaneous component, it introduces distortion into the sine drive signal.)

The goal of the control loop is to obtain a 2% control accuracy. For design, let us allow a maximum of 1% detector ripple. We can now calculate the compressor speed for a particular frequency. The integrator used to reject ripple does so at the rate of 6 dB/octave. If we assume that the detector is a full-wave rectifier or a square-law detector, then the ripple frequency is twice the fundamental frequency. The average detected value is roughly equal to the amplitude of the unsmoothed ripple. Therefore, the compressor loop bandwidth must be decreased to the point where the drive frequency is larger than the loop bandwidth by orders of magnitude. For example, for a fundamental drive frequency of 1000 Hz, the compressor feedback loop bandwidth must be no wider than 5 Hz to 10 Hz.

Feedback loop bandwidth of the compressor system serves as a measure of the ability of the compressor to control the amplitude of the accelerometer signal under the many fluctuating dynamic conditions that occur when the frequency is swept. It is expressed in radians per second (rad/s), $\omega_L (=2\pi f_L)$.

The expected error in control as the sine drive is swept through a resonance can be predicted by calculating the control error E(dB).

$$E = \frac{\dot{\psi}}{\omega_L} \qquad (1)$$

The quantity $\dot{\psi}$ is the amplitude slewing-rate capability of the system, measured in dB/sec. Amplitude slewing rate is also called "compressor speed." From Equation (1) we see it also is a measure of the bandwidth of the control loop as a servomechanism. The relationship to the servo bandwidth can be deduced as follows. Suppose that f(t) represents the output signal, and that f(t) has its envelope changing with time (A is a constant):

$$f(t) = A \cdot e^{-\omega_c t} \qquad (2)$$

Taking logarithms and differentiating yields ($\omega_c = 2\pi f_c$):

$$\dot{\psi} = \frac{dL(t)}{dt} = 8.68\ \omega_c = 54.5\ f_c \qquad (3)$$

There are two main operational parameters influencing the required range of values for the slewing rate. These parameters

are (1) the Q of the resonance that the drive frequency is presently sweeping through and (2) the frequency sweep rate. The effect of these in establishing an acceptable slew-rate is discussed below.

SYSTEM EMBODIMENT

The above discussion concerning the theory is applicable to either analog or digital systems (the latter our subject here).

Block Diagram. In the digital application, it is efficient that the portion of the diagram of Figure 1 which consists of the reference, summer, and integrator, should be in software in the computer. The sine generator and the variable-gain amplifier are implemented with devices handling the signal in analog form, but controlled digitally. The frequency of the sinewave locks to the number digitally supplied to the generator. The gains of the variable-gain amplifiers are set by numbers supplied by the computer. The detector can be handled either in an analog or in digital form. In the present system, it is handled digitally.

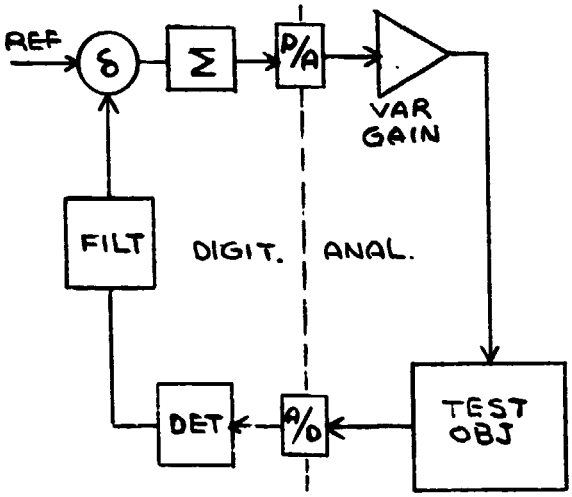

Figure 2 - Compressor Loop - Digital System

Figure 2 shows a simplified block diagram. Shown are the sampling and quantizing devices required by the computer: an A/D converter and multiplexer (MUX), as well as a D/A converter. The detector and its filter are achieved in software.

Non-Synchronous Sampling. The method of "detecting" the return signal is to take in a frame of data, τ seconds long; τ is very nearly equal to the period of the fundamental of the sinusoid. If p is the sampling rate, it is desirous to keep p synchronous with f, the frequency of the sinewave. Since f shifts in very fine steps, this means a continuous and very fine updating of p: the A/D converter and multiplexer dealing with the input signal must have their sample rates smoothly and infinitely programmable without losing timing accuracy. In view of the complexity of synchronous sampling, it is worth exploring the non-synchronous sampling of the cycle of duration τ, Figure 3: suppose we are attempting to find the rms value of the sinewave by taking the mean square value of N samples of the sinewave over one period. The sampling rate is such that there are (N+m) samples per cycle of the wave (m < 1). The first sample occurs when the argument of the sinewave has the value θ.

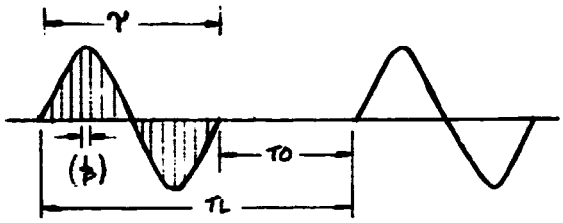

Figure 3 - Sampling: MUX and DATA

The computer forms the average, S_a^2, given by:

$$NS_a^2 = \sin^2(\theta + 2\pi/(N+m)) + \sin^2(\theta + 4\pi/(N+m)) + \ldots + \ldots + \sin^2(\theta + 2\pi(N-1)/(N+m)) \quad (4)$$

By trigonometric manipulation, the equation for NS_a^2 can be rewritten:

$$2NS_a = N - \tfrac{1}{2}\cos 2\theta \left[1 - \frac{\sin\frac{(m+\frac{1}{2})\cdot 4\pi}{N+m}}{\sin(\frac{2\pi}{N+m})}\right] + \sin 2\theta \left[\frac{\sin\frac{2\pi(m+1)}{N+m}\cdot\sin\frac{2\pi m}{N+m}}{\sin(\frac{2\pi}{N+m})}\right] \quad (5)$$

If m = 0, θ = 0, S_a becomes the true rms, S_o.

Also, $2NS_o = N$

and so $S_o = 0.707$

Examination of Equation (5) with N >> 1 indicates that it is certainly bounded by, for all m:

$$2NS_a^2 = N \pm 1 \quad (6)$$

Hence, $S_a = S_o(1 \pm \frac{1}{2}N)$ (7)

To control to better than ±0.3 dB, we must keep

$$N \geq 16 = 2^4 \quad (8)$$

Thus, as f shifts, we do not need to shift p, until Equation (8) is violated. When p is changed, we must change the cut-off frequency, associated with the anti-aliasing filter at the MUX input. We keep the -0.3 dB (cut-off) frequency, F, of a given filter, as the lowest value possible, satisfying

$$f \leq F \quad (9)$$

When f starts to exceed F, the filter is stepped to a larger value of F.

Suppose we are engaged in multiple-acceleration control; i.e., suppose we are controlling to the rms average or extremal of acceleration signals. We must bring in M time histories during the time τ. Then, the multiplex rate is raised to . A typical maximum allowable value for Mp set by hardware performance is 125,000 Hz. Hence, for eight input channels, the highest value permitted for f is given by setting

$$128\ F = 125{,}000$$

Thus $$f \leq 1000 \text{ Hz} \quad (10)$$

If we need to test at frequencies higher than 1000 Hz, 8 channels, we simply use more than one cycle of the sinewave.

M_k, number of input channels that can be handled by (MUX A-D) in K cycles of the operating frequency, f, is given by:

$$M_k\ F = 8000\ K \quad (11)$$

From the diagram of Figure 3 we note that the control algorithm is handled in the interval of time, T_L, minus the time τ. τ is now equal to (K/f) seconds. Since the need for using multiple cycles occurs only at the higher frequencies, little restriction is imposed when we are forced to go to multiple cycles.

Data Samples. For each input frame of the return signal therefore, we compute an rms value: for the purposes of control, the rms value so obtained constitutes a single data point. In assessing the return signal from the exciter, the actual time history is of no value. The information sought is the rms level. The servo speed must be geared to the rate of change of the information in the signal, not that inherent in its time history. Hence, the servo speed is actually slow enough so that we do not have the computer examine the return signal continuously. It can sample one cycle of the wave (for the time duration, τ) allowing a time, T_o, between frames to carry out the subsidiary computations in the computer (Figure 3). Thus, the control is a sampled-servo system with a sampling period, T_L:

$$T_L = \tau + T_o \quad (12)$$

During each time, T_o, the computer (CPU) computes the level of the return signal from the samples derived during the previous ingesting period, τ. It then derives a new control signal to be sent to the gain control register of an output variable-gain amplifier to correct for any deviation in the return level from that specified by the program. The output amplifier, under CPU control, carries out the logarithmic gain-control function discussed above.

Specimen Q. One parameter that has a large effect on the control performance is the maximum value of the specimen Q expected. In analog systems, the operator must set in via a front panel switch the expected specimen Q. With the digital system he must likewise indicate the Q to be expected via instructions to the CPU.

It is to the operator's advantage never to call for a larger Q than actually occurs. If the specimen has no sharp resonances, the operator calls for the low-Q parameter for the control. For higher Q values, he uses the medium-Q parameter and for very sharp resonances, he picks high-Q. The low-Q condition is defined as having Q-values between zero and 50; the medium-Q condition is defined as having Q values between 50 and 200; the high-Q case as having Q values larger than 200.

The digital system user has one important advantage over the user of an analog system. If he selects the wrong value of Q, the control automatically corrects his selection for the actual value of Q encountered. This feature is discussed below.

Control Loop Action. Figure 4 illustrates the control loop in further detail. x(t) is the return signal received from the accelerometer system and its signal conditioner. The gain of the system input amplifier, denoted by G_i, is set to a value consistent with the desired value of acceleration at the table, and the need to keep the rms level of x(t) near to a full-scale value. We must allow for the peak/rms ratio of the signal, plus a need to recover from a large, sudden signal at the table. It is indicated that the A/D must therefore be set to handle signal peaks at least twice the rms. The A/D converter has 12 bits, with 1 bit for sign, 1 bit for the average/peak allowance just discussed, 1 bit to allow for the fact that G_i can only be set in 3 dB steps. The rms level, therefore, approximates the 9th bit in the A/D converter. (NOTE: For what follows, Figure 10 provides a logic flow diagram.)

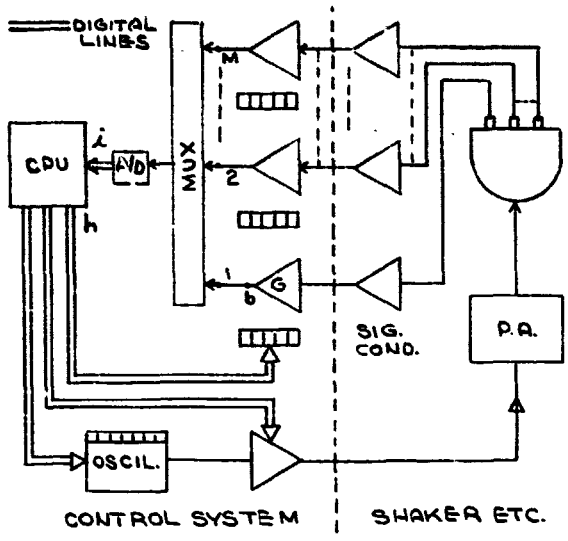

Figure 4 - Control Loop

The first step after A/D conversion is to compute the mean square of the signal; i.e., to compute over the cycle of interest, $\overline{x^2}$

$$Y = \overline{x^2} = 1/n \sum_{1}^{n} x_i^2 \tag{13}$$

Y is compared with the reference value, Y_R, and an error number, e, produced.

$$d = Y - Y_R \tag{14}$$

The reference level, Y_R, must be calculated by the computer for each point on the test profile, as determined by the control program.

For each amplitude value required by the program, there is an optimum value for the gain G_i, bringing the rms controlled level at point b, as close to the optimum value as the gain steps of the amplifier allow. To complete the calibration of the input circuitry to 1%, it is necessary for the program to adjust the reference level, Y_R, to compensate for the size of the minimum increment of gain in the amplifier G_i. But, changing the value of Y_R has the effect of altering the loop gain, and this effect must be removed: a gain-normalizing factor, G, is introduced:

$$e = G\,d \tag{15}$$

where $G = K/Y_R$

The quantity, e, is the final normalized error number. Error numbers e are summed, one number for each iteration of time, T_L. The sum produces the number, E′:

$$E' = \Sigma\, e \tag{16}$$

The number E′ is then scaled by a factor R as required by the compression rate being used. The combined effect of the loop time, T_L, and the loop gain (as finally set by R) determines the compression rate. After scaling by the quantity R, the quantity E′ is converted to the final amplitude level command (output signal).

$$D = RE' \tag{17}$$

There is then a final word conversion to convert D to a gain-command word to set the gain of the output amplifier.

The output amplifier is essential in performing the compression. It is impossible to set gains merely by shifting data words digitally in the CPU. There is no way to do this and maintain control accuracy over the wide dynamic range needed. There is only one way to achieve compression feedback having the sort of characteristics proven essential over the years, for effective sine-servo control, and that way employs a wide-ranging amplifier.

Compressor. The compression rate is affected by the Q of the specimen. If a high-Q specimen is being tested, it is necessary to slow the control loop down. Otherwise, the loop becomes unstable. In setting up a test, we set in a value of Q assumed to be the largest that we can expect across the frequency band of interest. Thus, we are in effect assuming a fixed Q across the band; and so the compression rate (i.e., ψ, Equation (3)) to be permitted at each present value of the frequency, f, must be proportional to f; the proportionality constant must obviously be inversely proportional to Q. Thus, the compression rate, ψ, can be written:

$$\psi \sim f/Q \tag{18}$$

The amplitude control loop as a servomechanism has a frequency response, f_c, that is related to ψ by Equation (3). Obviously, f_c is affected by T_L:

$$f_c \sim \frac{1}{T_L} \tag{19}$$

The gain R also affects f_c:

$$f_c \sim R \tag{20}$$

Thus, at any given frequency, in going from low-Q to high-Q conditions, the control-loop speed must be reduced; this can be accomplished by a combination of two techniques:

(a) Increase the "data sample" time, T_L.

(b) Decrease the loop gain, R, so that it takes more control iterations to correct an error.

By a mutual interaction of T_L and R, we force ψ, through f_c, to follow the curves of Figure 5. It is convenient with a binary CPU to alter the value of ψ for every octave change in f. Thus, for frequencies between $f = f_j$ and $f = 2f_j$, $T_L = T_{Lj}$; then for f between $f = 2f_j$ and $f = 4f_j$, we change T_L to $T_L = \frac{1}{2} T_{Lj}$. At the lower end of the frequency range, $T_{Lj}f_j$ can be kept constant for a given Q; a typical relationship is:

$$T_{Lj} \cdot f_j = 8.0 \qquad (21)$$

In moving from low-Q to medium-Q control, R is reduced by the factor 2^{-3}; to go to high-Q control, R is reduced further by a factor of 2^{-3}.

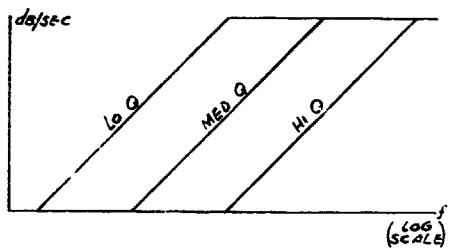

Figure 5 - Automatic Compression Rates

At the higher frequencies, relationship (21) cannot be followed beyond a certain frequency, since T_L cannot be reduced below the time duration needed for the computer to carry out the basic work that must be done between "data samples." Thus, T_L at the high end of the spectrum is fixed and R must be adjusted to compensate.

As mentioned above, the digital system can out-perform an analog sine control system in one important respect. The user selects whether he intends to run at the low-Q, medium-Q, or high-Q condition: if he chooses wrongly (i.e., if he selects too low a Q), the computer notes the instability of the control, and adjusts ψ automatically to compensate: the adjustment is done in steps of 2^{-1}, until stability is reached. (Of course, an upper limit for Q is also implied by the sweep rate selected, so that a sweep slow-down is required as well as a compression-rate slow-down; if such is indeed the case, though it could adjust the sweep rate, the system is not presently programmed to do so, but to abort! It would seem that changing the sweep rate is something the user should do.)

Logarithmic Frequency Sweep. The law usually followed in sine-sweep testing starts slowly at low frequencies and increases the rate of frequency change at higher frequencies; it follows the logarithmic law:

$$df/dt = q = bf \qquad (22)$$

Hence, $$\log_e(f/f_o) = bt \qquad (23)$$

If W is the sweep rate in octaves per minute,

$$W = 85\ b \qquad (24)$$

If T_s = the sweep time in minutes (the time to sweep from the lowest frequency, f_z, to the highest. f_u)

then, $$WT_s = \log_2(f_u/f_z) \qquad (25)$$

A digital system sweeps by incrementing the data in the frequency register of the oscillator at the correct rate. Thus, to carry out a given frequency sweep, the oscillator is addressed from time to time by the computer and fed new "frequency" words. It locks the frequency of the output sinewave to the latest "frequency" used. In order that no resonances are missed, we must keep

$$Df/f \leq \alpha/Q \qquad (26)$$

where α is a number less than unity. Let Df be the frequency increment. Combining equations, we can compute the corresponding time increment, Dt. A suitable value for K is 0.3. Hence,

$$Dt = 25/WQ \qquad (27)$$

It is reasonable to set

$$Dt \geq T_L \qquad (28)$$

An acceptable value for Dt is 0.1 seconds. Based on this value, we can set up the following table for the maximum value of W (i.e., W_1):

TABLE 1
Sweep Rate Vs Specimen Q

Condition	Assumed Maximum Q	W_1
Lo Q	50	5 oct/minute
Medium Q	200	1.25 oct/minute
High Q	1000	0.25 oct/minute

The operator of the system must restrain W_1 to fit the above table. Once he has chosen High Q, Lo Q or Medium Q, he must not then select an incompatible W_1. The above table summarizes basic physical limits imposed by the servo, and does not arise because either a digital or analog system is used. The size of the corresponding frequency increment is given by:

$$Df = \left[\frac{Wf}{85}\right] Dt \qquad (29)$$

Keeping Dt at 100 milliseconds independent of the present value of T_L puts Df at

$$Df = \frac{Wf}{850} \tag{30}$$

Thus, the computer arranges for finer frequency increments, when W is less. This is as it should be, since a reduced value of W can be taken as implying the possibility of encountering a resonance with a high Q and its corresponding narrower bandwidth. The resonance therefore needs smaller frequency increments to be excited properly.

Tracking Filter Mode. An important method of operation for any swept-sine vibration control system is to control on the level of the fundamental of the return acceleration signal, rather than on the composite rms. With analog systems, a tracking filter must be added to the control loop to filter the acceleration signal. With the digital system, no extra hardware is required, the filtering being done in software. The only hardware change is to use one channel of the input MUX to bring in a frame of the full-scale oscillator drive signal, before it is applied to the output attenuator. In other words, the oscillator output, $F_1(t)$, is treated like another return signal, and is multiplexed with the accelerometer signal or signals (for multiple accelerometer control). Let

$$F_1(t) = A \sin \omega t \tag{31}$$

From the input samples taken during the time, τ, the computer develops from each sample of $F_1(t)$, a second signal $F_2(t)$.

$$F_2(t) = \left[A^2 - F_1^2(t)\right]^{\frac{1}{2}} \tag{32}$$

$F_1(t)$ and $F_2(t)$ are used as reference signals. The phase difference between $F_1(t)$ and the data samples is not important provided the MUX has low jitter. Each sample of the input signal or signals being tracked is multiplied by the corresponding value of $F_1(t)$ and of its derived value $F_2(t)$. For each input signal, x(t), therefore, the computer computes the data gathered over each period, τ, two data values, Y_j and Z_j:

$$Y_j = \int_\tau x(t) \cdot F_1(t)\, dt \qquad Z_j = \int_\tau x(t) \cdot F_2(t)\, dt \tag{33}$$

Y_j and Z_j, of course, are computed by summation of the appropriate $x(t) \cdot F(t)$ products, for the data samples gathered over the time, τ. Thus, Y_j and Z_j are the j-th samples of two variables Y and Z. T_L seconds later, the (j+1)-st sample pair (Y_{j+1}, Z_{j+1}) is obtained.

Y_j and Z_j are fed to two identical low-pass filters within the software of the computer. These low-pass filters are obtained by digital filter techniques. Their outputs, Y_{oj} and Z_{oj}, respectively, are, of course, derived from the stream of values Y_j and Z_j. They are combined to obtain a single value, X_j:

$$X_j^2 = Y_{oj}^2 + Z_{oj}^2 \tag{34}$$

X_j^2 replaces X^2 in the servo block diagram.

In working out conditions for the tracking filter, the filter 3-dB bandwidth, B, must be wide enough to be useful. Very narrow values for B are much easier to design, but their utility and efficiency are limited to very special situations, since they force the user to restrict the sweep speed that can be permitted to very low values.

Since vibration phenomena are usually constant-Q in nature, it is very useful to have B proportional to f. Thus, as f increases B must be widened. This cannot be achieved indefinitely as f increases: there is a value of f beyond which it is not practical to widen B.

For servo-loop stability, we must assume that

$$BT_L >> 1. \tag{35}$$

This is a basic servo law that can never be violated by digital or analog equipment. Hence, corresponding to the conditions for which Equation (21) applies, et seq., we can draw up a similar set of conditions. We set B_M as the absolutely maximum value of B that can be permitted. Smaller values of B can always be obtained.

The value of B_M is influenced by R and T_L. The following table gives values of B that are representative of what can be obtained with acceptable values of T_L and R(T_L and R, of course, are affected by f):

TABLE 2
Acceptable Filter Bandwidths

f	B
250 Hz	2 Hz
500 Hz	4 Hz
1000 Hz	8 Hz
2000 Hz	15 Hz

Referring back to the discussion on compression speed, the CPU can use the largest value of the ratio (f/B) to be used in a given test, to set the Q value for determining ψ.

MULTIPLE INPUTS

For large fragile specimens, controlling to a signal computed from the outputs of a number of control accelerometers is very desirable. Two methods of control are: (a) Averaging, (b) Extremal selection. With method (a), as has been discussed above, all the return signals are multiplexed over the frame duration, τ. The sum of the sequence of all MUX samples, normalized by the number of input channels, gives a mean square value for control.

With method (b), control is switched to the return signal having the largest (or smallest) value. Either the rms or peak value can be used. In either case, each input must have its level computed separately during the time, τ, and the decision carried out as to the controlling channel immediately after the frame has passed.

The speed of selection is a popular (and probably critical) criterion in the specifying of a selection system for vibration control. It has been a big factor in the specification of analog selection circuits and should be equally important with digital systems. It is important, therefore, to establish the maximum useful selection speed. It turns out the selection speed depends on the speed of response (compression rate) of the control loop. It is no use selecting faster than the loop can respond, and extremely fast selection does not improve system performance. An estimate of the switching speed needed is important. Suppose we have two input signals and are operating in a selection mode. Suppose the first signal is in control, with the second signal initially set to zero amplitude. Suppose now the second signal increases in amplitude, the change following a step function: the level of the controlling signal is passed instantaneously. The pattern of change just described represents the worst possible case.

Assume, now, that the selection is instantaneous by some miracle of design. The control loop commences to reduce the error introduced at the compression rate. The loop reduces at the maximum rate of 8.68 dB/time constant. Three loop time constants reduce the error to 5% of its initial value.

Now suppose instead of the step-function change in the selection, we had the selection process follow a ramp function so as to take a time equal to one loop time-constant to reach the new error signal. Then the loop would require four time constants to reduce the error, instead of three for the case of instantaneous response, (a slow-down of 33.3%). This seems a small decrease in performance, even for the extreme operating conditions surmised. In practice, with slower signal changes and slower compression speeds, the slow-down is probably never larger than 10%.

Besides speed, signal weighting is another important factor affecting selection design. Signal weighting can be dealt with in a number of ways. The easiest method involves hardware only: it is simply to adjust the accelerometer sensitivity as fed into the input normalizing amplifier, if such exists. Otherwise, weighting can be done in software by introducing scale factors to the control loop via the CPU.

ALARM/ABORT IMPLEMENTATION

Alarm/abort limits are very useful features, easy to program into digital-control systems. When the acceleration level deviates from the desired by more than the alarm limit, the operator is notified. If it deviates by more than the abort limit, the test is terminated.

It is necessary to eliminate false alarms or false aborts. This can be done by having alarm and abort controls programmed to act in some manner as the following:

(a) A running count, n, is to be kept separately for alarm and for abort.

(b) Each period of time, T_L, the return signal is examined for exceeding the alarm and the abort levels. If it does exceed a level, the relevant count, n, is increased by unity.

(c) Each period of time, T_L, the return signal does not exceed a level, the relevant count, n, is decreased by unity.

(d) The value of n can never go negative.

(e) When n reaches the value N_o, the relevant level is considered to have been exceeded, and abort action is initiated.

N_o largely depends on experience. A value of two or three for N_o has proven satisfactory.

The sine control system is unique in one way. Its chief cause of consistent alarm/abort conditions is the encountering of a high-Q situation with too fast a compression speed set in by the operator. Thus, when the control loop sees an alarm condition, in addition to notifying the operator, it alters the compression loop gain by decreasing the value of R, as is described above. A 6 dB change is made.

After an alarm condition has been reached, and is reset to zero, the action can

commence again. If the alarm is again exceeded, R is again adjusted by 6 dB. Thus, it is possible for the system to eventually correct for a serious error in the original specification of Q. Thus, unlike any analog system, the system has the ability to adaptively adjust the control parameters, depending on the specimen Q.

SPECIMEN PROTECTION AND SAFETY

In common with random control, the specimen must be guarded against malfunctioning of CPU, amplifiers, MUX's, etc. Most malfunctions are caught simply by their effects of driving the signal outside alarm and abort limits.

One important item to be uniquely guarded against is failure of the accelerometer. Several algorithms are possible, but it has been proven that the best scheme here actually copies the analog protection device: it measures the rate of change of the signal level received from the accelerometer. If the increment in the time increment T_L is negative and exceeds a previously established value, A_M, the excessive demand is assumed to be due to lack of an accelerometer (return) signal. The seriousness in setting the value of A_M depends on the fragility of the specimen, and the program must permit the user to select A_M at will. Whenever an abort is called for, the computer attenuates the drive signal to the shaker smoothly and gracefully to zero, preventing any possible serious acceleration transients from occurring.

MIXED SINE/RANDOM

Mixed sine/random testing involves superimposing sine and random tests on a specimen simultaneously. The tests are programmed individually, and the first task of the control is to separate the return sine signal from the return random so that each type of signal can be used in its own control loop.

The sine component is easily pulled out of the random by using the tracking-filter mode. Narrowing down the bandwidth, B, of the tracking "filter," is easy to do with a digital system, and makes mixed sine/random easy to accomplish from the sine point of view.

The random signal is much more difficult to extract from the sine with a digital control system: the best way to extract the random seems to be as follows: (1) The composite return signal is fed to the FFT process; and a Fourier transform of the composite signal is produced, (2) At the present value of the frequency, f, of the sinewave, the FFT line is much higher in level because the energy of the sinewave is superimposed, (3) However, the computer is aware of the lines affected, since it has control of f, and for the line or lines in the neighborhood of f, the random closed loop control ceases to function; instead, the PSD level of the output signal is set locked to that worked out before f swept into the region of the lines. Once f sweeps past the line(s) in question, the closed-loop control is again free to operate for them.

The principle problem to be worked out with mixed sine/random is the adjustment of the signal levels through both the sine and random systems (the latter on a PSD basis), to allow for the presence of large, interferring signals. Fortunately, it has been proven practical to get excellent control for a considerable range (35 dB or more) in the value of the ratio of (random rms)/(sine rms), the range being centered at 0 dB.

EXAMPLES

Out of a multitude of test results, a few have been selected to illustrate the sort of equalization achievable under sine control.

The first test shows the equalization of a peak/notch filter used to simulate an actual shaker and specimen. See Figure 6.

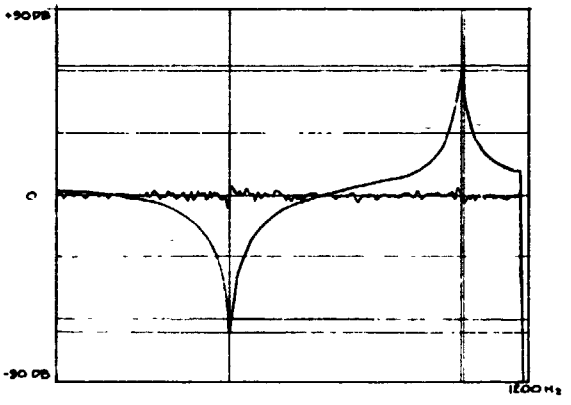

Figure 6 - Peak Notch Correction

A notch is set close to 500 Hz, and a peak close to 990 Hz: the Q of the notch is 61, and the Q of the peak is 72, for a total p/n spread of 73 dB. The sweep rate is 0.5 oct/min. The resulting control shows a maximum error of 0.6 dB. Further reduction of the error is possible, if system parameters are adjusted. For example, the MUX sample rate is set by Equation (8); if it is increased, relative to $(1/\tau)$, the error can easily be cut in half. However, the present values for the parameters would seem adequate for practical control.

Now we turn to a more interesting example. In this example, eight accelerometers are placed along a resonant beam, and mounted on a shaker. Control is affected as follows: control to the maximum level of inputs #A, #3, #4, #5, #6, #7, #8; input #A is the average of acceleration signals #1, #2; inputs #3 through #6 are the signals out of the corresponding accelerometers, weighted by a factor 0.25; inputs #7, #8, weighted by a factor 0.125.

The program specified is: 0.75 G, 10 Hz to 100 Hz; constant DA from 5 Hz to 10 Hz; sweep rate: 4 oct/min. Figure 7 shows the input program, with channel #? signal superimposed; we see at what frequency channel #2 in effect takes over all by itself, channel #1 yielding too weak a signal at those frequencies to contribute significantly to #A.

We also see where the signal from channel #2 does not control alone; either the average or one of the other signals controls in the regions where signal #2 drops away. Figure 8 shows the return signal from accelerometer #8; it must reach 6 G to take control, and only achieves this level when the drive frequency is 36 Hz approximately. Figure 9 plots all eight input acceleration signals, weighted.

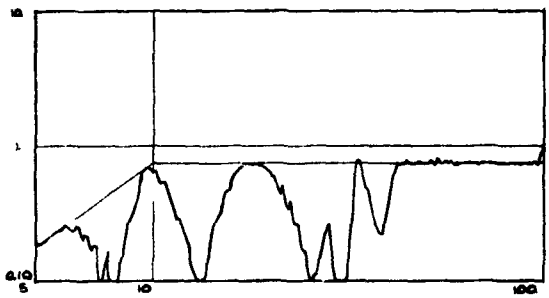

Figure 7 - Channel No. 2

CONCLUSION

Swept-sine vibration testing provides many interesting and unique aspects of interest in the techniques of shaker control. Control is essentially non-stationary in nature, as opposed to random control or shock pulse control. Adaptive servo techniques have proven practical and useful.

The control of swept-sine vibration testing involves handling of much wider dynamic ranges than are required with random or pulse control. And there is no opportunity here of glossing over the dynamic-range performance. The sinewave stands out clear and unencumbered.

The versatility of digital sine control is obvious. It will only be a matter of time when its potential will be fully realized for handling testing situations where analog devices have performed marginally at best; for example, it will not be long before it will be reported that a practical digital system has been developed for the simultaneous phase and amplitude control of multiple shakers connected by a common resonant load, the goal of considerable desire and effort over the past years.

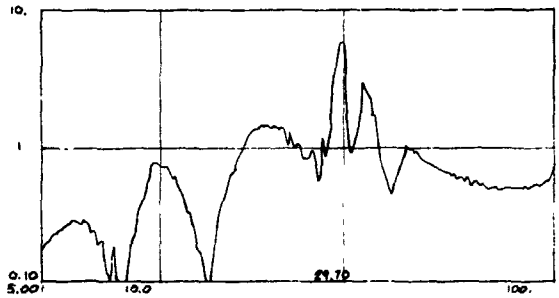

Figure 8 - Channel No. 8

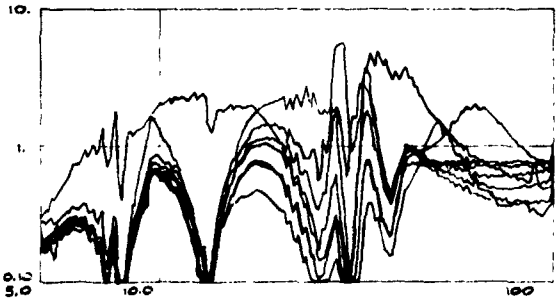

Figure 9 - All Channels - Eight-Channel Control

REFERENCES

a. F. C. Bosso, A. G. Ratz, S. F. Sullivan, "Field Experience with Digital Control Systems for Vibration and Acoustic Testing", No. 720821, Society of Automotive Engineers, Inc., 1972.

b. A. G. Ratz, "Digital Control Systems for Electrodynamic Vibration Exciters", Proc. ISA, 16th International Symposium, Seattle, 1970.

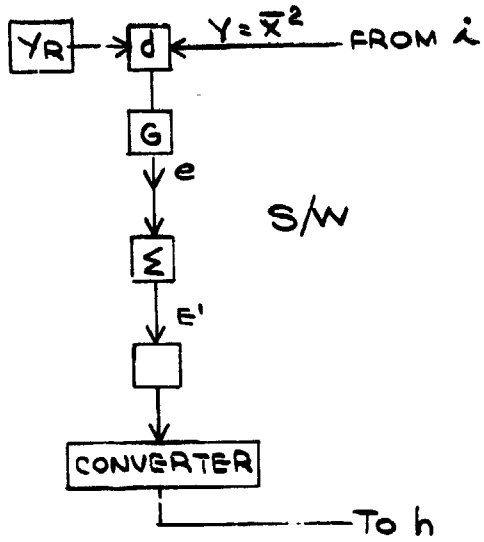

Figure 10 - Logic Flow (Ref: Figure 4)

TIME HISTORY SYNTHESIS FOR SHOCK TESTING ON SHAKERS

D. O. Smallwood
Sandia Laboratories
Albuquerque, New Mexico

Several digital methods now available for matching shock spectra with oscillatory type transients are reviewed and the merits of each discussed. The methods include WAVSYN. SHOC, sums of decaying sinusoids, fast-sine sweeps, modulated pseudo random noise, classical pulses, and the method of least favorable response. While the last method is not strictly a method for matching shock spectra, it is closely related. The discussion is limited to procedures for synthesizing the waveform. Additional parameters (in addition to the shock spectrum) which can be specified to limit the classes of functions available for performing a particular test are discussed.

INTRODUCTION

The need for an oscillatory-type pulse to represent certain field environments has been recognized for several years. During this period, it was also recognized that electrodynamic or electrohydraulic shaker systems were well-suited for reproducing these pulses. With the development of digital control techniques it became possible to reproduce very complex time histories. Therefore, considerable effort has been expended in developing these methods.

A common tool for measuring the character of a transient has been the shock response spectrum of the event. As a result, many current methods are based on producing a transient whose shock spectrum matches a specified shock spectrum. Although considerable controversy still exists regarding the value of the shock spectrum, its use is very common and will continue for years regardless of the outcome of the controversy. Because of its projected use and the fact that procedures which exist can result in quite different waveforms, it was felt that a review of the available techniques would be useful.

Both analog and digital methods are being used. However, the purpose of this paper is to review the digital techniques. The problem addressed in this paper is: given a specified shock spectrum how can a waveform be generated which will have the same (within some tolerance) shock spectrum. The companion problem of how to reproduce the synthesized time history is left for another paper.

Before the time history synthesis can be discussed, the limitations placed on the waveform by the shaker system will be reviewed.

The types of transient vibration or shock pulses which can be accurately reproduced on both electrodynamic and electrohydraulic exciters are very much dependent on the physical limitations of the exciters. These limitations are listed in Table 1 and are briefly discussed here.

TABLE 1
Exciter Limitations

Limitation Number	Initial	Final	Maximum
1	$\ddot{x}(0) = 0$	$\ddot{x}(T) = 0$	Limited
2	$\dot{x}(0) = 0$	$\dot{x}(T) = 0$	Limited
3	$x(0) = 0$	$x(T) = 0$ (Electrodynamic)	Limited

The initial and final acceleration and velocity of a transient must be

zero for both electrodynamic and electrohydraulic exciters. As with any type of testing machine, maximum attainable values of acceleration and velocity are limited. Acceleration is actually limited by the force capabilities of the exciter.

Flexures in electrodynamic exciters generate restoring forces which return the exciter table to its originating position (defined as zero), and limitation 3 holds. This is not a requirement for electrohydraulic systems; however, by imposing this limitation one can take advantage of both the forward and return portion of the stroke to generate the required transient. This effectively results in doubling the displacement capacity of the exciter for generating transients. Thus for the purposes of this discussion limitation 3 will also be considered a limitation for an electrohydraulic exciter.

The initial slope of a lightly damped shock spectrum is related to the velocity and displacement changes required. This is illustrated in Figure 1. Here is an example of waveforms for different values of the initial slope (i.e., the slope of the shock spectrum as the frequency approaches zero on a log-log plot). Note that the shaker limitations will require that only pulses of the last type M>12) can be reproduced on a shaker system. If the initial slope of the specified shock spectrum is not greater than 12 dB/octave there will exist a lower frequency below which the shaker displacement and velocity limits will not permit the spectrum to be matched. If the test item responds like a rigid body at all frequencies less than this lower limit an argument can be made that it is not important to match the spectrum in this range.

Techniques using oscillatory pulses whose shock spectra have an initial slope of S = 1, as for example decaying sinusoids, have been moderately successful because the shaker system will act as a high-pass filter removing the low frequency energy from the waveform. This, combined with the flexure restoring force, will force the velocity and displacement to return to zero. The manner in which the acceleration-time waveform is distorted to remove the velocity and displacement change will be characteristic of the individual shaker system used. This makes it difficult to predict the velocity and displacement waveforms until after the test is run. The velocity and displacement waveforms

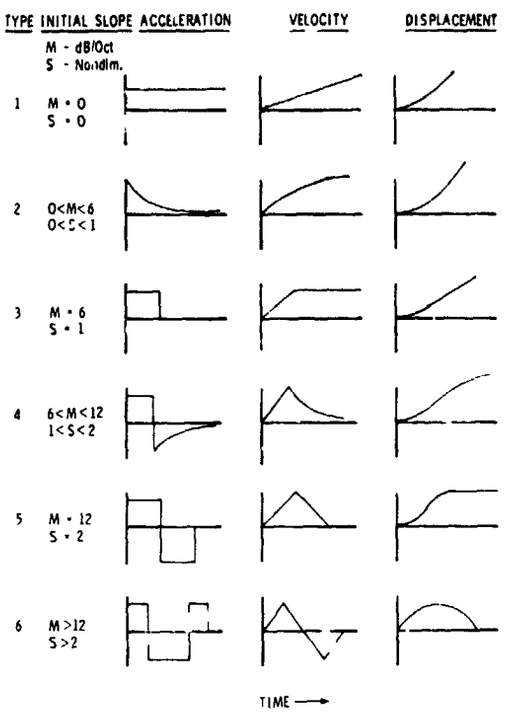

Fig. 1 - Initial Slope of the Shock Spectrum for Some Common Waveforms

are important as the shaker system places limits on the magnitudes which can be reproduced.

The shock spectrum at very high frequencies is identical to the peak amplitude of the input time history. Again the shaker limitations will determine if this level can be reproduced. In many real specifications the shock spectrum is not specified to a high enough frequency to determine the required peak input. In this case some flexibility is available in synthesizing the pulse.

With this introduction to the limitations of shaker systems and to the characteristics of a shock spectrum, the methods used to generate a time history whose shock spectrum will match a specified spectrum can be discussed.

PARALLEL FILTER METHODS

The first method discussed is the parallel filter method. This technique is a direct digital implementation of older analog methods [1]. Using this technique the waveform synthesis and shaker equalization are not separated but accomplished together with the test item mounted on the shaker. Using this method the required shock spectrum is

broken into regions (frequency ranges, typically 1/3 octaves). For each region the peak response is specified, along with a basic waveform whose energy is concentrated in the same frequency range. Any of the basic waveforms discussed later could be used. The most common ones are WAVSYN and decaying sinusoids. In the earlier analog methods the basic waveform was the response of a bandpass filter to an impulse. An initial amplitude for each basic waveform (one for each region or frequency band) is chosen and a composite waveform is formed by summing the waveforms. This time history is then applied to the power amplifier and the control accelerometer response is measured. The shock spectrum of the response is calculated and compared with the required spectrum. This information is then used to modify the amplitudes of the basic waveforms and the process is repeated as illustrated in Figure 2.

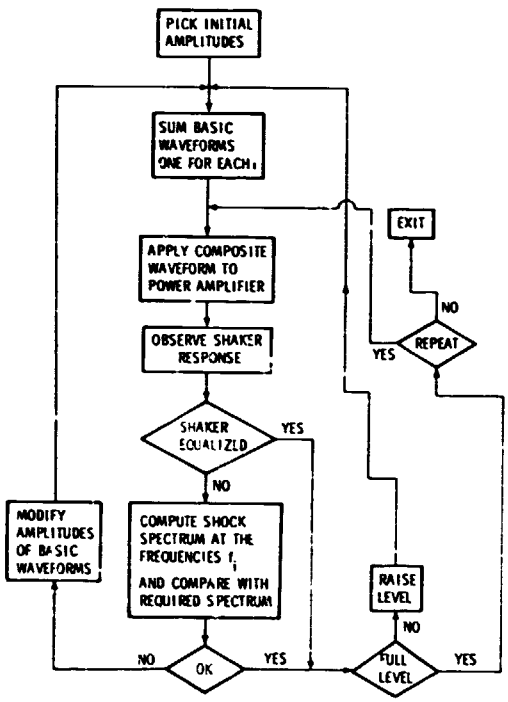

Fig. 2 - A Flow Chart for a Parallel Filter Iteration Method

A variation of the procedure outlined in Figure 2 is shown in Figure 3. The principal difference between this variation and the previous one is that the frequency components are added one at a time starting with the lowest frequency and working up to the highest frequency. When all the components have been added the complete spectrum is

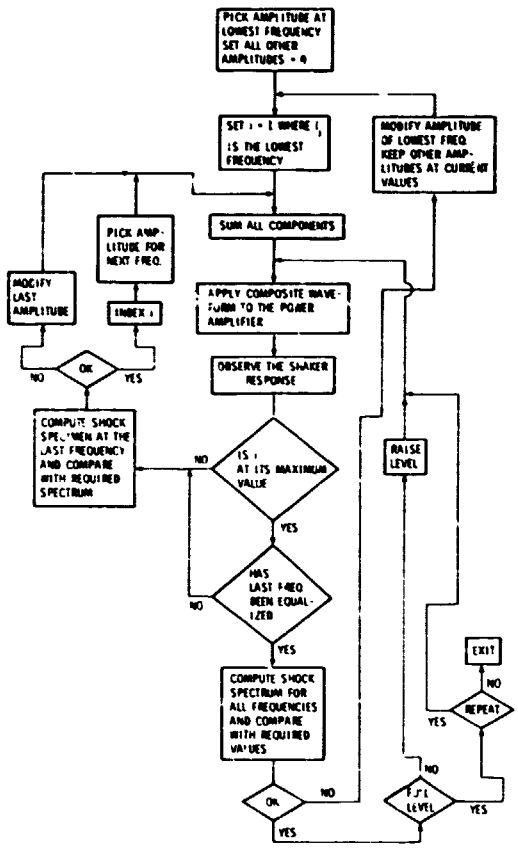

Fig. 3 - A Modified Flow Chart for a Parallel Filter Iteration Method

checked. If the spectrum is not within specifications the procedure is started over at the lowest frequency using the previously determined amplitudes as starting values. Using this technique only one frequency component at a time is modified. As a result, the method is more stable than the previous method (more likely to converge) as the interaction between components is less likely to cause problems. The advantage of the previous method is that if a stable solution is found, fewer pulses are required to equalize the system.

The only difference between the digital implementation and the older analog methods is that a larger variety of basic waveforms can be used, the shock spectrum is computed digitally, and more sophisticated and automated amplitude modification methods can be used. The advantages of these methods include: The methods are relatively easy to implement and use, as details of the time history are not controlled. Quite large values of the shock re-

sponse spectrum can be generated as the shaker is not required to be equalized over sharp notches in the frequency response function. This tends to concentrate the pulse energy in those frequencies where the shaker responds well. Also since equalization is good only in a broad sense, a large variety of shock spectra can be matched. The disadvantages include: Since details of the time history are not controlled, little is known about the velocity and displacement requirements. Because the shaker is not equalized with a fine frequency resolution, all frequencies may not be adequately tested. If the shock spectrum is analyzed with a finer resolution than the initial range, deviations from the required spectrum may be found.

TIME HISTORY SYNTHESIS

Several methods have been developed to synthesize a time history which will match a specified shock spectrum. The synthesis is usually done on a digital computer. It is assumed that this time history can be reproduced on a shaker system using methods originally developed by Favour and LeBrun [2] and will not be discussed in this paper. Several of the methods have checks included to determine the suitability of the transient for shaker reproduction. Reproducing the pulse on the shaker system is independent of the procedure to develop the waveform.

One method will be discussed in detail. The remaining methods will be discussed more briefly as the procedures are similar. The first method discussed is sums of decaying sinusoids (DS). The other methods discussed include WAVSYN, Shaker Optimized Cosines (SHOC), fast-sine sweeps, modulated random noise, modification of field time histories, classical pulses, and least favorable responses.

Sums of Decaying Sinusoids

It has been recognized for years that many field environments can be adequately represented by sums of decaying sinusoids, and as a result several authors [3, 4, 5] have suggested their use to match shock spectra. The usual basic waveform is given by

$$g_m(t) = A_m e^{-\zeta_m \omega_m t} \sin \omega_m t \qquad t \geq 0$$

$$= 0 \qquad t < 0$$

The basic waveform is shown as Figure 4, and the normalized shock spectra, for several values of ζ are shown as Figure 5. Several waveforms are added to synthesize a time history to match a complex shock spectra.

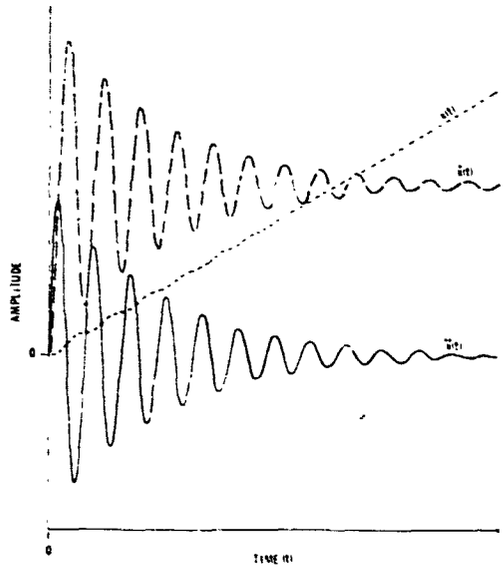

Fig. 4 - Decaying Sinusoid Acceleration, Velocity and Displacement Characteristics

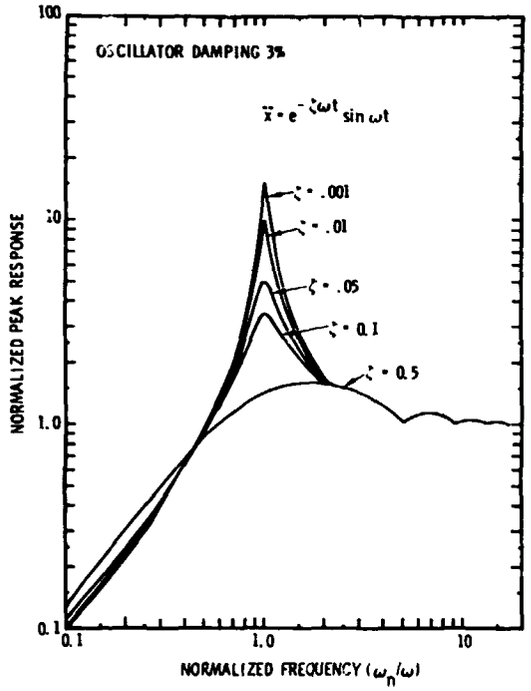

Fig. 5 - Normalized Shock Spectra for a Single Frequency Decaying Sinusoid

However, this waveform does not meet the requirements of a zero velocity and displacement change. If an attempt is made to reproduce this waveform, it will be slightly distorted by the shaker system removing the velocity and displacement change. Since the exact distortion will be a function of the shaker system, it becomes difficult to predict the velocity and displacement waveforms.

Two modifications of the basic waveform have been suggested. The author [3] suggested that a time-shifted, highly damped decaying sinusoid be added for velocity and displacement compensation. It is also possible to introduce time shifts to improve the appearance of the waveform. Allowing for time shifts of the individual components, the waveform becomes

$$\ddot{x}(t) = \sum_{m=1}^{L} U(t-\tau_m) A_m e^{-\zeta_m \omega_m (t-\tau_m)} \cdot \sin \omega_m (t-\tau_m)$$

$$+U(t+\tau)\, A_c e^{-\zeta_c \omega_c (t+\tau)} \cdot \sin \omega_c (t+\tau)$$

where

$$A_c = -\omega_c (\zeta_c^2 + 1) \sum_{m=1}^{L} \frac{A_m}{\omega_m (\zeta_m^2 + 1)}$$

$$\tau = \frac{\omega_c (\zeta_c^2 + 1)}{A_c} \left| \frac{2\zeta_c A_c}{\omega_c^2 (\zeta_c^2+1)^2} + \sum_{m=1}^{L} \left[\frac{A_m \tau_m}{\omega_m (\zeta_m^2+1)} + \frac{2\zeta_m A_m}{\omega_m^2 (\zeta_m^2 + 1)^2} \right] \right|$$

The magnitude (A_c) and the shift (τ) of the velocity and displacement compensating pulse are fixed by the other parameters. A plot of a typical waveform is shown as Figure 6.

Prasthofer and Nelson [4] suggested velocity and displacement compensation by adding two exponential pulses and a phase shift to the decaying sinusoid to give

$$\ddot{x}(t) = \sum_{m=1}^{L} g_m(t)$$

$$g_m(t) = A_m \left\{ K_1 e^{-at} - K_2 e^{-bt} + K_3 e^{-ct} \sin(\omega_m t + \theta) \right\}$$

where

$$\omega_c = \omega_m / \sqrt{1-\zeta_m^2}$$

$$a = \omega_c / 2\pi$$

$$b = 2\zeta_m \omega_c$$

$$c = \zeta_m \omega_c$$

$$K_1 = \frac{\omega_m a^2}{(a-b)\left[(c-a)^2 + \omega_m^2\right]}$$

$$K_2 = \frac{\omega_m b^2}{(a-b)\left[(c-b)^2 + \omega_m^2\right]}$$

$$K_3 = \left\{ \frac{(c^2-\omega_m^2)^2 + 4c^2\omega_m^2}{\left[(b-c)^2 + \omega_m^2\right]\left[(a-c)^2 + \omega_m^2\right]} \right\}^{1/2}$$

$$\theta = \tan^{-1} \frac{-2c\omega_m}{c^2-\omega_m^2} - \tan^{-1} \frac{\omega_m}{a-c} - \tan^{-1} \frac{\omega_m}{(b-c)}$$

The first two terms are added for velocity and displacement compensation. The phase shift, θ, is added to force the initial value to zero.

A plot of a typical modified pulse is shown as Figure 7.

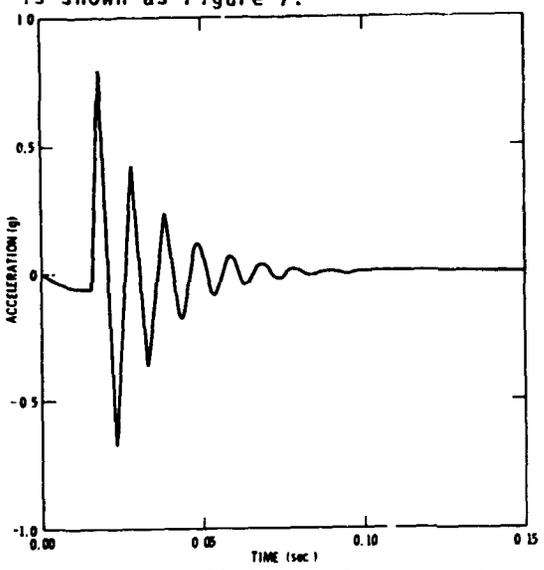

Fig. 6 - Modified Decaying Sinusoid

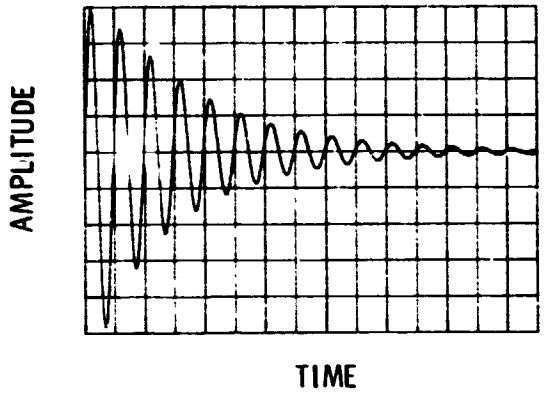

Fig. 7 - Modified Decaying Sinusoid

A set of curves can also be generated which gives the peak response ratios (the ratio of the peak response to the input amplitude at the frequency of highest response) as a function of the decay rate (ζ) of the decaying sinusoid and the damping factor (η) of the shock spectrum (Figure 8).

Example Using Decaying Sinusoids

Let us assume a test requires that a pulse be reproduced on an electro-hydraulic shaker system. The required shock spectrum is given in Figure 9. A typical field time history which resulted in the required composite shock spectrum is also included (Figure 10) for comparison purposes. The shaker limitations are: peak acceleration 50 g's o-p, peak velocity 120 in/sec o-p, and peak displacement 8 in p-p. The pulse will be composed of sums of decaying sinusoids compensated using the method suggested by the author.

The spectrum cannot be matched at the lowest frequency because the slope of the spectrum is less than 12 db/oct. In actual fact, a 16 ft/sec velocity change is associated with the spectrum. It will be assumed that the test item is not likely to have any resonances below 6 Hz or above 115 Hz and the spectrum will be matched from 4 Hz to 115 Hz. The first step is to assume all the decaying sinusoids will act independently. Using Figures 5 and 8 the amplitudes and decay rates for the components can be picked. A 4 Hz pulse is picked to raise the low end of the spectrum. A large decay rate is picked to keep the spectrum reasonably flat in this region. Further frequencies are picked at the peaks in the spectrum.

The initial estimates (Trial 0) are shown in Figure 11 and Table 2. From displacement considerations the compensating frequency is picked at 1 Hz with a decay rate of 1.0. The shock spectrum of the composite pulse is shown on Figure 12. The spectrum is low at 4 Hz due to the interaction of the 1 Hz pulse. The spectrum is also low from 4-12 Hz, high from 12-90 Hz, and low above 90 Hz. As expected the assumption of independence was only approximate. An iterative procedure is then used to modify the component amplitudes to match the spectrum at the frequencies of the decaying

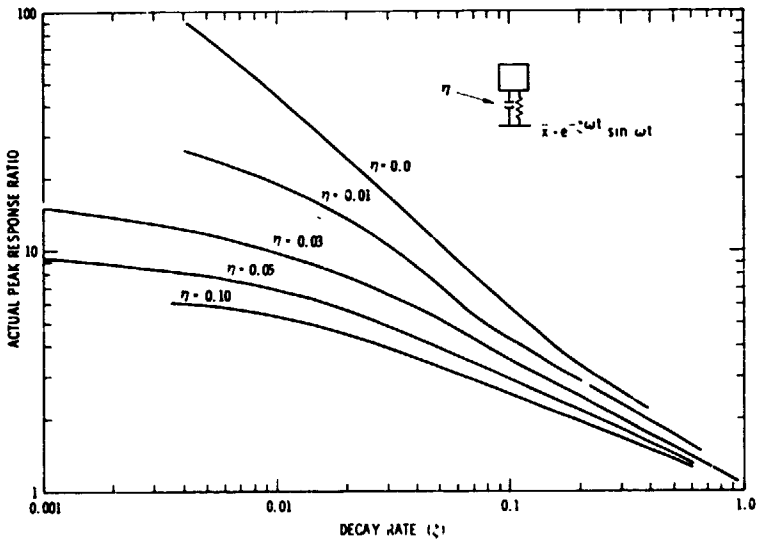

Fig. 8 - Peak Response Ratio for a Decaying Sinusoid

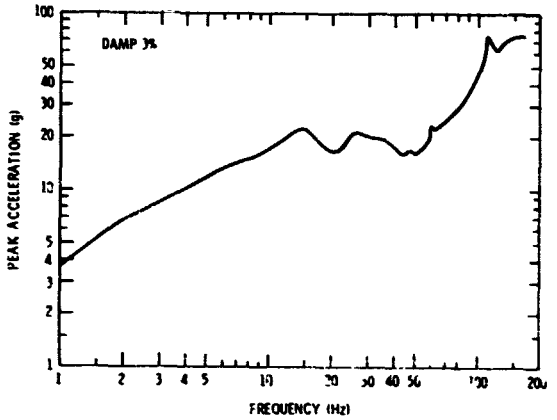

Fig. 9 - Example Specified Shock Spectrum

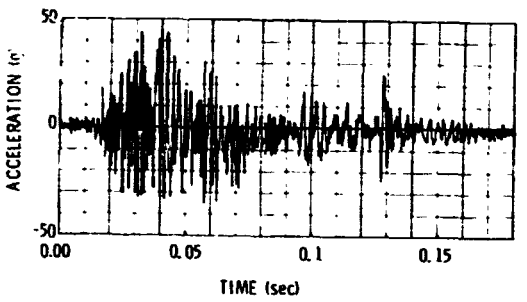

Fig. 10 - A Sample Time History

sinusoids. One possible iteration procedure is outlined in Figure 13. The results are shown in Figures 12 and Table 3 as Trial 1. Note that the solution does not converge; i.e., the amplitudes of the 36 and 47 Hz components were reduced to zero, but the spectrum was still too high. The high level is caused by the interaction of the lower frequency components. For the next trial (Trial 2), the decay rates of the 26 Hz, 36 Hz, 47 Hz, and 60 Hz components were lowered to reduce the interaction. Components at 8 Hz and 80 Hz were added to raise the level near those frequencies. The level of the shock spectrum at 112 Hz was also raised to improve the match at that frequency. Again an iteration procedure was used to determine the component amplitudes which would result in matching the required spectrum at the component frequencies. As before the amplitude of the 47 Hz component was reduced to zero. This time the spectrum was about 5% high at 47 Hz. The results are shown in Table 4 and Figure 12. At this point it was determined that the match was sufficient and the pulse parameters were within the shaker capabilities.

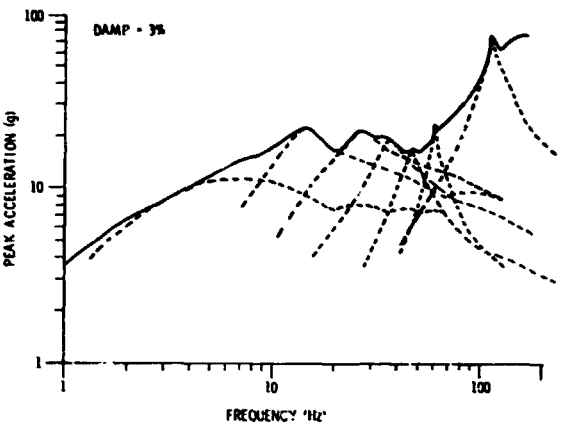

Fig. 11 - Composite Shock Spectrum Formed by Several Decaying Sinusoids

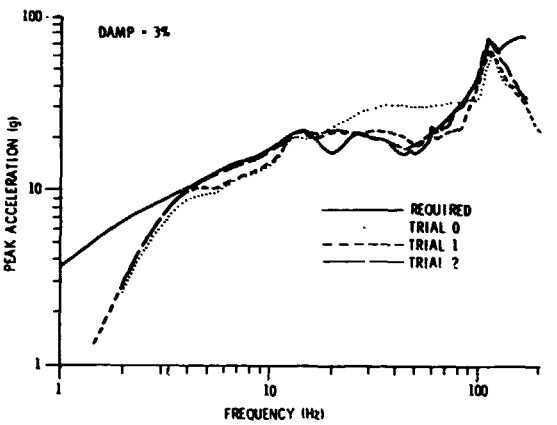

Fig. 12 - Shock Spectrum for Several Composite Waveforms Composed of Sums of Decaying Sinusoids

In this example an acceptable match was achieved in two iterations (Trial 0 is not counted, as it is usually skipped, but was included for illustrative purposes.) The time histories of the acceleration, velocity and displacement are included as Figures 14-16. The parameters in Table 4 can now be used to define a time history to be reproduced on the shaker system.

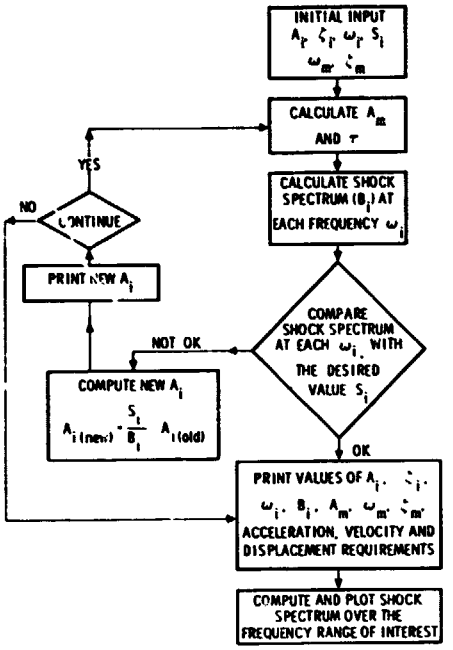

Fig. 13 - Flow Diagram for Picking Decaying Sinusoids to Match a Given Shock Spectrum

TABLE 2 - Parameters for Trial 0

I	FREQ (Hz)	ZETA	AMP (g)	TAU (sec)
1	1	1.0	-5.37	-0.141
2	4	0.5	7.1	0
3	14	0.2	8.8	0
4	26	0.2	8.8	0
5	36	0.1	5.7	0
6	47	.05	3.4	0
7	60	.01	2.3	0
8	112	.02	8.1	0

TABLE 3 - Parameters for Trial 1

I	FREQ (Hz)	ZETA	AMP (g)	TAU (sec)
1	1	1.0	-5.71	-0.138
2	4	0.5	8.67	0
3	14	0.2	10.1	0
4	26	0.2	8.52	0
5	36	0.1	0	0
6	47	.05	0	0
7	60	.01	2.22	0
8	112	.02	8.47	0

TABLE 4 - Parameters for Trial 2

I	FREQ (Hz)	ZETA	AMP (g)	TAU (sec)
1	1	1	-5.74	-0.141
2	4	0.5	6.47	0
3	8	0.3	4.45	0
4	14	0.2	11.1	0
5	26	.08	3.51	0
6	36	.05	0.646	0
7	47	.03	0	0
8	60	.005	1.78	0
9	80	.01	2.73	0
10	112	.02	9.93	0

Acceleration Range	+18.1, -9.0 g
Velocity Range	+63, -75 in/s
Displacement Range	+2.1, -4.9 in

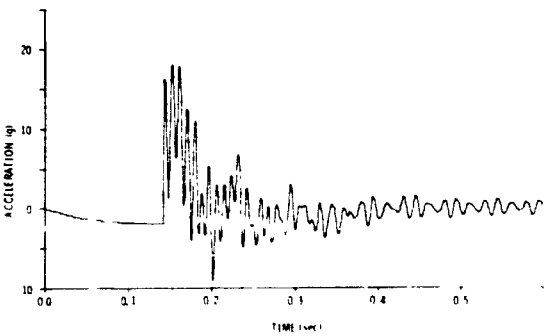

Fig. 14 - Acceleration of a Composite (Trial 2) Composed of a Sum of Decaying Sinusoids

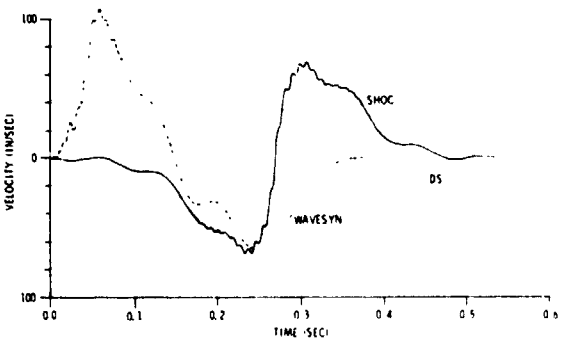

Fig. 15 - Velocity of Three Composite Waveforms

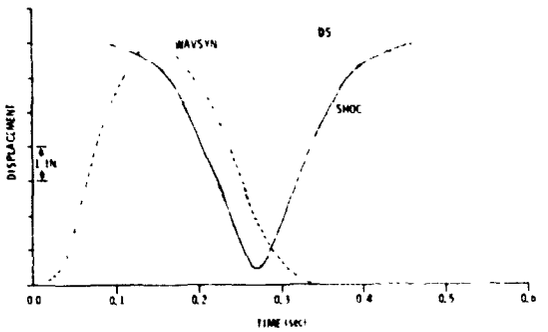

Fig. 16 - Displacement of Three Composite Waveforms

WAVSYN

A method developed for the U. S. Army is described by Yang. [6, 7] This method is called WAVSYN, The basic waveform is given by

$$g_m(t) = A_m \sin(2\pi b_m t)\sin(2\pi f_m t)$$

$$\text{for } 0 \le t \le T_m,$$

$$= 0 \qquad \text{for } t > T_m,$$

where $f_m = N_m b_m$,

$T_m = 1/(2b_m)$,

and N_m is an odd integer.

The waveform for $N_m = 5$ is shown as Figure 17.

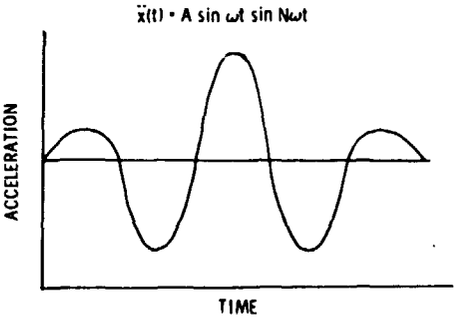

Fig. 17 - WAVSYN Time History, $N_m = 5$

A specified shock spectrum is then matched by summing several of the basic waveforms.

$$\ddot{x}(t) = \sum_{m=1}^{L} g_m(t + \tau_m).$$

The basic adjustable parameters are the number of pulses summed L, the frequencies f_m, the number of half cycles N_m, and the amplitudes of each component A_m.

The delay τ_m is used to improve the appearance of the time history (i.e., make the time history look more like field data) and does not seriously change the shock spectrum. Normalized shock spectra for N = 3, 5, 7, and 9 are shown in Figure 18. Note that the peak in the shock spectra occurs near f_m.

The shape or magnification can be modified by changing N_m. The frequency of the peak in the shock spectrum can be controlled with f_m and the magnitude of the whole curve can be moved up and down with A_m. Detailed procedures [6, 7] are described for matching a wide variety of shock spectra using the technique. An advantage of the technique is that the velocity and the displacement changes are zero. This is essential for accurate reproduction on a shaker system.

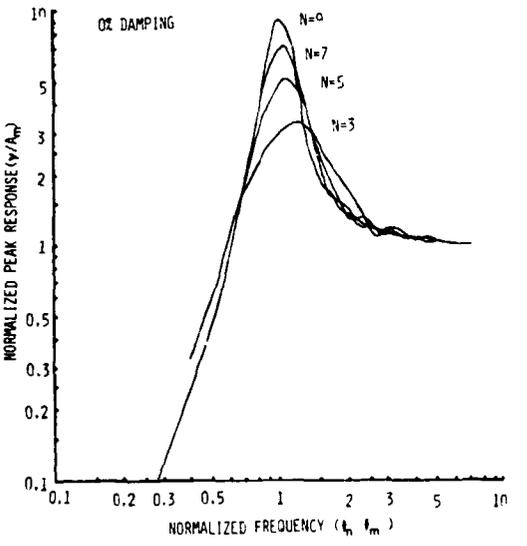

Fig. 18 - WAVSYN Shock Spectra

For comparison, the same shock spectrum as in the previous example was matched using WAVSYN. Eight components were used as listed in Table 5.

TABLE 5 - WAVSYN Components

No	f_m(Hz)	N_m	A_m(g)	τ_m
1	4	3	3.98	0
2	6	3	4.82	0
3	9	3	7.37	0
4	12.5	7	3.	0
5	27	5	4.3	0
6	33	7	0.94	0
7	70	11	2.44	0
8	112	19	8.86	0
Maximum Acceleration 20.9 g's				
Maximum Velocity 107 in/sec				
Maximum Displacement 7.10 in				

The acceleration, velocity, and displacement time histories are shown in Figures 19, 15, and 16. The shock spectrum is shown in Figure 20.

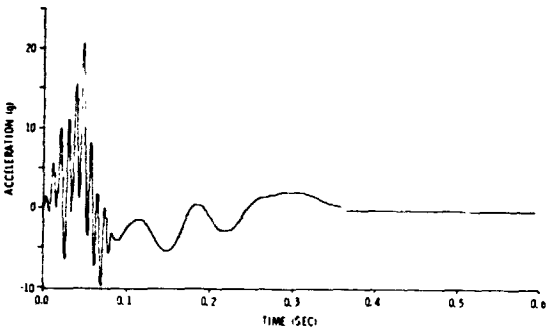

Fig. 19 - Acceleration Time History of WAVSYN Composite Pulse

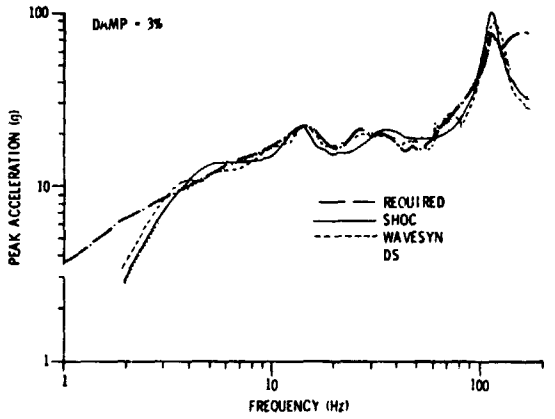

Fig. 20 - Shock Spectra Comparing Decaying Sinusoids, SHOC, and WAVSYN

SHOC

A method developed by the author [8] for matching shock spectra with an oscillating transient is called the SHOC (Shaker Optimized Cosines) technique. The basic waveform for this technique is given by

$$g_m(t) = A_m e^{-\zeta_m \omega_m t}\cos\omega_m t - B_m \cos^2 \frac{\pi t}{\tau} \qquad 0 \le t \le \tau/2$$

$$= 0 \qquad t > \tau/2$$

$$g_m(-t) = g_m(t),$$

$$\text{where } B_m = \frac{4A_m\zeta_m}{\tau\omega_m(\zeta_m^2+1)},$$

τ = the pulse duration

The first term is an exponential decaying cosine and the second term (a cosine bell) is added to force the velocity and the displacement changes to zero. The waveform is symmetric about the origin and builds up and then decays.

The basic waveform is illustrated as Figure 21. The normalized shock spectra for several values of ζ are shown as Figure 22. As in the case of WAVSYN, a parameter is available for modifying the shape of the curve (ζ_m), the frequency of the peak of the shock spectrum (ω_m) and the level of the curve (A_m).

As in the case of WAVSYN, several of these components are added to synthesize a waveform which will match a complex shock spectrum

$$\ddot{x}(t) = \sum_{m=1}^{L} g_m(t)$$

Also, as in WAVSYN, the velocity and the displacement changes are zero.

For comparison, the same shock spectrum as used in the two previous examples was matched using SHOC. Four components were used and are listed in Table 6.

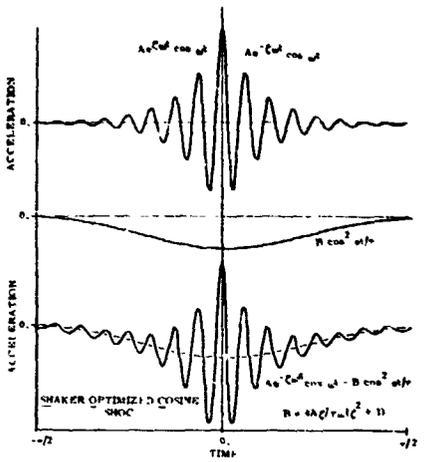

Fig. 21 - A SHOC Pulse

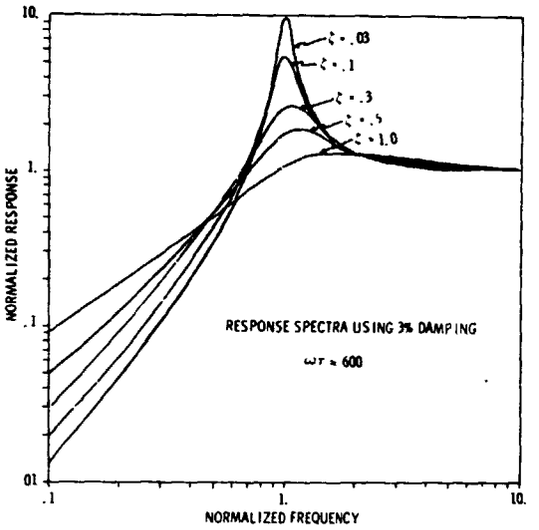

Fig. 22 - SHOC Shock Spectrum

TABLE 6 - SHOC Components

FREQ (Hz)	ζ	Amplitude	τ(sec)
4.0	1.0	10.0	0.54
13.0	0.1	2.5	
32.0	0.2	3.0	
112.0	.03	9.8	
Maximum Acceleration		23.7	
Maximum Velocity		69.5	in/sec
Maximum Displacement		6.5	in

The acceleration, velocity, and displacement time histories are shown in Figures 23, 15, and 16. The shock spectrum is shown in Figure 20. The three previous methods are also compared in Table 7.

Note that for this example the characteristics of all three pulses are quite similar, and the three methods would be expected to have a similar damage potential, although this has not been firmly established.

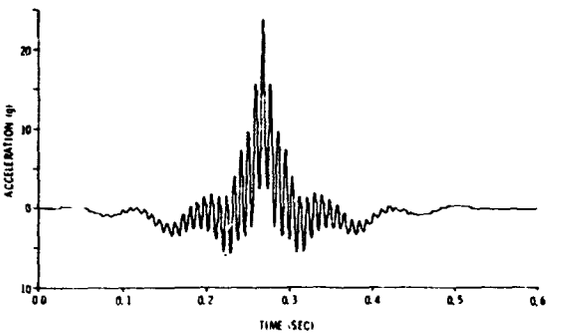

Fig. 23 - Acceleration of a Composite SHOC Pulse

Fast-Sine Sweeps

The first analytical procedure developed for matching shock spectra was a technique using fast-sine sweeps, which lasted from a few hundred milliseconds to several seconds. The early work in this area was done by Crum and Grant [9] and later expanded by several authors including Roundtree and Freberg [10]. The basic procedure is to assume an acceleration time history of the form

$$\ddot{x}(t) = A(t) \sin \theta(t)$$

A particular form is then chosen for for A(t) and θ(t) which includes a limited number of variable parameters. The derivative of θ(t) is the instantaneous frequency of the time history. Procedures are then given for picking the variable parameters to match the specified spectrum. Crum and Grant chose

$$A(t) = A \quad \text{(a constant)}$$

$$\theta(t) = -2\pi N' \ln\left(1 - \frac{f_o t}{N'}\right) \quad \text{increasing frequency}$$

$$\theta(t) = -2\pi N' \ln\left(1 + \frac{f_o t}{N'}\right) \quad \text{decreasing frequency}$$

TABLE 7 - Comparison of Decaying Sinusoids, WAVSYN, and SHOC

Method	Peak Input (G)	Duration(1) (ms)	RMS Duration(2) (ms)	Ratio of Peak Response to the Peak Input	Velocity Requirement (in/sec)	Displacement Requirement (in)
WAVSYN	21	300	71	4.3	110	7.1
SHOC	24	120	40	4.0	70	6.5
Sums of Decaying Sinusoids	19	210	88	4.7	70	6.9

(1) The duration is defined as the time beginning when the waveform first reaches 10-percent of its peak value and ending when it decays to 10-percent of its peak value for the last time.

(2) See Appendix A

where the variable parameters are the constant for A(t), the starting frequency f_o, and the effective number of cycles at each frequency N'. The effective number of cycles at each frequency (N') is based on the ratio of the shock spectra with a Q of 5 and 25, f_o was chosen as the lowest frequency of interest, and A was determined by the required amplitude of the shock spectrum. The form chosen by Roundtree and Freberg was a more general formulation given by

$$\frac{d\left(\ln A(t)\right)}{d\left(\ln f(t)\right)} = \beta, \quad A(0) = a, \quad f(0) = f_o,$$

$$\frac{df(t)}{dt} = Rf(t)^{\gamma},$$

$$\frac{d\theta(t)}{dt} = 2\pi f(t), \quad \theta(0)=0,$$

where the variable parameters are β, a, f_o, R, γ.

As mentioned earlier, the derivative of $\theta(t)$ is the instantaneous frequency f(t). β represents the rate of change of the amplitude function, A(t), with respect to the instantaneous frequency, f(t). The starting frequency is f_o. The initial value for the amplitude function A(t) is a. R and γ are used to control the rate of frequency change and the sweep duration. For example, if $\beta = 0$, the sweep amplitude is held constant, and if $\gamma = 0$, the sweep rate will be linear. The sweep will be exponential for $\gamma = 2$.

Roundtree and Freberg present graphs for picking values for the parameters based on the requested shock spectra computed at two different values of damping.

The methods of Crum and Grant have been used for several years. The methods of Roundtree and Freberg are too new to be well established. The advantage of these methods is that they produce pulses which are well suited for reproduction on shaker systems. It has also proved practical to match shock spectra at two different values of damping. The principle disadvantage is that the techniques produce pulses which do not resemble (in the time domain) many (if not most) field events. Another limitation is that the techniques have been highly developed for matching spectra which can be represented by a straight line on a log-log shock spectrum plot and adapt poorly for matching spectra with other shapes. A typical time history for these methods is shown in Figure 24.

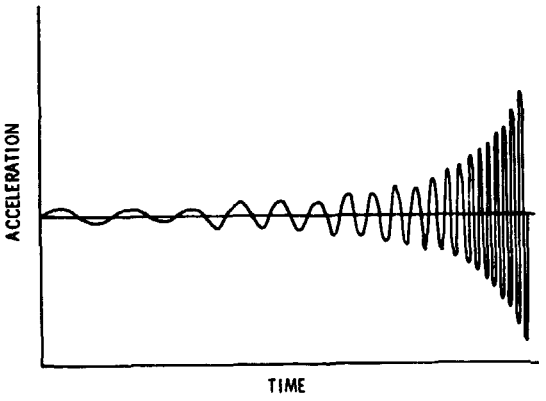

Fig. 24 - Time History of a Fast-Sine Sweep

Modulated Random Noise

Authors in the seismic field have long recognized the somewhat random nature of seismic records. As a result, numerous proposals [11, 12] have been made to derive a random process which, when multiplied by a suitable window, will provide an adequate simulation of seismic events. The attempt is to derive a waveform which will have the statistical characteristics of a seismic event. Since one of the tools used to characterize the seismic event is the shock spectrum of the event, the modulated random noise methods produce pulses which match a specified shock spectrum. However, it is important to recognize that these methods only match the shock spectrum in a probabilistic sense.

Bucciarelli and Askinaza [13] proposed that these same ideas could be used to simulate pyrotechnic shocks by using an exponential window.

$$\ddot{x}(t) = g(t)n(t)$$

where g(t) is a deterministic function of time which characterizes the transient nature of the event.

$$g(t) = \begin{cases} 0 & t<0 \\ e^{-\beta t} & t\geq 0 \end{cases}$$

The function n(t) is a representative of a stationary, broadband, zero-mean, noise process with a spectral density $S_n(\omega)$.

It is then proposed that the function $S_n(\omega)$ be chosen such that the average Fourier amplitude spectrum of $\ddot{x}(t)$ will be equal to the average Fourier amplitude spectrum of the field environment. It is shown that the following approximation will accomplish this purpose.

$$E[F(\omega)F^*(\omega)] \cong S_n(\omega)/2\beta$$

where

$$E[F(\omega)F^*(\omega)]$$

is the expected value of the field Fourier amplitude spectrum.

The above equations seem reasonable for the following reason. $S_n(\omega)$ is a stationary process with a fixed amount of energy per unit of time. As β becomes larger, the duration of the transient becomes shorter and $S_n(\omega)$ must be increased to maintain a given energy in the transient.

Tsai [14] then proposes that the random variation in the shock spectrum be removed in the following manner. Pick a sample $\ddot{x}(t)$. The shock spectrum of $\ddot{x}(t)$ is then computed. In areas where the shock spectrum is low, add energy to the waveform by adding sine waves to n(t). In areas where the shock spectrum is high, filter n(t) with a narrow-band notch filter. Compute the shock spectrum of the modified $\ddot{x}(t)$ and repeat the process until the desired shock spectrum is achieved. The final modified $\ddot{x}(t)$ will then be used as the test input. A procedure could probably be worked out to accomplish the same goal by modifying the Fourier amplitude of n(t) without resorting to adding sine waves and filtering [15,16].

This procedure looks quite interesting, but as far as the author knows, it has not been tried in the laboratory.

Modification of Field Time History

Workers in the seismic field have suggested a method very similar to the modulated random noise technique. For this method the original sample (x(t)) is an actual field time history (in the seismic field an earthquake record). The Fourier content of the waveform is then modified to force the shock spectrum of the time history to match a specified curve.

Classical Pulses

It may be desirable to reproduce a classical pulse (half-sine, terminal peak sawtooth, etc.) on a shaker system. In general these pulses are of Type 3 (Fig. 1) and cannot be reproduced without modification. The pulses can be easily corrected to a Type 5 pulse by adding a bias pulse of equal and opposite area at the end of the pulse. Pulses of this type can be reproduced with only the distortion introduced by the improper displacement boundary conditions. It is always possible to introduce a bias pulse which will also meet the displacement boundary conditions. For example, consider a terminal peak sawtooth pulse biased with a square wave as shown in Figure 25.

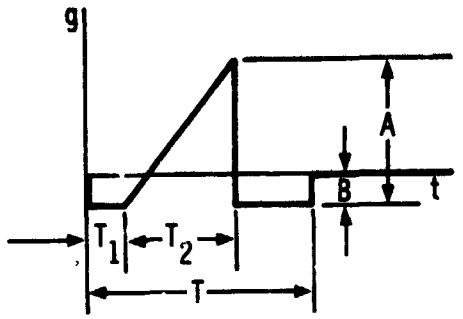

Fig. 25 - A Modified Terminal Peak Sawtooth

It is easy to see that the velocity change will be zero if

$$BT = 1/2\ A\ T_2.$$

If an expression is written for the acceleration of this waveform, and it is double integrated to solve for the displacement. The displacement boundary conditions can then be used to show that a zero displacement change can be achieved if

$$T_1 = \frac{T}{2} - \frac{2T_2}{3}$$

Thus two parameters are available (B, T_1) to control the velocity and displacement change of the composite waveform. A similar analysis can be done for other bias pulses and classical waveforms. If both the bias pulse and the classical waveform are symmetrical the solution is always to place the classical waveform in the center of the bias pulse.

A bias pulse which has been found to work quite satisfactorily is a cosine bell or Hanning pulse. The advantages of this bias pulse are: The waveform is zero and smooth at the ends, which usually improves the reproduction. The energy of the pulse is concentrated at the lower frequencies with a well-defined upper frequency and a sharp roll-off characteristic (18 dB/oct). This means that the effects of the bias pulse will be seen only at the lower frequencies. The frequency where the effects will start to be seen can be controlled with the duration of the bias pulse.

Least Favorable Response Techniques [17]

The basic assumption of the least favorable response techniques is that the magnitude of the Fourier spectrum has been specified. Since the undamped residual shock spectrum is related to the Fourier modulus, it could also be specified. It is then shown that if the frequency transfer function between the mechanical input and the response of a critical point on the test item (not the transfer function of the shaker system) can be characterized by

$$H(\omega) = |H(\omega)|\ e^{i\theta(\omega)},$$

then the peak response of the critical point on the structure will be maximized by the input

$$X(\omega) = X_e(\omega)e^{-i\theta(\omega)},$$

where $X_e(\omega)$ is the specified Fourier modulus, and

$$\ddot{x}(t) = \frac{1}{2\pi}\int_{-\infty}^{\infty} X(\omega)e^{i\omega t}\, d\omega.$$

where $\ddot{x}(t)$ is the required time history at the input to the test item.

The Fourier transform of the response of the critical point ($Y(\omega)$) is given by

$$Y(\omega) = X(\omega)H(\omega)$$

$$= X_e(\omega)\,|H(\omega)|.$$

The function $Y(\omega)$ is real. This response can be seen to produce a maximum response by thinking of a transient as being composed of a sum of many sinusoids. If the phase angle of all the sinusoids is zero at some point in time all the components will constructively add, and produce the largest possible peak. It is also shown in Appendix A that this response will have a minimum rms duration.

Modern methods make the computation of the above equations relatively easy. It is proposed that the phase angle (θ) of the frequency transfer function be measured in the laboratory. This function, together with the specified Fourier modulus ($X_e(\omega)$) is then used to compute the test input $\ddot{x}(t)$. Note that the above technique considers the actual test item response, while the shock spectrum approach considers only the response of single degree of freedom systems with known damping. The least favorable response method does assume a linear system with a well-defined critical response.

The method does guarantee that the largest possible peak response will be achieved (hence a guarantee of a conservative test). Shock spectrum techniques cannot make this guarantee for multiple degree of freedom systems. Several examples [17, 18] using the LFR method have indicated peak responses on the order of 1 to 2.5 times a typical peak response to a field event.

This method has been used on one known test series [18] and the results are compared with the shock spectrum methods. As the method requires considerable computations and the reproduction of a complicated computed waveform, digital methods are required for its application.

A spin-off, from the least favorable response techniques, is to assume a unity transfer function (i.e., $H(\omega) = 1$). This means that the peak input will be maximized. If we think of a transient as being a finite amount of energy with a specified frequency distribution (Fourier modulus), the procedure will produce a transient which will transfer this energy to the test item with the largest possible peak input and in a minimum amount of time.

The input to the test item is given by

$$\ddot{x}(t) = \frac{1}{2\pi}\int_{-\infty}^{\infty} X_e(\omega) e^{i\omega t}\, d\omega.$$

Note that $X_e(\omega)$ is a real positive function. Therefore, $x(t)$ will be a real even function. As a result, a typical input defined in this manner will look similar to a SHOC pulse. The resulting input is independent of the test item characteristics, and hence eliminates the need to define the transfer function $H(\omega)$. The only required parameter is the Fourier modulus (or the equivalent undamped residual shock spectrum). For example, the least favorable input with a unity transfer function for a transient with the same Fourier modulus as the transient shown in Figure 14 is given as Figure 26. The rms duration of this transient is 64 msec. One test series [18] indicates that this may be a reasonable approach.

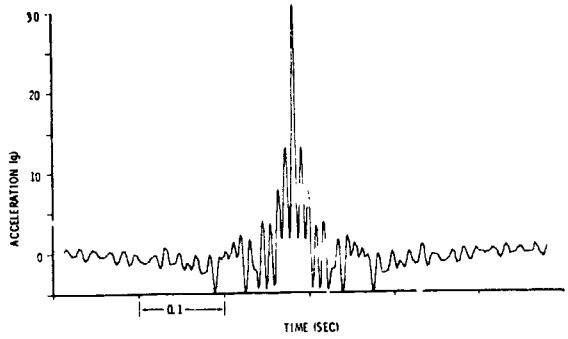

Fig. 26 - A Least Favorable Input with a Unity Transfer Function

ADDITIONAL PARAMETERS (IN ADDITION TO THE SHOCK SPECTRUM) WHICH MAY BE SPECIFIED

Since there are many methods for matching the shock spectrum, it would be desirable to specify additional parameters limiting the class of functions which may be used for a particular test. Several parameters have been suggested and a short discussion of several methods will follow.

Limit the Duration of the Transient

It has been suggested that limits could be placed on the minimum and maximum allowable durations for the transients. It is felt that if the shock spectrum is matched and the duration is comparable, the "damage" should be nearly the same. For complex waveforms, careful attention should be given as to how the duration is defined. The author is not aware of any test program where this specification has actually been used.

Require the Shock Spectrum at Two Different Values of Damping to be Matched

Since damping is the poorest known parameter in many systems, it is felt that if the shock spectrum is matched at two different values of damping (for example, a Q of 5 and 25) the resulting transient should be a reasonable simulation for all values of damping. However, it is a very difficult problem to find a transient which will match a shock spectrum at two values of damping except for a limited class of functions. In fact it is not even clear that a solution always exists. It is true that a solution can exist, for example, a set of shock spectra with different damping values for a known time history. But if those spectra are modified (for example, smoothed, raised in level, or enveloped), it is not clear that a solution will still exist.

Specify the Allowable Ratios of the Peak Shock Response and the Peak Input Level

The attempt is to prevent or encourage the use of oscillatory-type input as opposed to a single-pulse (for example, a half-sine) input. Note that, if the shock spectrum is plotted at a high enough frequency, the maximax shock spectrum reflects the peak input level and this specification is redundant.

This specification would be useful to confirm the value of the maximax spectrum at very high frequencies. TRW has included this requirement in a recent specification which required that the amplification of the response spectrum over the peak-g input would be in the range of 2.5 to 5. This requirement was added to prevent a single pulse or a very long transient from being used.

Specifically Exclude Certain Methods

If the test requester is aware that certain methods are not likely to produce a good simulation, a very effective measure is to simply exclude their use. The limit of this procedure is to exclude all the methods but one. In fact, a knowledgeable requester can specify not only the method, but the parameters needed to define the transient. For example, if decaying sinusoids are specified, then the component frequencies, decay rates, and amplitudes can be listed. In essence, the specification will require a certain time history be used. It should be remembered that if this is done, only those testing laboratories which have implemented the particular method can perform the test. Thought must also be given to requirements for a successful test. One is tempted to place requirements on the fidelity of the time history reproduction. However, most available techniques for reproducing a time history assume a linear system. If the test item is non-linear, the reproduction of a given time history may be poor through no fault of the testing laboratory.

CONCLUSIONS

It is apparent from the preceding discussion that a large variety of methods are now available for matching a shock spectrum on a shaker system. These methods can produce quite different waveforms, and it is not clear that they will all produce equivalent results. It is important that a shock spectrum not be considered as a sufficient specification to define an environment. The "characteristics" of the field waveform should be considered. The personnel who write test specifications must be aware that several procedures could be used to match a specified shock spectrum, and careful consideration should be given as to which procedure will (or will not) produce an acceptable test.

Nomenclature

A - amplitude

a - constant

B - a constant

b - constant, also a frequency

c - constant

E - expected value

f - frequency

g - a basic waveform from which a composite is formed, also an exponential window

i - $\sqrt{-1}$

K - constant

L - the number of basic waveforms which have been added to form a composite waveform

M - slope on a log-log plot in dB/octave

N - number of half cycles, an odd integer

N' - an effective number of cycles at each frequency in a fast sine sweep

Q - quality factor, $\frac{1}{2\zeta}$

R - a constant

S - nondimensional slope on a log-log plot, also auto (power) spectral density

T - a pulse duration

t - time

U - a unit step function

X - Fourier transform of $\ddot{x}$

X_e - a specified Fourier modulus

$\ddot{x}$ - acceleration

$\dot{x}$ - velocity

x - displacement

β - a constant

Γ - a constant

ζ - a decay rate

η - damping coefficient for a shock response spectrum

θ - phase angle

τ - a time delay or shift

ω - circular frequency

Subscripts

c - a velocity and displacement compensating pulse

i - an index

m - an index

Superscripts

$\bullet$ - complex conjugate

REFERENCES

1. G. W. Painter and H. J. Perry, "Simulating Flight Environment Shock on an Electrodynamic Shaker," Shock and Vibration Bulletin, No. 33, Part 3, March 1964, pp. 85-96.

2. J. J. Favour, J. D. LeBrun, and J. P. Young, "Transient Waveform Control of Electromagnetic Test Equipment," Shock and Vibration Bulletin, No. 40, 1969.

3. D. O. Smallwood and A. R. Nord, "Matching Shock Spectra with Sums of Decaying Sinusoids Compensated for Shaker Velocity and Displacement Limitations," Shock and Vibration Bulletin, No. 44, Part 3, pp. 43-56, 1974.

4. D. B. Nelson and P. H. Prasthofer, "A case for Damped Oscillatory Excitation as a Natural Pyrotechnic Shock Simulation," Shock and Vibration Bulletin No. 44, Part 3, pp. 57-71, 1974.

5. J. Carden, T. K. DeClue, and P. A. Koen, "A Vibro-Shock Test System for Testing Large Equipment Items," 44th Shock and Vibration Bulletin, Supplement 1, August 1974, pp. 1-26.

6. R. C. Yang, "Safeguard BMD System - Development of a Waveform Synthesis Technique," Document No. SAF-64, The Ralph M. Parsons Company, 28 August, 1970.

7. R. C. Yang and H. R. Saffell Development of a Waveform Synthesis Technique - A Supplement to Response Spectrum as a Definition of Shock Environment," Shock and Vibration Bulletin, No. 42, Part 2, January 1972, pp. 45-53.

8. D. O. Smallwood and A. F. Witte, "The Use of Shaker-Optimized Periodic Transients in Matching Field Shock Spectra," Shock and Vibration Bulletin, No. 43, Part 1, pp. 139-150.

9. J. D. Crum and R. L. Grant, "Transient Pulse Development," Shock and Vibration Bulletin, No. 41, Part 5, December 1970, pp. 167-176.

10. R. C. Rountree and C. R. Freberg, "Identification of an Optimum Set of Transient Sweep Parameters for Generating Specified Shock Spectra," Shock and Vibration Bulletin, No. 44, Part 3, 1974, pp. 177-192.

11. R. Levy, F. Kozin, and R. B. B. Moorman, "Random Processes for Earthquake Simulation," Journal of the Engineering Mechanics Division, Proceedings of the American Society of Civil Engineers, April 1971, pp. 495-517.

12. R. L. Barnoski and J. R. Maurer, "Transient Characteristics of Single Systems of Modulated Random Noise," Journal of Applied Mechanics, March 1973, pp. 73-77.

13. L. L. Bucciarelli and J. Askinazi, "Pyrotechnic Shock Synthesis Using Nonstationary Broad Band Noise," Journal of Applied Mechanics, June 1973, pp. 429-432.

14. Nien-Chien Tsai, "Spectrum-Compatible Motions for Design Purposes," Journal of the Engineering Mechanics Division, Proceedings of the American Society of Civil Engineers, April 1972, pp. 345-356.

15. D. O. Smallwood, " Methods Used to Match Shock Spectra Using Oscillatory Transients," Institute of Environmental Sciences, 1974 Proceedings, pp. 409-420.

16. R. H. Scanlan and K. Sachs, "Earthquake Time Histories and Response Spectra," Journal of the Engineering Mechanics Division, Proceedings of the American Society of Civil Engineers, Volume 100, No. EM4, August 1974, pp. 635-655.

17. D. O. Smallwood, "A Transient Vibration Test Technique Using Least Favorable Responses," Shock and Vibration Bulletin No. 43, Part 1, pp. 151-164.

18. A. F. Witte and D. O. Smallwood, "A comparison of Shock Spectra and the Least Favorable Response Techniques in a Transient Vibration Test Program," Institute of Environmental Sciences, 1974 Proceedings, pp. 16-29.

19. A. Papoulis, The Fourier Integral and Its Applications, McGraw-Hill, 1962, p. 62.

APPENDIX A
RMS Duration of a Transient

A transient f(t) is defined with a Fourier transform F(ω). The rms duration (D) of the transient is defined as,

$$D^2 = \frac{1}{E}\int_{-\infty}^{\infty} t^2 |f(t)|^2 dt \qquad (A\text{-}1)$$

where

$$E = \int_{-\infty}^{\infty} |f(t)|^2 dt. \qquad (A\text{-}2)$$

E is sometimes referred to as the energy of the pulse. It will be required that E is finite, requiring that f(t) approach zero faster than $1/t^2$, as t approaches both positive and negative infinites. In a general sense, the rms duration of a transient will be a function of the time origin chosen. To avoid this difficultly, it is requried that the time origin be chosen in such a manner as to minimize the rms duration. If some other origin is chosen a time shift (T) can be introduced which will minimize the rms duration,

$$T = \frac{1}{E}\int_{-\infty}^{\infty} t|f(t)|^2 dt. \qquad (A\text{-}3)$$

The rms duration is a measure of the central tendency of a transient. For example, consider a transient of some finite energy composed of all frequencies in equal amounts. An impulse (or delta function) will represent the transient in this class with a minimum duration. A long-duration, low-level random waveform will represent the transient with a maximum duration. The rms duration of several common transients is given in Table A-1.

It can be shown [19] that the rms duration is also given by,

$$D^2 = \frac{1}{2\pi E}\int_{-\infty}^{\infty}\left[\left(\frac{dA}{d\omega}\right)^2 + A^2\left(\frac{d\phi}{d\omega}\right)^2\right]d\omega \qquad (A\text{-}4)$$

where

$$F(\omega) = A(\omega)e^{i\phi(\omega)}.$$

If $A(\omega)$ is specified the minimum rms duration is given by

$$\frac{d\phi}{d\omega} = 0$$

or

$$\phi(\omega) = \text{constant}$$

The constant can be zero. Eq. A-4 implies that the rms duration is related to the smoothness of the Fourier spectrum, both the magnitude and the phase. The smoother the Fourier spectrum, the shorter the rms duration.

TABLE A-

The rms Duration of Some Common Transients

Function	Equation		rms Duration
Square Wave	$f(t) = 1$	$0<t<T$	0.29 T
	$= 0$	elsewhere	
half sine	$f(t) = \sin\frac{\pi t}{T}$	$0<t<T$	0.23 T
	$= 0$	elsewhere	
terminal peak sawtooth	$f(t) = t/T$	$0<t<T$	0.19 T
	$= 0$	elsewhere	
triangle	$f(t) = 1 - 2\lvert t\rvert/T$	$-\frac{T}{2}<t<\frac{T}{2}$	0.16 T
	$= 0$	elsewhere	
haversine	$f(t) = \frac{1}{2}\left(1 + \cos\frac{2\pi t}{T}\right)$	$0<t<T$	0.13 T
	$= 0$	elsewhere	
parabolic cusp	$f(t) = \left(\frac{2}{T}\lvert t\rvert - 1\right)^2$	$-\frac{T}{2}<t<\frac{T}{2}$	0.11 T
	$= 0$	elsewhere	
exponential single side	$f(t) = e^{-at}$	$t>0$	$\frac{1}{2a}$
	$= 0$	$t<0$	
exponential	$f(t) = e^{-a\lvert t\rvert}$		$\frac{1}{\sqrt{2}a}$
exponential decaying sinusoid	$f(t) = e^{-a\omega t}\sin\omega t$	$t>0$	$\frac{1}{2a\omega}$
	$= 0$	$t<0$	
	for $a<<1$		

MODAL ANALYSIS USING DIGITAL TEST SYSTEMS

Mark Richardson
Hewlett Packard Company
Santa Clara, California

Modal Analysis methods based upon the measurement and post test processing of transfer functions in digital form are discussed. The analysis which shows how modal data can be identified from transfer function measurements is reviewed. Then various techniques of transfer function measurement using a Fourier analyzer are presented. This is followed by a discussion of alternative methods for identifying modal data from transfer function measurements.

I. INTRODUCTION

An analog tracking filter can be viewed as a device which gives the spectral content of a time domain signal, one frequency at a time. By comparison, the digital Fourier transform can be viewed as a parallel processor which gives the entire frequency spectrum of a time signal in a selected bandwidth.

Since the digital Fourier Analyzer provides a broad band frequency spectrum very quickly (e.g. = 100 ms to give 512 spectral lines), it can be used for obtaining broad band response spectrums from a structure which is excited by a broad band input signal.

Furthermore, if the input and response time signals are measured simultaneously, Fourier transformed, and the transform of the response is divided by the transform of the input, a transfer function between the input and response points on the structure is measured. (Division of one frequency domain function by another is straightforward when the data is in digital form.) Hence, a digital Fourier Analyzer which can simultaneously measure two (or more) signals is an ideal tool for measuring transfer functions quickly and accurately. Furthermore, since the modes of vibration of an elastic structure can be identified from transfer function measurements, a multichannel Fourier Analyzer with additional processing capability can also be used for identifying modal parameters from test data.

Modal Analysis is the process of characterizing the dynamic properties of an elastic structure by identifying its modes of vibration. A mode of vibration is a global property of an elastic structure. That is, a mode has a specific natural frequency and damping factor which can be identified from response data at practically any point on a structure, and it has a characteristic "mode shape" which identifies the mode spatially over the entire structure.

Modal testing is performed on mechanical structures in an effort to learn more about their elastic behavior. Once the dynamic properties of a structure are known its behavior can be predicted, and therefore controlled or corrected.

Resonant frequencies, damping factors and mode shape data can be used directly by a mechanical designer to pinpoint weak spots in a structure design, or this data can also be used to confirm or synthesize equations of motion for the elastic structure. These differential equations can be used to simulate structural response to known input forces and to examine the effects of perturbations in the distributed mass, stiffness, and damping properties of the structure in more detail.

In this paper the measurement of transfer functions in digital form, and then the application of digital parameter identification techniques to identify modal parameters from the measured transfer function data are discussed. It is first shown that the transfer matrix, which is a complete dynamic model of an elastic structure can be written in terms of the structure's modes of

vibration. This special mathematical form allows one to identify the complete dynamics of the structure from a much reduced set of test data, and is the essence of the modal approach to identifying the dynamics of a structure.

Next, various considerations which apply to broad band testing using a Fourier Analyzer are discussed. Ways in which spectral resolution, measurement noise, and multipoint excitation can be handled with a digital machine are also discussed.

Finally, the application of transfer function models and identification techniques for obtaining modal parameters from the transfer function data are discussed. Several alternative single degree-of-freedom and multi-degree-of-freedom methods are covered.

The results presented in this paper are not intended to be a survey of digital modal testing, but rather a summary of experience gained at Hewlett Packard in the development of an all-digital modal analysis test system.

II. THE STRUCTURE DYNAMIC MODEL

In the majority of present day modal analysis practice, the motion of the physical system is assumed to be adequately described by a set of simultaneous second-order linear differential equations of the form

$$M\ddot{x}(t) + C\dot{x}(t) + Kx(t) = f(t) \qquad (1)$$

where

$f(t)$ = applied force vector
$x(t)$ = resulting displacement vector
$\dot{x}(t)$ = resulting velocity vector
$\ddot{x}(t)$ = resulting acceleration vector

and M, C, and K are called the mass, damping, and stiffness matrices. If the system has n-dimensions (n - degrees-of-freedom) then the above vectors are n-dimensional and the matrices are (n×n).

For a two dimensional system, two differential equations of motion would be written:

$$\begin{bmatrix} m_{11} & m_{12} \\ m_{21} & m_{22} \end{bmatrix} \begin{bmatrix} \ddot{x}_1(t) \\ \ddot{x}_2(t) \end{bmatrix} + \begin{bmatrix} c_{11} & c_{12} \\ c_{21} & c_{22} \end{bmatrix} \begin{bmatrix} \dot{x}_1(t) \\ \dot{x}_2(t) \end{bmatrix} +$$

$$\begin{bmatrix} k_{11} & k_{12} \\ k_{21} & k_{22} \end{bmatrix} \begin{bmatrix} x_1(t) \\ x_2(t) \end{bmatrix} = \begin{bmatrix} f_1(t) \\ f_2(t) \end{bmatrix} \qquad (2)$$

or performing the indicated matrix multiplication:

$$m_{11}\ddot{x}_1(t) + m_{12}\ddot{x}_2(t) + c_{11}\dot{x}_1(t) +$$
$$c_{12}\dot{x}_2(t) + k_{11}x_1(t) + k_{12}x_2(t) = f_1(t)$$

$$m_{21}\ddot{x}_1(t) + m_{22}\ddot{x}_2(t) + c_{21}\dot{x}_1(t) + c_{22}\dot{x}_2(t)$$
$$k_{21}x_1(t) + k_{22}x_2(t) = f_2(t) \qquad (3)$$

Each equation is a statement of Newton's second law which balances inertia, damping and restoring forces against each of the applied input forces. The mass, stiffness and damping matrices contain the necessary mass, stiffness and damping coefficients so that the equations of motion yield the correct responses when input forces are applied.

The mass, stiffness and damping matrices are usually assumed to be real valued and symmetric.

A considerable amount of modal analysis practice has developed around the so called normal mode testing. In the theory of normal modes, it is assumed that the damping matrix is either proportional to the mass and stiffness matrices (proportional damping), or can be replaced by a complex valued stiffness matrix (structural damping), or doesn't exist at all. It has been shown recently, (refs. 1 and 2) that without these assumptions a meaningful transformation of equation (1) to modal coordinates is possible using conjugate pairs of complex modal vectors. Furthermore, a generalized modal transformation of equation (1) has recently been developed (ref. (3)) which does not require the mass, stiffness and damping matrices to be real valued or symmetric.

In the approach to modal testing presented here, modal parameters are identified from transfer function measurements. Therefore, it is convenient to write equations (1) in their equivalent transfer function form.

Taking the Laplace transform of the system equations gives:

$$B(s)X(s) = F(s) \qquad (4)$$

where

$F(s)$ = Laplace transform of applied force vector
$X(s)$ = Laplace transform of resulting displacement vector
$B(s) = Ms^2 + Cs + K$
s = Laplace variable (a complex number)

$B(s)$ is referred to as the system matrix. The transfer matrix $H(s)$ is defined as the inverse of the system matrix, that is:

$$H(s) = B(s)^{-1} \qquad (5)$$

Hence, $H(s)$ satisfies the following equation:

$$X(s) = H(s)\,F(s) \qquad (6)$$

which is equivalent to equation (4).

Each element of the transfer matrix is a transfer function. For an n-dimensional system, H(s) is an nxn matrix, which can be written:

$$H(s) = \begin{bmatrix} h_{11}(s) & \cdots & h_{1n}(s) \\ \vdots & & \vdots \\ h_{ij}(s) & & \\ \vdots & & \vdots \\ h_{n1}(s) & \cdots & h_{nn}(s) \end{bmatrix} \quad (7)$$

where $h_{ij}(s)$ is the transfer function in the $i^{\underline{th}}$ row and $j^{\underline{th}}$ column of the transfer matrix. Note that transfer functions are defined in terms of the Laplace variable s. The transfer function is a complex valued function, i.e. it has a real and imaginary part. Figure 1 shows the real part of a typical transfer function plotted as a function of the s-variable.

Note that the Fourier transform gives the value of the transfer function along the imaginary axis in the s-plane, referred to as the <u>frequency</u> axis. The transfer function evaluated along the frequency axis is also referred to as the <u>frequency response function</u>. The real axis in the s-plane is referred to as the <u>damping</u> axis. The reason for this will be made clear later on.

It will be shown in the next section that it is possible from measured frequency response functions to identify all the parameters necessary to completely specify the matrix of transfer functions H(s), for an elastic structure. The transfer matrix contains all the information necessary to completely specify the dynamics of the structure and it has been shown that the mass, stiffness and damping matrices can be recovered once the transfer matrix H(s) is known.

III. MODES OF VIBRATION

In this section, modes of vibration are defined in mathemetical terms and it is shown that the transfer matrix can be written in terms of modal frequency, damping and modal vectors. This special mathematical form is the key to modal testing using transfer functions and has implications both in the measurement and post test analysis portions of this approach.

Recall that the elements of the system matrix B(s) are quadratic functions of the Laplace variable (s). And, since the transfer matrix H(s) is defined as the inverse of the system matrix, it follows that the elements of H(s) are ratios of polynomials in s, with the determinant of B(s) in each denominator.

That is the ij^{th} element of H(s) can be written:

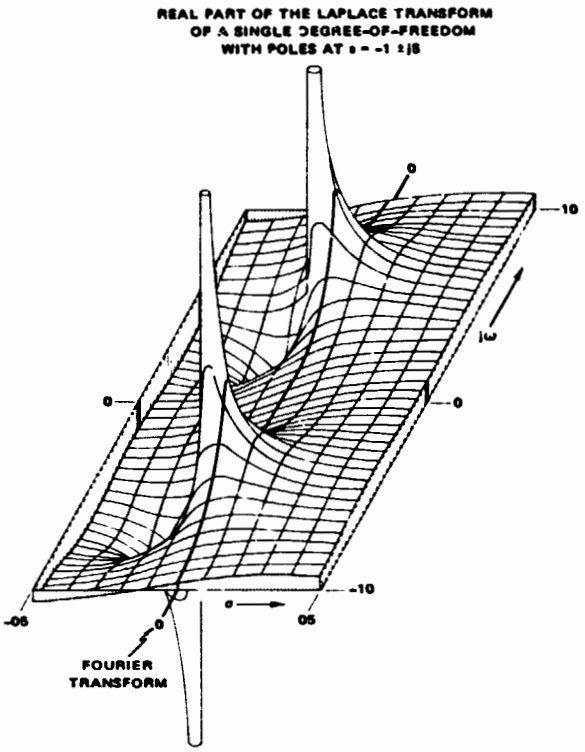

Figure 1. Real Part of a Transfer Function

$$h_{ij}(s) = \frac{b_1 s^{2n-2} + b_2 s^{2n-1} + \ldots + b_{2n-1} s + b_{2n-2}}{\det (B(s))} \quad (8)$$

where the b's are polynomial coefficients. If the system is n-dimensional then det (B(s)) is always a polynomial of order 2n, which has 2n roots, i.e. values of s for which det (B(s)) = 0.

If the roots of det (B(s)) are assumed to be <u>distinct</u>, then H(s) can always be written in the partial fraction form:

$$H(s) = \sum_{k=1}^{2n} \frac{a_k}{s - p_k} \quad (9)$$

where

p_k = k^{th} root of det (B(s)) = 0

a_k = residue matrix for the k^{th} root. (nxn for an n-dimensional system)

The roots p_k are referred to as <u>poles</u> of the transfer function. When the system is

subcritically damped, the poles are complex numbers and occur in complex conjugate pairs. Figure 1 shows a pair of complex conjugate poles locations at s = -1 ± j5 Hertz. When the structure is critically or supercritically damped, the poles are real valued and lie along the real axis in the s-plane.

At the locations ($s=p_k$) it is clear from expression (9) that the transfer function value goes to infinity, i.e. its denominator goes to zero.

In physical terms, this is where the structure is said to resonate or become resonant. Refer to Figure 1 again. For the example plotted there, when the structure is subjected to an input frequency of 5 Hertz, it will resonate because a pole is located at s = -1 + j5 Hertz. And the lighter the damping is, i.e. the closer the pole is to the frequency axis, the more the structure will resonate after external forces are removed. In the extreme case where the poles are located right on the frequency axis the structure would resonate forever when excited by an external force.

Each complex conjugate pair of poles corresponds to a mode of vibration in the structure. They are complex numbers, written as

$$p_k = -\sigma_k + i\omega_k \ , \ p_k^* = -\sigma_k - i\omega_k \qquad (10)$$

where * denotes the conjugate, σ_k is the modal damping coefficient, (assumed to be positive in value) and ω_k is the natural frequency. These parameters, which are the coordinates of the poles in the s-plane are shown in Figure 2.

An alternative set of coordinates can also be defined for describing the pole locations. The resonant frequency is given by:

$$\Omega_k = \sqrt{\sigma_k^2 + \omega_k^2} \qquad (11)$$

and the damping factor or percent of critical damping is given by:

$$\zeta_k = \frac{\sigma_k}{\Omega_k} \qquad (12)$$

When $\zeta_k = 1$, mode (k) is critically damped; and when $\zeta_k < 1$, mode (k) is subcritically damped.

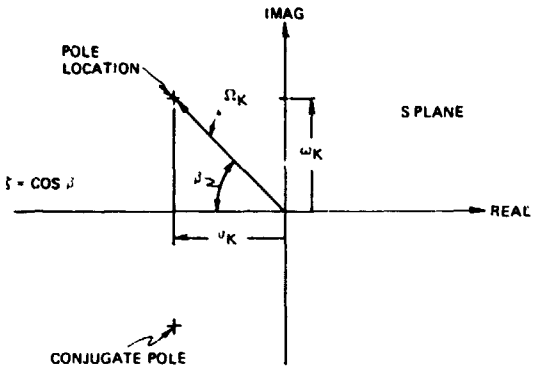

Figure 2. Poles of a Mode (k)

Modal vectors (u_k) are defined as solutions to the homogeneous equation

$$B(p_k)\ u_k = 0 \qquad (13)$$

u_k = n-dimensional complex vector.

It has been shown (ref. 2) that when they are defined in this way, the transfer matrix can be written in the form:

$$H(s) = \sum_{k=1}^{2n} \frac{A_k u_k u_k^t}{s-p_k} \qquad (14)$$

where the superscript t denotes the transpose and A_k is a scaling constant. In other words, the modal residue matrix a_k for mode (k) can be written in terms of the modal vector u_k as

$$a_k = A_k u_k u_k^t \qquad (15)$$

Furthermore, it is shown in ref.(2) that the transfer matrix can be written as a summation of (n) conjugate pairs:

$$H(s) = \sum_{k=1}^{n} \left[\frac{u_k u_k^t}{s-p_k} + \frac{u_k^* u_k^{*t}}{s-p_k^*} \right] \qquad (16)$$

where u_k^* is the conjugate of u_k and p_k^* is the conjugate of p_k. ($A_k = 1$ without loss

of generality.) Each of the terms in the summation in expression (16) is an nxn matrix which represents the contribution of each mode (k) to the transfer matrix.

For a 2-dimensional system, there can only be two modes of vibration. Therefore, there are two sets of complex conjugate pairs of modal vectors and poles, i.e.

$$p_1,\ u_1 = \begin{bmatrix} u_{11} \\ \\ u_{21} \end{bmatrix};\ p_1^*,\ u_1^* = \begin{bmatrix} u_{11}^* \\ \\ u_{21}^* \end{bmatrix}$$

$$p_2,\ u_2 = \begin{bmatrix} u_{12} \\ \\ u_{22} \end{bmatrix};\ p_2^*,\ u_2^* = \begin{bmatrix} u_{12}^* \\ \\ u_{22}^* \end{bmatrix} \qquad (17)$$

and the transfer matrix is written as the sum of submatrices

$$H(s) = \begin{bmatrix} \frac{u_{11}u_{11}}{s-p_1} & \frac{u_{11}u_{21}}{s-p_1} \\ \frac{u_{21}u_{11}}{s-p_1} & \frac{u_{21}u_{21}}{s-p_1} \end{bmatrix} + \begin{bmatrix} \frac{u_{11}^*u_{11}^*}{s-p_1^*} & \frac{u_{11}^*u_{21}^*}{s-p_1^*} \\ \frac{u_{21}^*u_{11}^*}{s-p_1^*} & \frac{u_{21}^*u_{21}^*}{s-p_1^*} \end{bmatrix} + \begin{bmatrix} \frac{u_{12}u_{12}}{s-p_2} & \frac{u_{12}u_{22}}{s-p_2} \\ \frac{u_{22}u_{12}}{s-p_2} & \frac{u_{22}u_{22}}{s-p_2} \end{bmatrix} + \begin{bmatrix} \frac{u_{12}^*u_{12}^*}{s-p_2^*} & \frac{u_{12}^*u_{22}^*}{s-p_2^*} \\ \frac{u_{22}^*u_{12}^*}{s-p_2^*} & \frac{u_{22}^*u_{22}^*}{s-p_2^*} \end{bmatrix} \qquad (18)$$

It is important to note that each row and column of the numerators in the above matrices contains the same modal vector, multiplied by a component of itself. In other words, the modal vectors and pole locations can be identified from <u>any</u> row or column of the transfer matrix except those corresponding to components of a modal vector which are zero, known as <u>node points</u>. This leads to perhaps the most significant premise of modal testing using this approach.

Only <u>one</u> row or column of the transfer matrix needs to be measured in order to identify all the modal parameters of a structure provided the following assumptions are met

1. The motion is linear, described by the linear second - order equations.
2. The symmetry of motion or reciprocity property is valid (i.e., B and H matrices are symmetric).
3. No more than one mode exists at each pole location of the system transfer matrix.

In practice, the pole locations p_k and one row or column of the residue matrix a_k are actually identified from one row or column of measured transfer function data. Suppose that the q^{th} row or column of the tranfer matrix was measured. Then the q^{th} row or column of a_k, call it r_{qk}, would be identified from the data. It is straightforward to show that the entire residue matrix can be constructed from the identified q^{th} row or column using the formula

$$a_k = \frac{r_{qk} r_{qk}^t}{r_{qqk}} \qquad (19)$$

where r_{qqk} is the q^{th} component of the residue vector. If a single exciter is used to measure the q^{th} column of the transfer matrix, then r_{qqk} is the residue at the <u>driving point</u>.

COMPLEX MODE SHAPE

The structural model used in the foregoing development required that the damping matrix be symmetric and real valued. Without further restrictions on damping, such as the proportional damping assumption, the mode vectors can in general be complex valued.

When the mode vectors are real valued, then they are the equivalent of the <u>mode shape</u>, i.e. the observed spatial motion of the mode. In the case of complex mode vectors, the interpretation of the mode shape is slightly different. Recall that the transfer matrix for a single mode (k) can be written

$$H_k(s) = \frac{a_k}{s-p_k} + \frac{a_k^*}{s-p_k^*} \qquad (20)$$

where a_k = (nxn) complex residue matrix.

p_k = pole location of mode (k).

A component of $H_k(s)$ can therefore be written

$$h(s) = \frac{r_k}{2i(s-p_k)} - \frac{r_k^*}{2i(s-p_k^*)} \qquad (21)$$

where $\frac{r_k}{2i}$ = complex residue of mode (k).

The inverse Laplace transform of the transfer function of expression (21) is the impulse response of mode (k). In other words, if only mode (k) of the structure could be excited with a unit impulse function, its time domain response would be

$$x_k(t) = |r_k| e^{-\sigma_k t} \sin(\omega_k t + \alpha_k) \qquad (22)$$

where $|r_k|$ = magnitude of the residue

α_k = phase angle of the residue

$$= \arctan \frac{\text{Imaginary part } (r_k)}{\text{Real part } (r_k)}$$

Note: It is convenient to remove a factor of 2i from the residue in expression (21) in order to simplify the above result.

Expression (22) is a sinusoidal waveform with frequency ω_k multiplied by the decaying exponential function $e^{-\sigma_k t}$ as shown in Figure 3. Hence, the response is a decaying sinusoid where the amount of decay (damping) is controlled by the parameter ω_k. A phase shift in the impulse response is introduced by the phase angle α_k of the complex residue (modal vector). Note that when the residue vector is real valued ($\alpha_k = 0°$) there is no phase delay in the impulse response of mode (k).

It is this phase delay which is represented by the complex mode shape.

III. MODAL TESTING CONSIDERATIONS

In the last section, it was shown that only one row of column of the transfer matrix need be measured in order to identify the parameters necessary to characterize the modes of vibration of the structure.

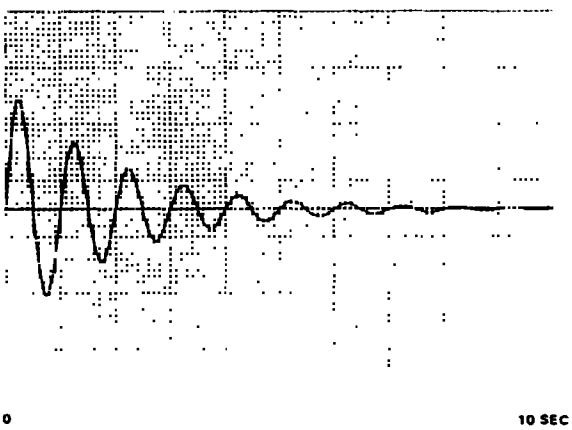

Figure 3. Impulse Response of a Mode (k)

In this section, various methods of measuring transfer functions with a digital machine are discussed. In addition, digital techniques for reducing measurement noise and increasing frequency resolution are discussed.

1. TWO CHANNEL MEASUREMENT WITH BROADBAND EXCITATION

Sine wave excitation can be used to measure transfer functions using a Fourier Analyzer, but it has some clear disadvantages compared to other types of signals. Sine testing is slow since it only excites the structure at one frequency at a time, while the digital FFT is capable of generating all frequency lines in a band of interest simultaneously. Therefore, a broadband excitation signal such as an impulse or random noise source which excites the structure over a spectrum of frequencies simultaneously makes transfer function measurement faster with a Fourier Analyzer.

Secondly, since modal analysis assumes that the dymanic behavior of the structure is linear, any measured non-linear behavior will tend to invalidate the modal parameter estimates. A broadband random signal is actually helpful in removing the effects of non-linear behavior from the measured transfer function data.

TRANSIENT TESTING

A fast method of performing transient testing is to use a hand held hammer with a load cell attached to impact the structure. The load cell measures the input force, and accelerometers mounted on the structure measure the response signals. The setup time required to use this method is negligible compared to the mounting and alignment of shakers. A typical test setup is shown in Figure 4.

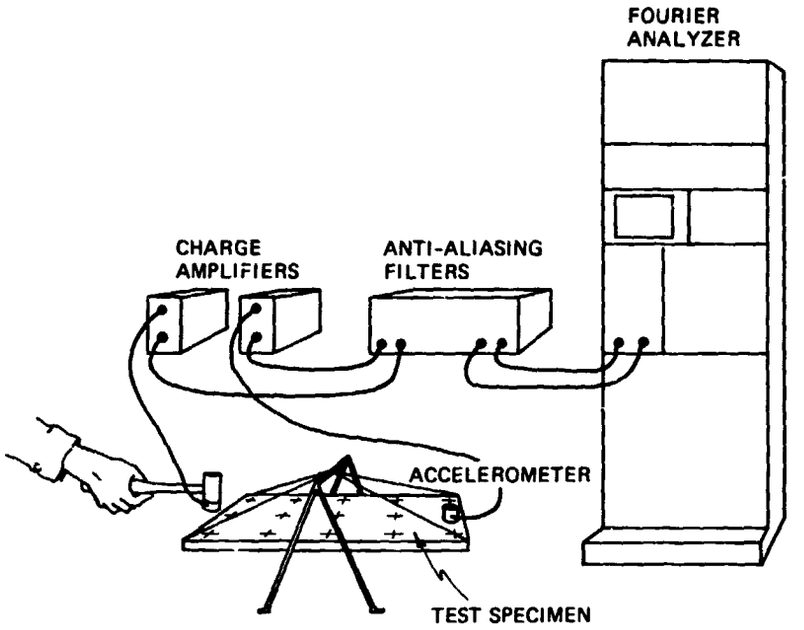

Figure 4. Hammer Test Setup

Whether a hammer or shaker is used to impact the structure, the signal measuring equipment must contain a triggering mechanism capable of capturing the majority of this short duration signal.

The primary drawback of the transient testing method is that the power spectrum of the impulse cannot be controlled as well as a random spectrum. Figure 5.A shows a typical impulse signal and its corresponding power spectrum. This particular signal provides energy from DC (0 frequency) to 5 KHz, but the energy density may not be high enough to excite an entire structure. The only way of providing more energy is to hit the structure harder, which may destroy it!

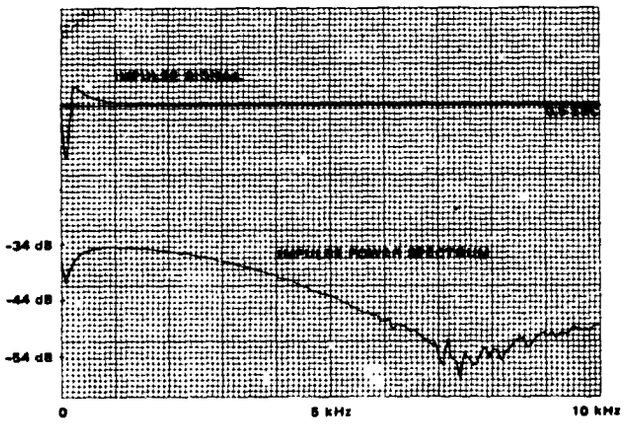

Figure 5A. Impulse Signal and Power Spectrum

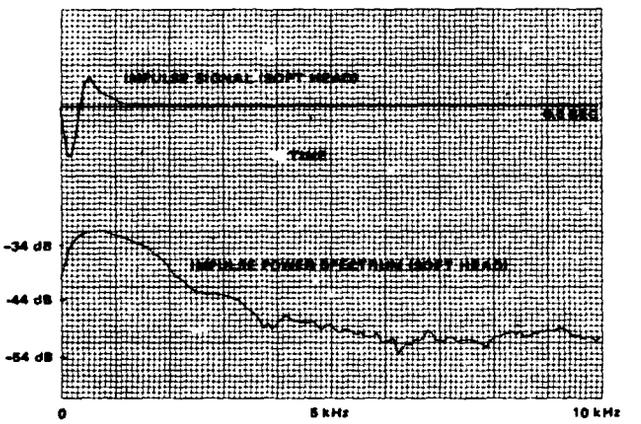

Figure 5B. Impulse Signal and Power Spectrum

On the other hand, a softer head can be placed on the hammer or shaker head to soften the impact. This has the effect of changing the impulse to a wider time width pulse, and the bandwidth of the corresponding power spectrum will in general be less than that of the impulse. Figure 5.B illustrates this case. This method can be used to concentrate more energy at lower frequencies but still may not provide the energy levels necessary to test a large, heavily damped structure.

RANDOM TESTING

Two primary advantages of using a shaker driven by a broadband random signal are that it is more controllable than a tran-

sient signal and when used in conjunction with power spectrum ensemble averaging (described later), noise and non-linear components of the structural dynamics can be removed from the measured data.

A random signal can be generated in several different ways:

METHOD #1.

A straightforward approach is to use a random signal generator and pass the signal through a band pass filter to concentrate the energy in a band of interest. Figure 6. illustrates this case. Generally, the signal spectrum will be flat except for filter roll-off at the ends of the spectrum and you can only control the overall level of the signal (i.e. the overall spectrum level). One drawback of this approach is that although the shaker is being driven with a flat spectrum signal, the structure is excited by a signal with a different spectrum due to the impedance match between the structure and the shaker head. To overcome this, a signal with a shaped spectrum must be output to the shaker.

Another more serious drawback of this method is that the measured signals (input and response) are not periodic in the measurement time window. A key assumption of digital Fourier Analysis is that a measured time waveform be periodic in the measurement time window. If it is not, the corresponding frequency spectrum will contain so called "leakage". That is, energy from the non-periodic parts of the signal will "leak" into the periodic parts of the spectrum, this giving an inaccurate result. Figure 7. illustrates the difference between a signal which is periodic in the window and one which is non-periodic. Figure 7.A. shows a sine wave of period T. The measurement window covers the first time interval (0, T) but note that if the measurement were repeated again in the internal (T, 2T), the exact same waveform would be measured. When a signal repeats in each successive time period (T), it is said to be periodic in the window (0, T).

Note that the non-periodic signal in Figure 7.B. does not repeat in each successive time period (T). In summary a signal x(t) is periodic in a window (T) if and only if

$$x(t + T) = x(t)$$

Typical input and response signal pairs for transient and random measurements are shown in Figure 8. The transient waveform in Figure 8.A. are periodic in the window. However, the random signals are non-periodic in the window (0, T) since they do not repeat in successive windows of length T.

The Hanning Window

The Hanning window is normally used, to reduce leakage in the spectrum of a non-periodic random signal.

The Hanning window is shown in Figure 9. When a non-periodic time waveform is multi-

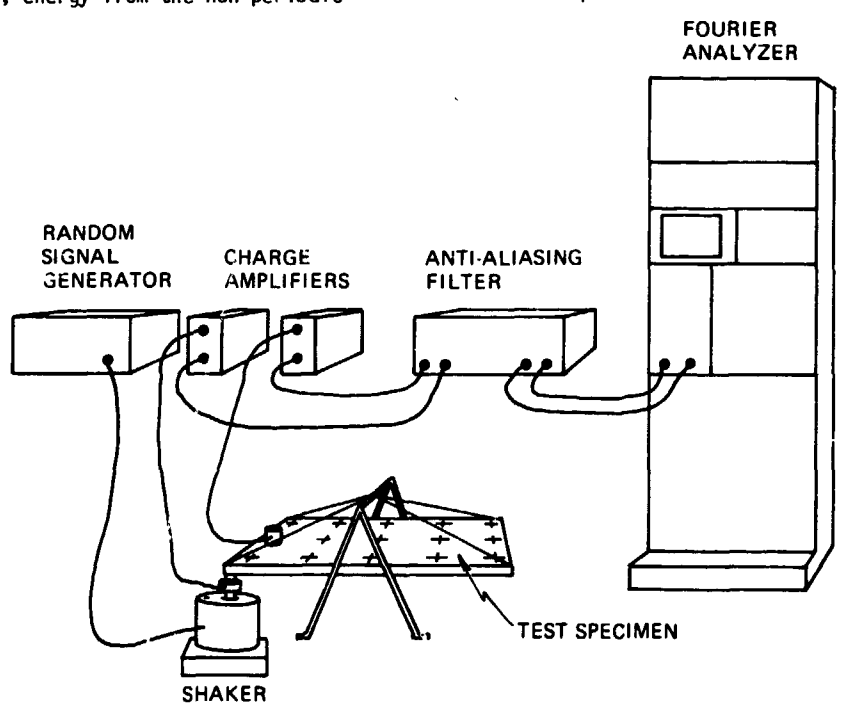

Figure 6. Random Test Setup

plied by this window, the values of the signal in the measurement window more closely satisfy the requirements for a periodic signal.

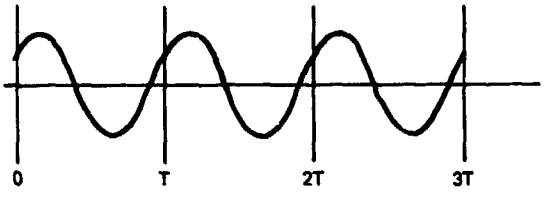

Figure 7A. Signal Periodic in Window

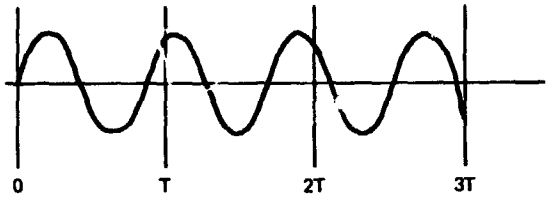

Figure 7B. Signal Non-periodic in the Window

Therefore, leakage in the spectrum of a signal which has been multiplied by the Hanning window is greatly reduced.

However, multiplication of two time waveforms, i.e. the non-periodic signal and the Hanning window, is equivalent to convolution of their corresponding Fourier transforms. Hence, although multiplication of a non-periodic signal by the Hanning window reduces leakage, the spectrum of the signal is still distorted due to convolution with the Fourier transform of the Hanning window, i.e. its line shape.

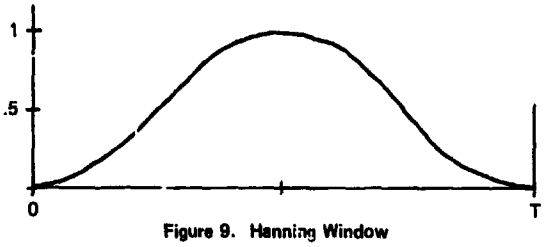

Figure 9. Hanning Window

Therefore, when a non-periodic random noise source is used to excite the structure, a Hanning window must be applied to the measured time-domain signals and the effect of this window must be deconvolved from the transfer function. This is easily done using digital techniques provided that the spectrum of the input signal is flat.

METHOD #2

To avoid the problems of using a non-periodic random signal, it is possible with a digital computer to generate a random signal and then output it to the shaker through a digital to analog converter (DAC). To do this, enough random data is synthesized in the computer to drive the shaker for T sec-

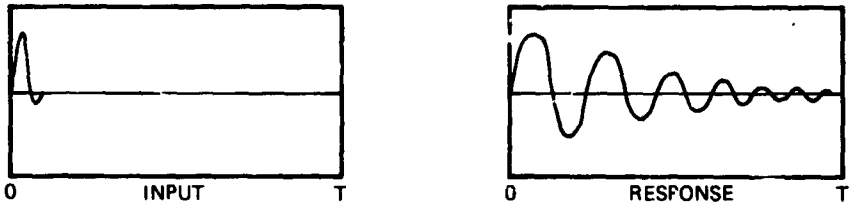

Figure 8A. Transient Input and Response Signals

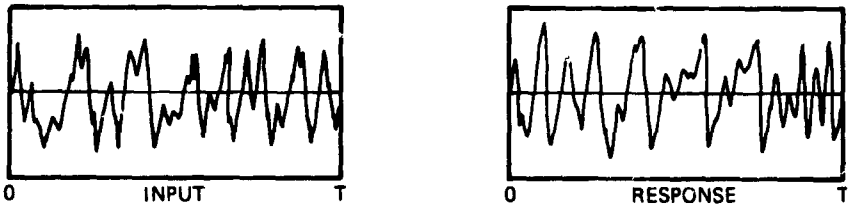

Figure 8B. Random Input and Response Signals

onds, and this data is then repeatedly output through the ADC every T seconds. The random signal is periodic since it repeats every T seconds, and is referred to as a pseudo random signal. This method of excitation not only removes windowing problems, since the measured signals are periodic, but allows you to shape the spectrum of the random signal line by line to compensate for loading of the shaker by the structure.

However, because it is periodic, a pseudo random signal will not effectively remove nonlinear distortion components from the measurement.

METHOD # 3

The best possible random signal is one that is both periodic in the window, i.e. satisfies the conditions for a periodic signal and yet changes with time so that it excites the structure in a truly random manner.

This type of signal is referred to as a periodic random signal. It starts out exciting the structure in the same manner as a pseudo random signal. Then, after the structure has reached a steady state condition, i.e. the transient part of its motion has died out, a measurement is taken. Then, instead of continuing with the same pseudo random signal, a different one is synthesized and output to the structure. This new excitation will excite the structure in a different steady state manner than the previous one, and when the power spectrums of these two measurements and many others are averaged together, non-linear distortion components are removed from the measured result. Reference (4) explains these methods in more detail.

2. REDUCING MEASUREMENT NOISE

One of the problems of any modal testing system is that extraneous noise from various sources in the measurement equipment or on the structure itself is measured along with the desired signals. Figure 10 below depicts this situation for the case involving transfer function measurements.

where

$F(\omega)$ = Fourier transform of measured input signal

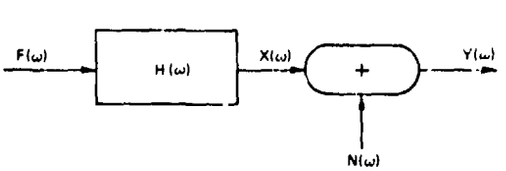

Figure 10. Measurement of Signal plus Noise

$Y(\omega)$ = Fourier transform of measured response signal

$N(\omega)$ = Fourier transform of noise

$X(\omega)$ = Fourier transform of desired response measurement

$H(\omega)$ = Transfer function of structure

Since we are interested in identifying modal parameters from measured transfer functions, the variance on the parameter estimates is reduced in proportion to the amount of noise reduction in the measurements. Two methods of noise reduction which take advantage of the digital data form and the data processing capabilities of a Fourier Analyzer are discussed here. One is an averaging technique applied at measurement time, and the other is a smoothing technique which is applied after the measurements have been made.

COMPUTATION OF THE TRANSFER FUNCTION IN THE PRESENCE OF NOISE

In Figure 10. above, we wish to compute $H(\omega)$ from the measured and transformed signals $F(\omega)$ and $Y(\omega)$. Recall that $H(\omega)$ is defined as the ratio $X(\omega)/F(\omega)$. Dropping the frequency dependence from the notation, Figure 10. yields the expression

$$Y = HF + N \tag{23}$$

All quantities in equation (23) are scalers. The input (or auto) power spectrum is defined as

$$G_{ff} = FF^* \tag{24}$$

and the cross-power spectrum as

$$G_{yf} = YF^* = (HF+N)F^* = HG_{ff} + NF^* \tag{25}$$

where * denotes the complex conjugate of the transform.

Now consider averaging the quantity G_{yf}.

The average value of G_{yf} from n different measurement s is

$$\overline{G}_{yf} = \frac{1}{n} \sum_{i=1}^{n} G_{yf}(i) \tag{26}$$

where $G_{yf}(i)$ is the i^{th} measurement taken.

Therefore,

$$\overline{G}_{yf} = \overline{HG}_{ff} + \overline{NF^*} = H\overline{G}_{ff} + \overline{G}_{nf} \tag{27}$$

where H_1 is assumed to be invariant (i.e. not changing from measurement to measurement) and $\overline{G}_{ff}$ and $\overline{G}_{nf}$ are defined similarly to $\overline{G}_{yf}$.

Now if the noise is assumed to have zero mean value and to be incoherent with the input signal, then

$$H = \frac{\overline{G}_{yf}}{\overline{G}_{ff}} - \frac{\overline{G}_{nf}}{\overline{G}_{ff}} \qquad (28)$$

As the number of averages grows larger, the noise term is reduced and the ratio $\overline{G}_{yf}/\overline{G}_{ff}$ more accurately estimates the true transfer function.

Figure 11. shows the effect of averaging on a typical transfer function measurement.

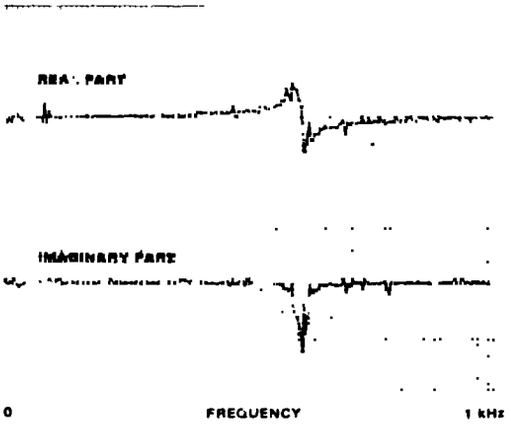

Figure 11A. Measurement with 3 Averages

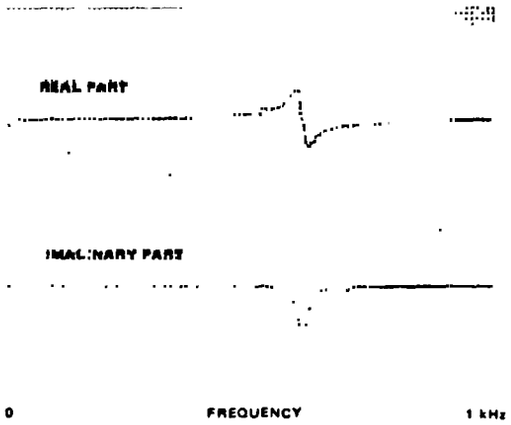

Figure 11B. Measurement with 50 Averages

THE COHERENCE FUNCTION

Whenever transfer functions are measured on a digital Fourier Analyzer in the manner just discussed, the coherence function can also be easily computed. The coherence function denoted $\gamma^2(\omega)$ is defined as the ratio

$$\gamma^2 = \frac{\text{(response power caused by applied input)}}{\text{(measured response power)}} \qquad (29)$$

The coherence function is also dependent upon frequency. Recall from Figure 10. that the measured response power spectrum contains the power caused by the input and the power due to extraneous noise sources. The measured response power spectrum is written

$$\begin{aligned} G_{YY} &= (HF+N)\,(HF+N)^* \\ &= |HF|^2 + H^*NF^* + HFN^* + NN^* \end{aligned} \qquad (30)$$

or

$$G_{yy} = |H|^2 G_{ff} + H^* G_{nf} + HG_{fn} + G_{nn} \qquad (31)$$

The response power caused by the input is

$$G_{xx} = HF(HF)^* = |H|^2 G_{ff} \qquad (32)$$

While the cross power spectrum between measured input and response is

$$G_{yf} = HG_{ff} \qquad (33)$$

Substituting these into the definition for coherence and taking average values from a large number of measurements, as explained with the previous transfer function calculation, gives

$$\gamma^2 = \frac{|\overline{G}_{yf}|^2}{\overline{G}_{ff}\overline{G}_{yy}} \qquad (34)$$

From the definition, it is clear that when the measured response power is in fact caused by the measured input power, the coherence value is one, for all frequencies. But when the measured response power is greater than the measured input power because some extraneous noise source is contributing to the output power, then the coherence value will be less than one (but greater than zero) for those frequencies where the noise source adds power to the response signal.

Hence, the coherence function is used to indicate the degree of noise contamination in a transfer function measurement and it can be used in a qualitative way to determine how much averaging is necessary to remove

noise from the measurement. Figure 12. shows coherence functions corresponding to the transfer function measurement in Figure 11. Note that with more averaging the estimate of coherence contains less variance, thus giving a better estimate of the noise energy in the measured signal.

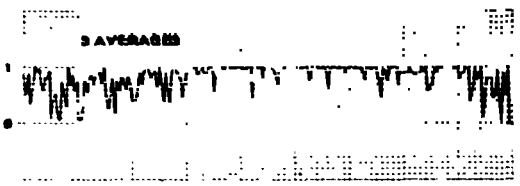

Figure 12A. Coherence of Measurement with 3 Averages

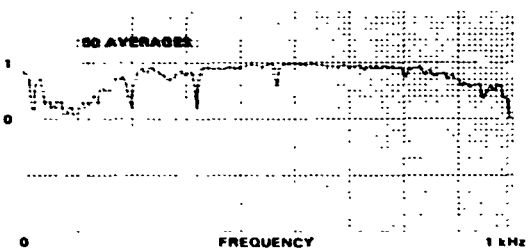

Figure 12B. Coherence of Measurement with 50 Averages

Figure 13. contains a block diagram of the power spectrum averaging process used in a digital machine to reduce noise in transfer function measurements.

EXPONENTIAL SMOOTHING

If after a reasonable amount of averaging, the transfer function measurements are still relatively noisy, the noise can be further removed by means of an exponential smoothing process. Many different types of schemes could be used to smooth data, but the exponential function is advantageous in this case because its effect on the data is known.

Recall from section II that the inverse Fourier transform of a transfer function is the sum of the impulse responses of the modes in the measurement bandwidth, i.e.

$$x(t) = \sum_{k=1}^{m} |r_k| e^{-\sigma_k t} \sin(\omega_k t + \phi_k) \qquad (35)$$

An example of this sum of decaying sinusoids is given in Figure 14.A. Measurement noise adds uniformly to this impulse response and therefore gives the result shown in Figure 14.B.

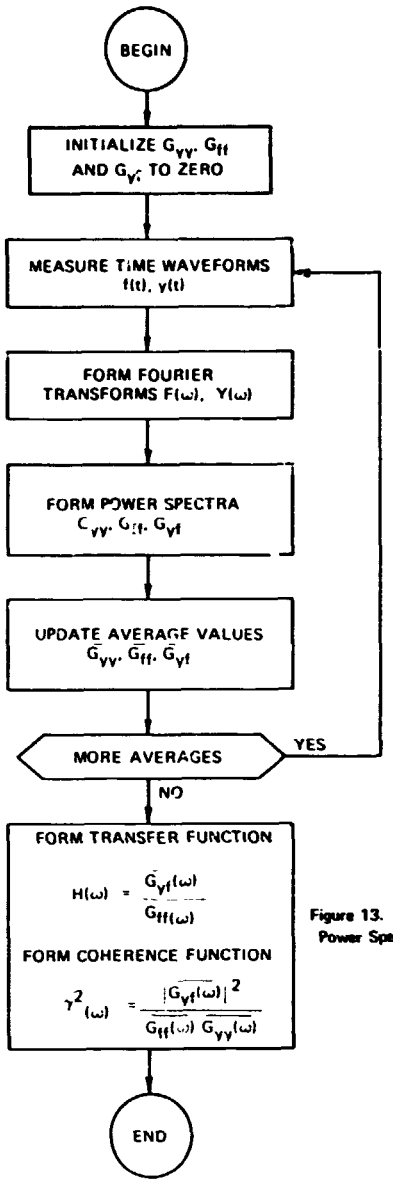

Figure 13. Measurement by Power Spectrum Averaging

Since the noise is distributed evenly throughout the block and the signal decays exponentially, the signal-to-noise ratio of the combined signal also decays exponentially.

Now if the measurement plus noise is multiplied by a decreasing exponential function (called an exponential window), as shown in Figure 15., the noise at the right hand end of the block is truncated, while the signal toward the left hand end is preserved. The overall signal to noise ratio of the data is increased since the combined signal plus noise is weighted more heavily in favor of the signal and less in favor of the noise. When the resulting waveform is transformed back to the frequency domain, the corresponding

transfer function has been smoothed, as illustrated in Figure 16. Furthermore, the width of the modal resonances, which are governed by the amount of damping in each mode have increased by a known amount. If the exponential window is represented by

$$\omega(t) = e^{-bt} \qquad (36)$$

b = a known constant, then the impulse response after windowing is

$$x(t) = \sum_{k=1}^{m} |r_k| e^{-(\sigma_k + b)t} \sin(\omega_k t + \alpha_k) \qquad (37)$$

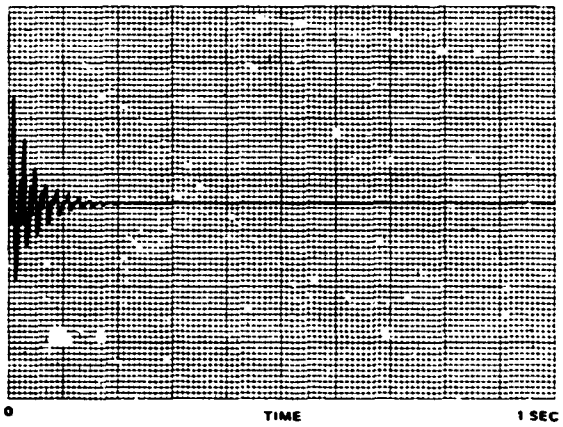

Figure 14A. Impulse Response

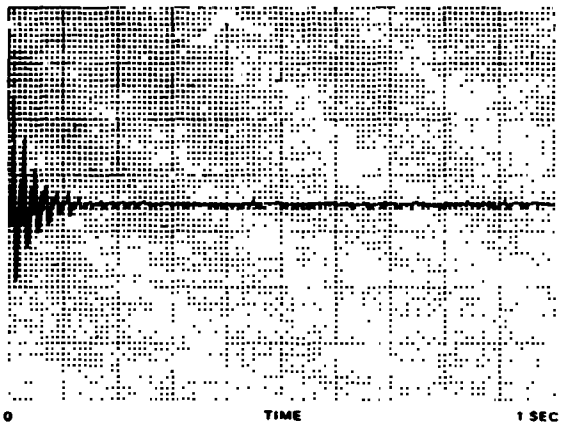

Figure 14B. Impulse Response plus Random Noise

In other words, a known amount of damping (b) is added to each mode with each multiplication of the impulse response by the exponential window.

The smoothed transfer function data can therefore be used to identify modal parameters and the correct damping coefficient can be recovered by subtracting the amount of damping due to the smoothing process from the identified damping value.

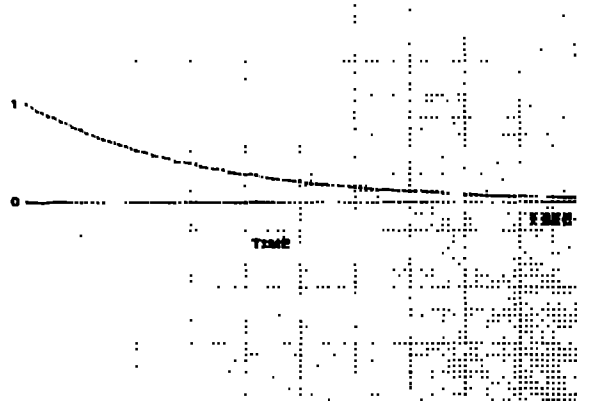

Figure 15. Exponential Window

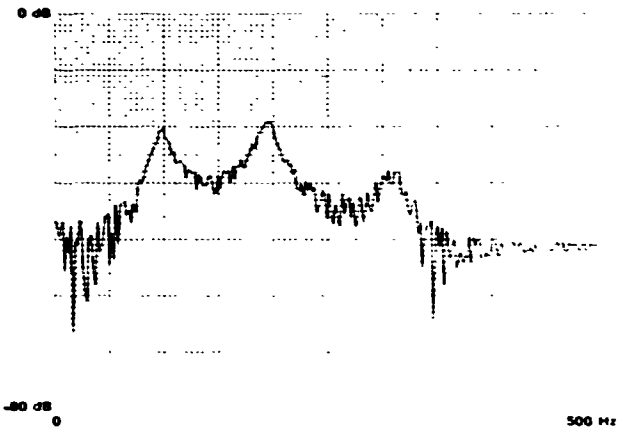

Figure 16A. Transfer Function Before Smoothing

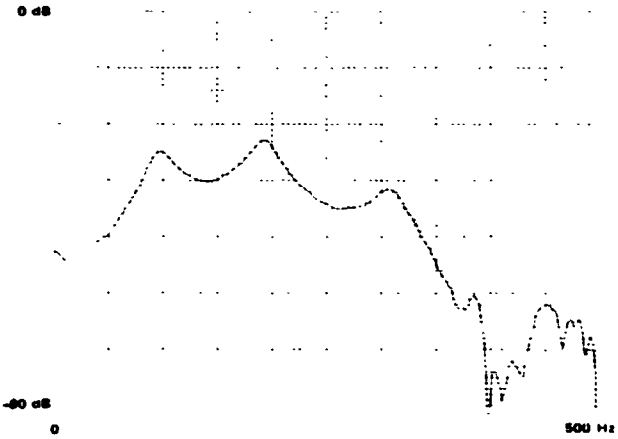

Figure 16B. Transfer Function After Smoothing

The drawback of this approach to noise removal is that if modes are closely spaced in frequency, exponential smoothing will smear them together so that they are no longer discernable as two modes.

3. GAINING FREQUENCY RESOLUTION

Normally, the Fourier transform is computed in a frequency range from zero frequency (D.C.) to some maximum frequency (F_{max}). This digital Fourier transform is spread over a fixed number of frequency lines (typically 1024) which therefore limits the frequency resolution between lines.

Band-selectable Fourier Analysis, the so called ZOOM transform, is a measurement technique in which Fourier transform based digital spectrum analysis is performed over a frequency band whose upper and lower frequencies are independently selectable. A comparison of Band-selectable Fourier Analysis (BSFA) and standard (Baseband Fourier Analysis is shown in Figure 17.
BSFA can provide an improvement in frequency resolution of more than a factor of 100, as well as a 10 dB increase in dynamic range, compared to Baseband Fourier Analysis. It is also called the ZOOM transform since it zooms in on a portion of a Baseband spectrum and "magnifies" it with more lines of definition, much as a camera zoom lens magnifies a picture. The topics of resolution and dynamic range are discussed separately below.

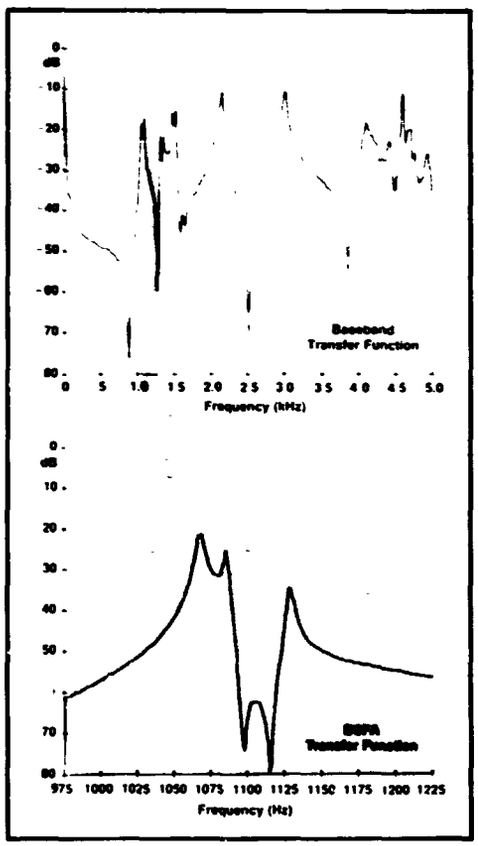

Figure 17. Base Band vs. Zoom Transform

INCREASED RESOLUTION

In any measurement technique, the resolution achievable in the frequency domain is determined by the length of time that the time-domain signal is observed. Specifically, the frequency domain resolution is the reciprocal of the time length of the measurement ($\Delta f = 1/T$).

Baseband Fourier Analysis provides uniform frequency resolution from D.C. to F_{max} (one-half the sampling frequency). Thus, the frequency resolution can also be expressed as $\Delta f = F_{max}/(N/2)$, where N is the block size; the number of samples describing the real time function. There are N/2 complex (magnitude and phase) samples in the frequency domain.

In actual practice, F_{max} is fixed by the frequencies of major experimental interest, and by aliasing considerations. Thus, the only way to improve frequency resolution in Baseband Fourier Analysis is to increase the block size. There are two reasons why this is an inefficient way to increase frequency resolution:

A. Digital processing times increase with block size.

B. The maximum block size is limited to some relatively small number of samples, based on Computer memory size.

BSFA solves these problems by providing greatly increased resolution about points of interest in the frequency domain, without requiring an increase in the system's block size.

This is done by digitally filtering the incoming time-domain data, and storing only the filtered time-domain data, corresponding to the frequency domain band of interest. Since the frequency resolution is still the reciprocal of the time length of the incoming signal, the digital filters must process T seconds of data to obtain a frequency resolution in the analysis band of $\Delta f = 1/T$. The resolution obtained in the frequency band of interest is approximately

$$\Delta f = \text{bandwidth}/(N/2) \qquad (38)$$

Thus, by restricting attention to a narrow region of interest below F_{max}, an increase in frequency resolution proportional to F_{max}/BW (where BW is the BSFA measurement bandwidth) can be obtained.

INCREASED DYNAMIC RANGE

BSFA can provide increased dynamic range re-

lative to Baseband Fourier Analysis. This is due to the increased "processor gain" on the analog to digital converter (ADC) quantization noise. However, a BSFA system can take advantage of this processor gain only to the extent that is made possible by the noise level and out-of-band rejection of the pre-processing digital filters. Certain BSFA filters can provide more than 90 dB of signal-to-noise and out-of-band rejection (Ref 5.).

Processor gain refers to the effect of increased frequency resolution on white noise in the presence of a narrow-band signal, such as a sine wave. The sine wave energy exists at a single frequency. Its peak value is, therefore, independent of the frequency resolution. The white noise peak amplitude, however, is reduced 3 dB in power each time frequency resolution is increased by a factor of 2. BSFA provides increased processor gain by increasing frequency resolution in the analysis band (relative to the baseband measurement).

4. SINGLE POINT EXCITATION

Having discussed how single transfer functions are measured, this section returns to the fundamental modal testing problem, measurement of one row or column of the transfer matrix. Consider the following two-dimensional example which defines the transfer matrix as:

$$\begin{bmatrix} X_1(s) \\ X_2(s) \end{bmatrix} = \begin{bmatrix} h_{11}(s) & h_{12}(s) \\ h_{21}(s) & h_{22}(s) \end{bmatrix} \begin{bmatrix} F_1(s) \\ F_2(s) \end{bmatrix} \quad (39)$$

In order to measure the first row of transfer functions along the frequency axis in the s-plane, that is to measure the frequency response functions

$$h_{11}(\omega) = h_{11}(s)\Big|_{s=i\omega}, \; h_{12}(\omega) = h_{12}(s)\Big|_{s=i\omega} \quad (40)$$

the structure should first be excited at point #1 and its response simultaneously measured at point #1. Then the first transfer function $h_{11}(\omega)$ is computed by forming the ratio of

$$h_{11}(\omega) = \frac{X_1(\omega)}{F_1(\omega)}, \; F_2(\omega) = 0 \; * \quad (41)$$

$F_1(\omega)$ = Fourier transform of the input at point #1

$X_1(\omega)$ = Fourier transform of the response at point #1

Next, the structure would be excited at point #2 and the response at point #1 simultaneously measured. Then the transfer function $h_{12}(\omega)$ is computed by forming the ratio

$$h_{12}(\omega) = \frac{X_1(\omega)}{F_2(\omega)}, \; F_1(\omega) = 0 \quad (42)$$

$F_2(\omega)$ = Fourier transform of the input at point #2

Note that the first row of the transfer matrix is the same as the first column since H(s) is symmetric, i.e. $h_{12}(s)=h_{21}(s)$.

To measure one column of the transfer matrix, the exciter is placed at one point on the structure (point #1 to measure column #1; point #2 to measure column #2) and the responses at points #1 and #2 are measured. For instance, column #2 would be measured by forming the ratios:

* This measurement is actually made using expression (28) but for simplicity it is represented here as the ratio of transformed response over input.

$$h_{12}(\omega) = \frac{X_1(\omega)}{F_2(\omega)}, \; F_1(\omega) = 0 \quad (43)$$

as defined before, and

$$h_{22}(\omega) = \frac{X_2(\omega)}{F_2(\omega)}, \; F_1(\omega) = 0 \quad (44)$$

where $X_2(\omega)$ = Fourier transform of response at point #2.

The method just described requires that the structure be excited at only one point at a time, i.e. single point excitation.

5. MULTI-POINT EXCITATION

In many cases a structure may be so large or heavily damped that a single point exciter does not put enough energy into the structure to excite the modes of interest. In addition, the structure may have multiple modes at the same frequency. In these cases, two or more exciters may be required to excite the structure. All of these inputs and the corresponding responses must of course be measured and because the data is in digital form, the desired row or column of the transfer matrix can still be

formed using matrix algebra.

In general, the transfer matrix is defined by

$$X(s) = H(s)\ F(s) \qquad (45)$$

Post multiplying by the conjugate transpose (denoted by T) of the transformed input vector gives

$$X(s)\ F^T(s) = H(s)\ F(s)\ F(s)^T \qquad (46)$$

then solving expression (46) for H(s) gives

$$H(s) = X(s)\ F^T(s)\ [F(s)\ F(s)^T]^{-1} \qquad (47)$$

If m-inputs are used to excite an n-dimensional system ($m \leq n$), then the corresponding m columns of H(s) can be computed using expression (47). Note that the inputs cannot be completely correlated or the indicated inverse will not exist.

Consider the following case where two inputs, located at points i and j on the structure are used

$$H(s) = \begin{bmatrix} X_1(s) \\ \\ X_n(s) \end{bmatrix} [F_i^*, F_j^*] \left[\begin{bmatrix} F_i \\ F_j \end{bmatrix} [F_i^*, F_j^*] \right]^{-1} \qquad (48)$$

Dropping the s-variable dependence from the notation in expression (48) gives

$$H(s) = \begin{bmatrix} X_1 F_i^* & X_1 F_j^* \\ \vdots & \vdots \\ X_n F_i^* & X_n F_j^* \end{bmatrix} \begin{bmatrix} F_i F_i^* & F_i F_j^* \\ F_j F_i^* & F_j F_j^* \end{bmatrix}^{-1} \qquad (49)$$

$$= QP^{-1}$$

Q is an n x 2 matrix and P is a 2 x 2 matrix. The inverse of P can be written in closed form using Cramar's rule, and the indicated multiplication of expression (49) can be carried out using the Fourier transforms of input and response signals to yield frequency response functions corresponding to the i^{th} and j^{th} columns of the transfer matrix.

This procedure can be extended to larger numbers of inputs but the required algebra involving the input and response Fourier transforms becomes more complex.

IV. MODAL PARAMETER IDENTIFICATION

When a structure is excited by a broad band input force many of its modes of vibration (degrees-of-freedom) are excited simultaneously. Since the structure is assumed to behave in a linear manner its transfer functions are really the sums of the resonance curves for each of its modes of vibration, as shown in Figure 18.

In other words, at any given frequency the transfer function represents the sum of motion of all the modes of vibration which have been excited. However, near the natural frequency of a particular mode its contribution to the overall motion is generally the greatest. The degree of mode overlap, i.e. the contribution of the tails of adjacent modal resonance curves to the transfer function magnitude at a modes' natural frequency, is governed by the amount of damping of the modes and their frequency separation. Figure 19 illustrates light and heavy modal overlap. Figure 19.A. shows modes with light damping and sufficient separation so that there is little modal overlap. Figure 19.B. shows modes with heavy damping and/or sufficiently high modal density

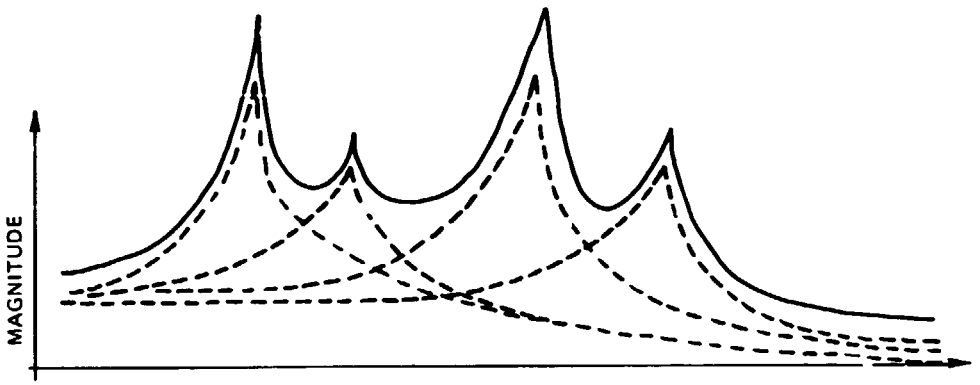

Figure 18. Magnitude of a Multi Degree-of-Freedom System Transfer Function

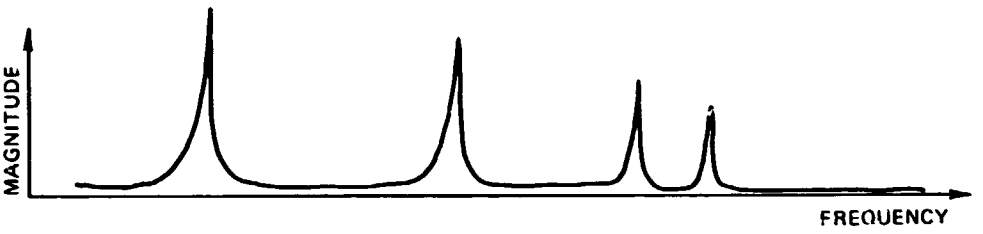

Figure 19A. Light Modal Overlap

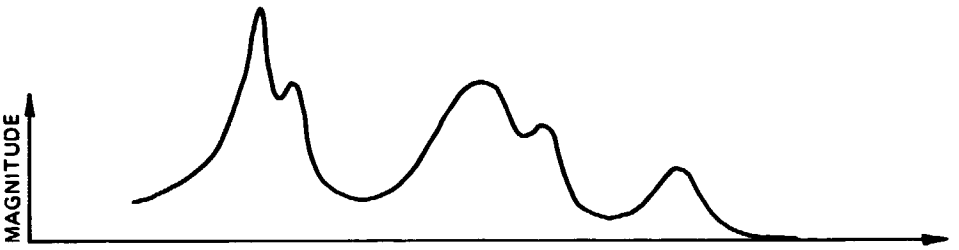

Figure 19B. Heavy Modal Overlap

(little frequency separation) such that there is plenty of modal overlap. This condition is also referred to as modal coupling.

In cases where modal overlap is light, the transfer function data can be considered in the vicinity of each modal resonance as if it were a single degree-of-freedom system. In other words it is assumed that the contribution of the tails of adjacent modes near each modal resonance is negligibly small. On the other hand when modal overlap is heavy a single degree-of-freedom approach to modal parameter identification will not work; the parameters of all the modes must be identified simultaneously.

1. Single Degree-of-Freedom Models

The majority of modal parameter identification techniques used today are based upon single degree-of-freedom models. This is so because the presently popular normal mode multi-shaker testing techniques are predicated upon the excitation of one mode of vibration at a time and hence the measured transfer function primarily reflects the motion of a single mode of vibration.

Recall from expression (21) that the transfer function of a single mode (k) of a linear system can be represented as

$$H_k(s) = \frac{r_k}{2i(s-p_k)} - \frac{r_k^*}{2i(s-p_k^*)} \qquad (50)$$

where

p_k = pole location in the s-plane

r_k = complex residue

This complex resonance curve generated by expression (50) along the frequency axis ($s=i\omega$) is shown in Figure 20.

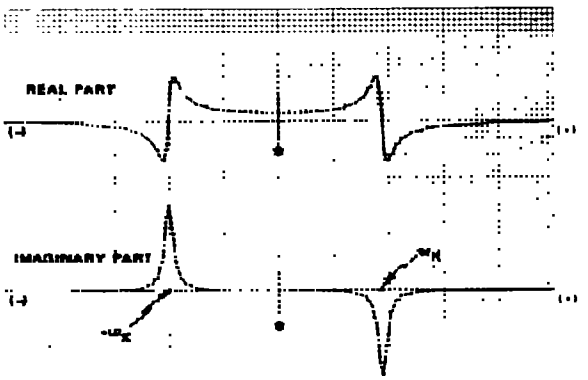

Figure 20. Resonance Curve for Single-Degree-of-Freedom

The resonance curve is generated by summing two terms together, one that describes the motion primarily around the positive frequency ω_k, and one that describes the motion primarily around the negative frequency $(-\omega_k)$.

Normally the transfer function is only measured for positive frequencies, i.e. along the $+i\omega$ axis, and it is clear that for positive frequencies the majority of the modal resonance is described by the formula

$$H_k(s) = \frac{r_k}{2i(s-p_k)} \qquad (51)$$

The frequency response function $H_k(\omega)$ can be

written in real and imaginary parts as

$$\mathrm{Re}[H_k(\omega)] = \frac{1}{2}\left[\frac{r2_k(\omega_k-\omega)+r1_k\sigma_k}{(\omega_k-\omega)^2+\sigma_k^2}\right]$$

$$\mathrm{Im}[H_k(\omega)] = \frac{1}{2}\left[\frac{r2_k(\omega_k-\omega)-r1_k\sigma_k}{(\omega_k-\omega)^2+\sigma_k^2}\right] \qquad (52)$$

where

$r_k = r1_k + ir2_k$

$p_k = -\sigma_k + i\omega_k$

$s = i\omega$

Now at modal resonance, i.e., $\omega = \omega_k$, it is clear from the expressions above that

$$\mathrm{Re}\,[H_k(\omega_k)] = r2_k/2\sigma_k$$

$$\mathrm{Im}\,[H_k(\omega_k)] = -r1_k/2\sigma_k \qquad (53)$$

MODE SHAPE FROM QUADRATURE RESPONSE

The real part of $H_k(\omega)$ is also referred to as the coincident or in-phase response, and the imaginary part of $H_k(\omega)$ is called the quadrature or out-of-phase response. The so called co-quad plot is simply the transfer function plotted in rectangular (real-imaginary) coordinates along the frequency axis.

In cases of light damping the residues are found to be almost always real valued. Therefore r2=0 and $\mathrm{Re}(H_k(\omega))=0$. When this assumption is valid the mode shape can be identified by merely picking the quadrature response of each measurement at the modal resonant frequency. Figure 21 illustrates this case.

MODE SHAPE BY CIRCLE FITTING

Another single degree-of-freedom approach to identifying the mode shape is based upon use of the Nyquist (or real vs. imaginary) plot of the transfer function. Expression (51) for a single mode (k) can be rewritten

$$H_k(\omega) = \frac{1}{2}\left[\frac{|r_k|e^{i\alpha_k}}{(\omega_k-\omega)+i\sigma_k}\right] \qquad (54)$$

where

$|r_k|$ = magnitude of complex residue

α_k = phase angle of residue

= arctan $(\mathrm{Im}(r_k)/\mathrm{Re}(r_k))$

If the residue is real valued and of unit magnitude then

$$\mathrm{Re}[H_k] = \frac{1}{2}\left[\frac{(\omega_k-\omega)}{(\omega_k-\omega)^2+\sigma_k^2}\right]$$

$$\mathrm{Im}[H_k] = \frac{1}{2}\left[\frac{-\sigma_k}{(\omega_k-\omega)^2+\sigma_k^2}\right] \qquad (55)$$

It is straightforward to show that

$$\mathrm{Re}[H_k]^2 + \left(\mathrm{Im}[H_k] + \frac{1}{4\sigma_k}\right)^2 = \frac{1}{16\sigma_k^2} \qquad (56)$$

That is, the modal resonance curve is a circle in the Nyquist plane with radius 1/4 σ_k and centered at -i/4 σ_k as shown in Figure 22.

The complex residue vector $|r_k|e^{i\alpha_k}$ merely

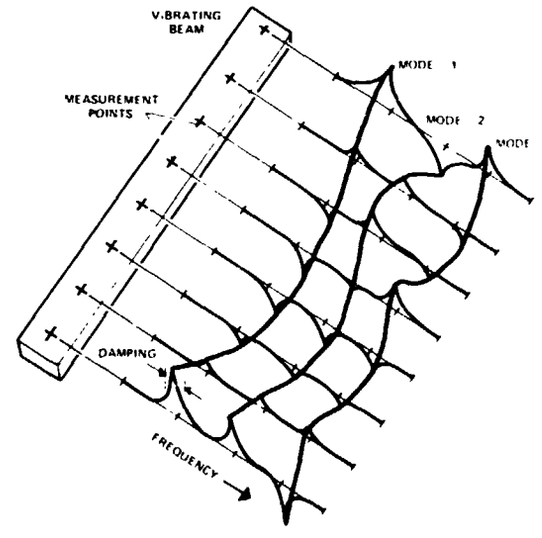

Figure 21. Mode Shape from Quadrature Response

expands the radius of the circle and rotates the circle in the Nyquist plane by the clockwise angle α_k away from the negative imaginary axis, as shown in Figure 23.

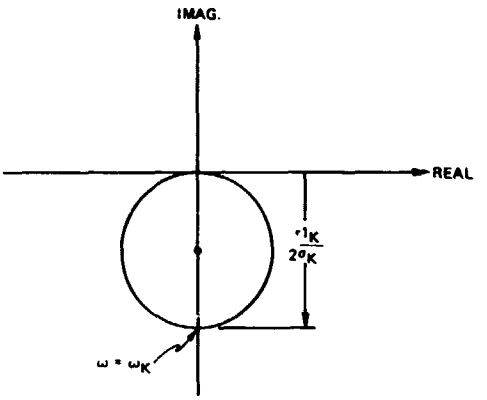

Figure 22. Modal Resonance in Nyquist Plane

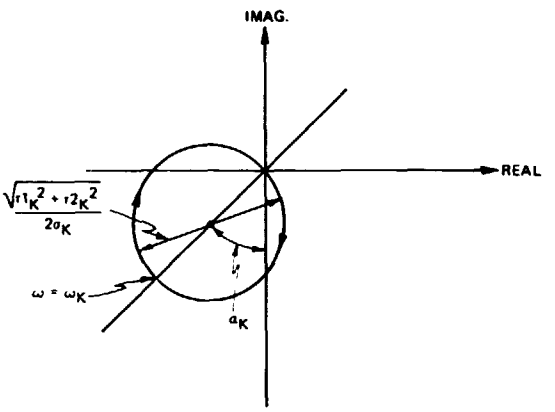

Figure 23. Complex Modal Resonance in Nyquist Plane

In general circle fitting involves the fitting of a circle in parametric form

$$(x + a)^2 + (y + b)^2 = c^2 \qquad (57)$$

by a least squared error procedure to a number of measured transfer function data points in the vicinity of each modal resonant frequency. In the process the center of the circle (a, b,) and its radius (c) are identified. The radius of the circle is then used as the magnitude of a component of the mode shape and the phase angle is computed as

$$\alpha_k = \arctan\left(\frac{b}{a}\right) \qquad (58)$$

The complete mode shape is obtained by fitting circles to each measurement of an entire row or column of the transfer matrix. This method, which is referred to as the Kennedy-Pancu method (Ref. 6), is generally more accurate than simply using the quadrature response.

MODE SHAPE BY COMPLEX DIVISION

This technique is also based upon the resonance curve for the positive frequency pole of a single mode, which is described by

$$H(\omega) = \frac{r}{2i(s-p)} \qquad (59)$$

Since p, the pole location, is assumed to be constant no matter where a transfer function measurement is made on the structure, then the ratio of two transfer functions (n) and (m) is

$$\frac{H_n}{H_m} = \frac{r_n}{r_m} \qquad (60)$$

In other words dividing one transfer function by another yields a complex scalor at all frequencies. Therefore if a single transfer function (m) is divided into all other measurements from a row or column of the transfer matrix, and several values of the resultant quotients in the vicinity of each modal resonance are averaged together after each divide operation, the complex vector

$$\begin{bmatrix} r_1/r_m \\ r_2/r_m \\ \cdot \\ \cdot \\ r_n/r_m \end{bmatrix} \qquad (61)$$

is identified, which is proportional to the mode shape.

This method is also better than the quadrature response method since, like the circle fitting method, it uses a number of data points in the vicinity of the modal resonance. However, it is sensitive to shifts in the modal frequency from measurement to measurement. When these shifts do occur, the resulting mode shape has small phase changes in it.

MODE SHAPE BY A DIFFERENCE FORMULA

This formula is based upon the differencing of transfer function data between adjacent frequency lines. In fact both residues and pole locations can be determined by this differencing approach.

Let the transfer function for a single mode (k) at frequency ω_j be defined by

$$H_j = \frac{1}{2}\left[\frac{r_k}{\psi_j + i\sigma_k}\right] \qquad (62)$$

where $\psi_j = \omega_k - \omega_j$,

and at the previous frequency ω_{j-1} by

$$H_{j-1} = \frac{1}{2}\left[\frac{r_k}{\psi_{j-1} + i\sigma_k}\right] \quad (63)$$

The product of these two values is

$$H_j H_{j-1} = \frac{1}{4}\left[\frac{r_k^2}{(\psi_j + i\sigma_k)(\psi_{j-1} + i\sigma_k)}\right] \quad (64)$$

and the backward difference ($\Delta H_j = H_j - H_{j-1}$) is

$$\Delta H_j = \frac{1}{2}\left[\frac{r_k(\omega_j - \omega_{j-1})}{(\psi_j + i\sigma_k)(\psi_{j-1} + i\sigma_k)}\right] \quad (65)$$

Dividing the difference into the product gives the desired residue value

$$r_k = \frac{1}{2}\left[\frac{H_j H_{j-1}}{(\omega_j - \omega_{j-1})\Delta H_j}\right] \quad (66)$$

Hence by forming the product and difference of adjacent frequency lines of data the residue is estimated using the above formula, which also includes the frequency resolution between lines ($\omega_j - \omega_{j-1}$). This formula applies at all frequencies and, as in the previous case, is best applied to data in the vicinity of the modal resonance and then an average of the results computed.

POLE LOCATION BY A DIFFERENCE FORMULA

Suppose that expression (62) is first multiplied by ω_j to give

$$Y_j = \frac{1}{2}\left[\frac{\omega_j r_k}{\psi_j + i\sigma_k}\right] \quad (67)$$

and then the difference ($\Delta Y_j = Y_j - Y_{j-1}$) formed

$$\Delta Y_j = \frac{1}{2}\left[\frac{(\omega_j - \omega_{j-1})(\omega_k + i\sigma_K)\, r_k}{(\psi_j + i\sigma_k)(\psi_{j-1} + i\sigma_k)}\right] \quad (68)$$

Then the desired parameters ω_k and σ_k are obtained by forming the ratio

$$\omega_k + i\sigma_k = \frac{\Delta Y_j}{\Delta H_j} \quad (69)$$

and this formula also applies at each frequency ω_j.

Both of the above differencing formulas can be derived using higher order differences also.

2. MULTIPLE DEGREE-OF-FREEDOM MODELS

All of the above methods work reasonable well when the amount of overlap between modes is small. However, in cases where the amount of modal overlap is sufficient to cause significant errors by the single degree-of-freedom techniques a multi-degree-of-freedom identification technique must be used.

In general some type of curve fitting technique which matches the following summation expression evaluated along the frequency axis ($s=j\omega$) to measured frequency response function data is necessary.

$$H(s) = \sum_{k=1}^{m}\left[\frac{r_k}{2i(s-p_k)} - \frac{r_k^*}{2i(s-p_k^*)}\right] \quad (70)$$

For each mode (k) the four parameters frequency, damping and complex residue (two parameters) must be estimated simultaneously.

LEAST SQUARES ESTIMATION

One technique that has been successfully applied at Hewlett-Packard is the application of equation (70) by an iterative least squared error technique to the complex transfer function data. The iterative equations result from a minimization of the error function

$$\varepsilon = \sum_{j=1}^{N}\left(H_j - H(\omega_j)\right)^2 \quad (71)$$

where

H_j = the measured data at frequency ω_j

$H(\omega_j)$ = the analytical model at frequency (ω_j)

N = data block size

With each iteration of the algorithm new values of all four unknowns for each mode are estimated which further reduce the error between the measured and analytical waveforms. Figure 24, illustrates a multi-degree-of-freedom curve fit using this process.

MEAS. MODE	FREQ(HZ)	DAMP(%)	RESIDUE AMPL	RESIDUE PHS
1	45.5497	.2475	87.1859	186.1
2	66.9754	1.5672	118.8888	2.5
3	129.1113	.1831	189.8194	163.1
4	144.4386	.1003	446.5688	349.8
5	240.5947	.1553	685.3258	354.4
6	256.5869	.2026	97.7994	156.4
7	303.5578	.1004	475.4058	181.8
8	319.2497	.7852	229.3784	182.8
9	328.2283	.2584	286.7471	169.2
10	375.5362	.0579	899.5685	358.1
11	413.4484	.1138	981.4277	169.2
12	422.8821	.3129	346.5385	186.6

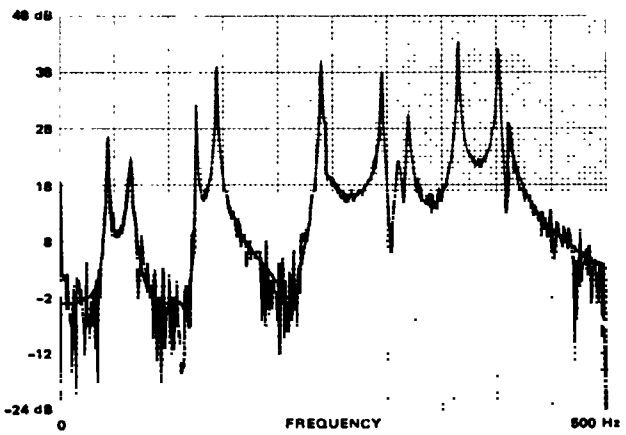

Figure 24. Magnitude Curve - Multi Degree-of-Freedom Curve Fit

An Alternate Approach

From inspection of expression (70), it is clear that the transfer function is a linear function of the residues r_k.

Therefore, if the pole locations p_k were known, the residues r_k could be identified using a least squared error procedure that involves solving a set of simultaneous linear equations. Hence, a simultaneous linear equation solution algorithm combined with a search procedure which iterates toward an optimum estimate of p_k is another approach to identifying modal parameters with a multi-degree-of-freedom model.

With either of the iterative techniques just mentioned the modes must somehow be identified beforehand and initial estimates of their pole locations given as starting values. Modes are generally identified from their resonance peaks on the transfer function magnitude curve. This can be done either by a computerized peak picking procedure, or by hand. Starting estimates of modal damping and residue can usually be satisfactorily identified using one of the previously described single degree-of-freedom methods or some other technique.

This apparent disadvantage, i.e. having to identify the modes before the least squared fitting process begins, turns out to be an advantage from an operational standpoint. In a test situation the machine operator is able to maintain control over the modal parameter identification process by specifying modes at certain frequencies even though from particular measurements their presense may not be apparent.

THE COMPLEX EXPONENTIAL ALGORITHM

A direct solution of the modal parameter identification problem underwent a considerable amount of development for the U.S. Navy several years ago (Ref. 7). It is referred to as the complex exponential algorithm. The approach is direct in the sense that no starting modal estimates are necessary. The algorithm works with the inverse transform of the transfer function i.e., the impulse response. Expression (22) the characteristic damping sinusoidal response, can also be written using complex exponential functions as

$$x(t) = \sum_{k=1}^{m} \frac{1}{2i}\left[r_k e^{p_k t} - r_k^* e^{p_k^* t}\right] \qquad (72)$$

Using the complex exponential algorithm this expression is curve fit to one measured row or column of the impulse responses (corresponding to a row or column of the transfer matrix) and the parameters p_k and r_k are identified in each measurement.

The algorithm is a two step process which solves for all the polynomial roots p_k first (recall that the poles p_k are roots of the polynomial set (B(s) = 0) and then the residues r_k. Originally the algorithm would find (n/4) modes in a impulse response that is (n) data points long. However, it has been improved recently so that parameters for a prespecified number of modes are identified. Nevertheless, the weakness of this approach is that the machine operator has no control over the root solving process and hence the algorithm will put modes wherever necessary to fit the data. There-

fore the same mode may not be identified in different transfer function measurements, thus making it difficult to identify a mode shape by this process.

V. CONCLUSIONS

The development of all-digital systems to collect and process dynamic vibration data from mechanical structures is beginning to mature more quickly as test engineers realize the power of the digital Fast Fourier transform as a tool for transfer function measurement. The testing and analysis techniques presented here are but some of the approaches that can be used with measurements that are in digital form.

Although analog based single mode testing techniques are currently more widely used than the digital techniques presented here, there are some inherent advantages to broad band testing e.g., speed, accuracy, resolution, noise rejection, and repeatability, which indicate that more Fourier transform based systems will be used for modal testing and analysis in the future.

ACKNOWLEDGEMENTS

Ron Potter, Senior Engineer, Santa Clara Division of Hewlett-Packard, and Dave Brown, Associate Professor of Mechanical Engineering, Universiry of Cincinnati, have both contributed substantially to my understanding of Modal Analysis. The development of many of the ideas and formulations in this paper are due primarily to their valuable assistance during the course of my work on the Hewlett-Packard Modal Analysis System.

REFERENCES

(1) Richardson, M., and Potter, R., "Identification of the Modal Properties of an Elastic Structure from Measured Transfer Function Data" 20th I.S.A., Albuquerque, N.M., May 1974.

(2) Potter, R., and Richardson, M., "Mass, Stiffness and Damping Matrices from Measured Modal Parameters" I.S.A. Conference and Exhibit, New York City, October, 1974.

(3) Potter, R., "A General Theory of Modal Analysis for Linear Systems", Hewlett-Packard Company, 1975 (to be published).

(4) Roth, P.R., "Effective Measurements Using Digital Signal Analysis" IEEE Spectrum, Pp. - 62, 70, April, 1971.

(5) McKinney, W.H., "Band-Selectable Fourier Analysis" Pp.-18, 24, Hewlett-Packard Journal, April, 1975.

(6) Kennedy, C.C., and Pancu, C.D.P., "Use of Vectors in Vibration Measurement and Analysis" J. Aerospace Sci., Vol. 14, No. 11, 1947, Pp. 603-625.

(7) Spitznogle, F.R. and Quazi, A.H., "Representation and Analysis of Time Limited Signals Using a Complex Exponential Algorithm" J. of the Acoustical Soc. of America, Vol. 47, No. 5 (part 1), Pp 1150, 1155, May 1970.

HARDWARE/SOFTWARE DEVELOPMENT TECHNIQUES TO SUPPORT COMPUTER CONTROLLED TEST SYSTEMS

Laurie R. Burrow, Jr.
Spectral Dynamics Corporation of San Diego
San Diego, California

An economical systems approach is described for controlling a desired random spectrum shape at a reference point. Hardware concepts for performing a "Power of 2" inverse FFT from a 500-point real time spectrum and software considerations for control and simple user dialog are presented. Examples are given of a complete test sequence including system calibration, establishing safety criteria, and displaying calibrated results. The extension of this concept to shock analysis and control is also given.

INTRODUCTION

The process of using the Fast Fourier Transform (FFT) algorithm coupled to a computer for generating and controlling a random vibration test has evolved into a practical and realistic concept today.

The basic approach is that of measuring a response from a control accelerometer using a forward transform, then comparing this with an operator-entered reference spectrum. Next, creating a spectrum that when converted to a random time function by use of the inverse FFT and used to excite the shaker system, would result in a response spectrum that matched the reference spectrum within prescribed limits. An investigation into the available systems indicated that a less complex and less costly approach was needed to really make digital random control and its inherent benefits available on a practical basis.

The purpose of this paper is to describe the hardware and software design considerations for the Spectral Dynamics Digital Random Control System. Many system details not considered pertinent are omitted. As in most cases, we were somewhat biased in our approach due mainly to our years of experience in the environmental field, as well as our practice of making minimum use of other manufacturers' hardware in SDC systems.

SPECTRAL DYNAMICS' APPROACH

Originally, it was intended that a version of the SD360 Digital Signal Processor (DSP), Fig. 1, would be used to perform forward and inverse Fourier Transforms because of its high processing speeds. The basic cost of FFT hardware caused a re-evaluation of plans for a Digital Random Control System. After a review of the analyzers available, a high speed 500-line Real Time Spectrum Analyzer, Fig. 2, was chosen as the Power Spectral Density Analyzer since it had the required analysis speed, economy, and reliability. Having made this decision, a basic approach was formulated which needed to be unique since an analyzer was being used that was not geared to "Powers of 2" as are typical FFT implementations. Thus, the RTA would be used to perform the PSD response measurements from the control accelerometer and software used to perform the inverse FFT in the computer.

MARKET INPUTS GUIDE DESIGN PHILOSOPHY

The Basic System requirements as viewed by SDC Marketing after observations and discussions with various customers were:

1) Personnel cutbacks in Aerospace and Government laboratories resulted in very high workloads on system operators, and many new and less experienced people were called upon to operate complex systems. As a result, operator errors and setup errors of systems were on the increase.

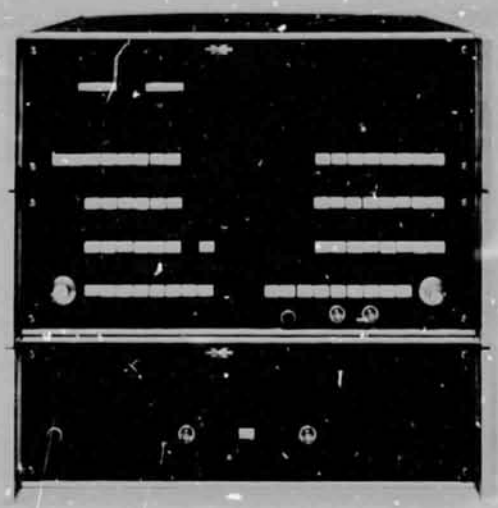

Figure 1. SD360 Digital Signal Processor

2) Commensurate with simple operation and setup is that package protection considerations must be given high priority to remove as much operator decision making as practical.

3) Experience with our Computerized Spectrum Processing System and Campbell Diagram Systems indicated that use of a teletype or other keyboard input device is very difficult for the average operator; therefore, every effort should be made to minimize or eliminate dependence on a teletype.

4) To give test conductors, inspectors, and design engineers total "visibility" during a test by visual observation of the Response Spectrum on a real time basis. It was noted that many customers owning Random Control systems, either analog or digital, were using real time analyzers for an independent verification of equalization due to the lack of a real time display from existing systems.

5) To make a system as inexpensive as practical so as to be attractive as a replacement for an older analog system.

6) To make a system with equalization speeds equal, or faster, than the analog systems, to allow test profiles to be equalized conservatively at 1.5 dB, over a dynamic range of greater than 60 dB.

7) To retain expansion capability for shock synthesis, and consider sine and, eventually, modal analysis by adding additional hardware.

8) To make the system such that those wishing to do R & D evaluations of fixtures, etc., using random or psuedo random could do so.

9) To use the stand-alone hardware approach, enabling separate use of the Analyzer as a data reduction tool and the computer for calculations. Also, hardware approach would allow independent dual real time display of the averaged and unaveraged Response Spectrum.

SOFTWARE CONSIDERATIONS

The Analyzer/Computer system uses a Digital Equipment PDP-11 16-bit minicomputer with the following features which make it ideal for use in a digital control system:

a) Asynchronous operation - System components run at their highest possible speed, replacement with faster devices means faster operations without other hardware or software changes.

b) Modular component design resulting in ease and flexibility in configuring systems.

c) Direct Memory Access capability.

d) Automatic priority interrupt system of 4 levels permits grouping of interrupt lines according to response requirements.

e) Vectored interrupts - yielding fast interrupt response to system peripherals.

f) Automatic powerfail and restart operation.

g) A single communications path (UNIBUS) structured for easy communication with a wide variety of peripherals and special interfaces.

In addition to these hardware features, PDP-11's are used in SDC systems because of their software support, accepted reliability and performance, and a worldwide service system.

Software can be roughly categorized as high level (FORTRAN, FOCAL, BASIC, etc.) and low level (machine language, assembly language). Relative to low level languages, high level languages generally:

a) Require less program development time;

b) Are easier to modify;

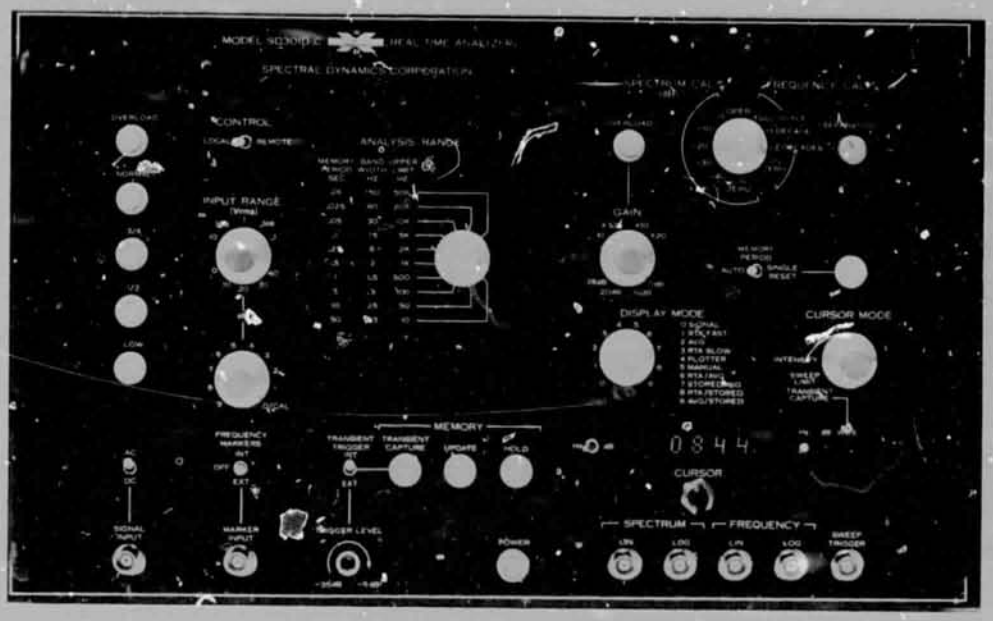

Figure 2. SD301D-C Real Time Analyzer

c) Require more memory storage; and

d) Execute slower.

An optimized blend of a high level DEC language called FOCAL, and low level assembly language is used in the system. This blend yields a software package that, while designed to perform a specific task, is extremely flexible and fast.

FOCAL (FOrmula CALculator) is an easily learned, highpowered, compact programming language. It is an interpreter level language, which means that a program may be written, debugged, modified, and executed "on-line" without the usually lengthy "compile" process required of compiler level languages, such as FORTRAN.

FOCAL is similar to BASIC in its use and structure with two significant exceptions. FOCAL permits line and character-by-character editing (modifying) of program statements. This edit feature, along with the "interpretive" nature of FOCAL, reduces program development time significantly. Secondly, the FOCAL interpreter only occupies approximately 2400 words of core as opposed to BASIC which occupies almost 4000 words of core.

FOCAL is used to perform tasks that do not require optimum speed, but require greatest flexibility. These include:

a) User dialog/communication with the system - FOCAL provides a simple, efficient means for transferring test information into the computer.

b) Report headings and data tabulations - Assuming the system output device is a low to medium speed device such as a teletype or printer, FOCAL is sufficiently fast to handle output. This frees the programmer from having to write simple, yet tedious and cumbersome data format conversion routines, output routines, etc.

c) Overall system control and sequencing - FOCAL can call on assembly language routines to perform high-speed input/output operations and high-speed "number crunching" (such as an FFT) routines. Since FOCAL can pass information to these routines via parameters, and can be easily and quickly modified to call on these routines in different sequence, overall system operation remains flexible, yet fast.

d) "Modeling" of program tasks - In the early stages of program development, many programs can be written and tested in FOCAL, and once proved feasible, converted to the faster assembly language version. For example, a new algorithm for combining narrowband data into 1/3 octave data can be tested and debugged almost completely at the FOCAL level where program creation, modification, and evaluation is desired.

The assembly language portions of the software are the workhorses of the system. Although usually most difficult to write and more time consuming to debug than the FOCAL routines, these program sections handle the high-speed input/output functions and data manipulations that are beyond the capabilities of most high level languages. These routines are usually modular in form, and are made as general and flexible as possible without sacrificing speed and memory allocation. This usually results in assembly language modules that may be used in many systems and/or applications with little or no modification necessary.

Figure 3 shows a typical group of FOCAL statements whereby dialog is set up with the operator of the System.

```
4.05  S D=FN(PAN,12);S DN=FX(1,FN(DST,10))
            -D*200
4.10  D 4.95
4.15  T "DEFINE?";D 5; I(X-0Y)4.2,4.5
4.20  T "LIST?";D 5;I(X-0Y)4.25,4.6
4.25  T "EDIT?";D 5;I(X-0Y)4.3,4.7
4.30  A "PLOT RANGE (DB): ",X;I(X)4.45,
        4.45;X FN(PLOT 8,X)
4.45  T "DISABLE TEST?";D 5;I(X-0Y)4.9,
        4.8,4.9
4.50  D 20;G 4.9
4.60  D 21;G 4.9
4.70  D 22;C 4.9
4.80  ..: FN(PAN,2,D);D 20.4
4.90  X FN(PAN,8)
4.95  T %2,1,"TEST NUMBER:",D,1
```

Figure 3. Typical Group of FOCAL Statements

```
3.10  X FN(PAN,6,0);X FN(PAN,10,4)
```

Figure 4. Typical Program Control Transfer

Figure 4 shows typical "calls" or transfer of program control to high-speed assembly language routines. As an example, the routine, FN (PAN,6,4) has one parameter. The FN tells the program that it is a user-defined function; the PAN,6 tells the program which function; and the four is the parameter. This particular function defines at what pretest level the system switches from psuedo random to random drive. When the assembly language program has been executed, the routine returns to FOCAL and proceeds to execute the next sequential program statement.

With a compact interpreter language, operator dialog can be rapidly constructed for entering test profiles and limits, as well as listing and editing test profiles. Everything connected with the use of the teletype is as simple and short as possible for the average user, but for the more sophisticated user, there is the ability to change certain parameters as desired for special applications and conditions. For example, the dialog can be modified so as to be in Spanish, German, French, etc., averaging times can be changed, psuedo random can be used, etc.

SYSTEM CONTROL PANEL

Since much of the effort put into the SDC Digital Random System centered around the requirement that the system be safe and easy to operate, a new instrument was designed to serve as the system control panel, as well as to house certain system peripherals, such as programmable amplifiers, output low pass filter, and system timing. As a matter of fact, once the test profiles are entered into the system, there is little need for the operator to concern himself with anything other than the control panel and the scope display.

By referring to Figure 5, it can be seen that a different approach than most of the other systems that were available on the market was taken. The test operators may enter tests and recall tests by simply assigning a number to a particular test and then using this number, recall and run those tests using the "Test No" selector. Provisions for inserting ten different test profiles and then recalling, running the tests, plotting the results, etc., without any further intervention of the teletype were made. Thus, the teletype can be removed from the system and stored until additional test profiles or new profiles are desired to be entered. The control panel is sectioned in such a manner as to make its use as simple as practical.

The teletype button, which is on the lefthand side of the control unit in the first section, is used to initiate dialog with the teletype connected to the system. Below that, is a Post Test Data switch whereby different responses and records made during a test can be recalled, displayed, or plotted. The next section to the right is for calibration of the system and the actual process of starting and running a test. The user can define up to four levels below full test so that equalization can be accomplished in steps. The present pretest-level condition of a test is indicated by the LED indicators. This is particularly helpful if many non-linearities are encountered or if there is concern over equalization dynamic range.

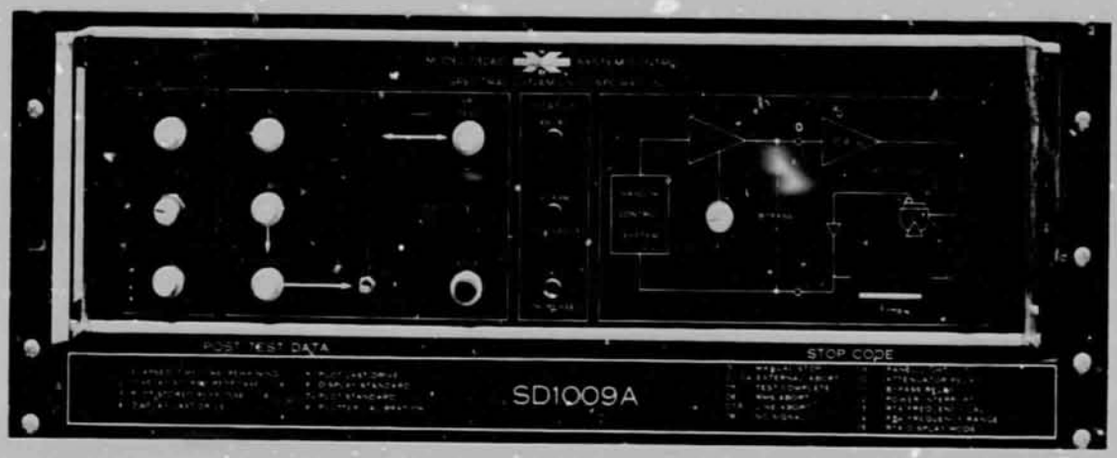

Figure 5. Digital Random System Control Panel

The toggle switch in this section is used for several purposes:

a) During calibration of a test, the toggle switch can be used to adjust the full test level if it is desired to run the same profile shape at a different full test level;

b) After starting a test, the toggle switch can be used to manually control the test level through the various pretest levels; and

c) After a test is terminated, the toggle switch can be used to set the plotter Y-axis span in dB and to select whether or not the plots are "autoranged" or plotted on the same scale as the standard spectrum.

Also in this section is the test number switch whereby a particular test profile can be selected, recalled and run. Below the test number switch is the system STOP button. At any time, the test can be terminated by the STOP button.

The "Status" section in the center of the panel tells whether the test has aborted, whether the system is not equalized within tolerance, or whether additional output gain is needed to reach the full test level.

The righthand section gives the operator a block diagram of how the system is set up and the condition of the test at any particular time. The LED readout on the lower righthand side of the panel is utilized for a multitude of functions. During a test, they indicate the actual overall g_{rms} level of the test, but at any time, this g_{rms} display can be over-ridden by pressing the time button and the actual elapsed time of a test will be displayed.

During a run, if for any reason the test aborts or is stopped, the LED indicators provide 15 different stop codes to inform the operator why the test stopped. These codes can be seen below the control panel on an auxiliary panel that is labeled, "Stop Codes." Also, on the same panel on the left, are the Post Test Data conditions and the data that can be retrieved from the system after a test has been terminated. When plotting data, the LED indicator tells the operator what g^2/Hz value to label the upper decade of his plot.

SYSTEM CONFIGURATION - Conceptual Block Diagram

Figure 6 illustrates the conceptual block diagram of the system. A brief explanation of signal flow through the system follows.

The output of the signal conditioning amplifiers is fed directly into a programmable attenuator. This programmable attenuator, which is under control of the minicomputer, has a primary function to optimize the input signal level of the Real Time Analyzer so that the system is always operating in an optimized dynamic range condition for the analysis of the response pickup. This is a very important consideration since dynamic range, when analyzing random data, is very

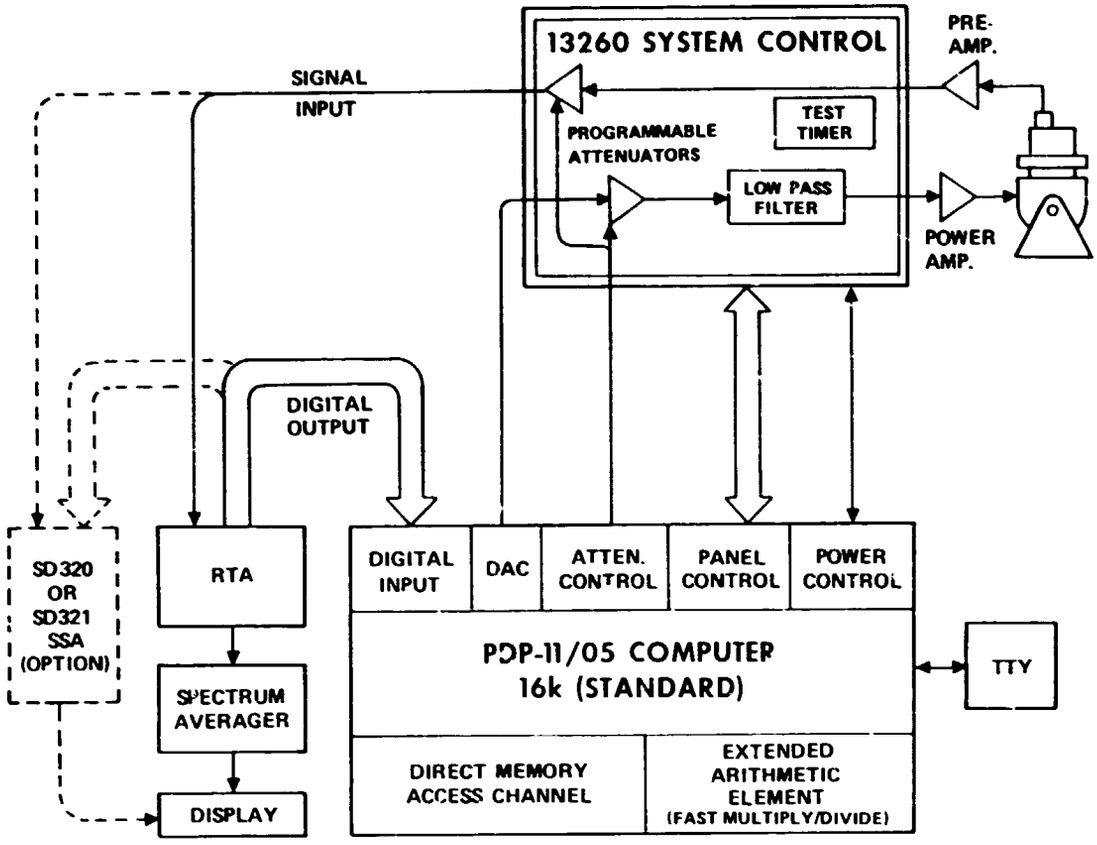

Figure 6. System Block Diagram

important. One of the most common mistakes made when doing random data analysis is not to have the input amplifiers of the Real Time Analyzer up to their maximum level.

The outputs from the Real Time Analyzer go in two directions. One output is fed to the spectrum averager and then to the display oscilloscope. The Real Time Analyzer used has the ability to simultaneously display both the averaged and the unaveraged spectrum data on the oscilloscope, thus alerting the operator for sudden and unexpected changes in the spectrum which, due to the averaging process, would show some time later on the screen. This unaveraged display capability, while new to most operators, is an extremely valuable tool for observing sudden changes in response spectrum.

Another output from the Real Time Analyzer is from the Analog-to-Digital Converter that converts the spectrum amplitude into digital data output to the minicomputer. This data is fed into the computer memory, averaged, and used as the basis for doing the follow-on calculations.

After the input data is compared to the reference spectrum, limit checked, etc., a random time function is fed from the minicomputer through a direct memory access channel and a digital-to-analog converter. This random time function is fed through an additional programmable attenuator whose output is passed through a low pass filter to remove harmonic components that might be generated in the output and then is fed on to the power amplifier and into the shaker. The programmable output attenuator adjusts the correct overall rms level into the power amplifier.

Additional inputs and outputs from the System Control unit are for sensing and controlling the indicator lights of the panel, and for supplying power to the panel. Also contained in the System Control unit is a hardware test timer and provisions for external hardware abort connections. All the essential design requirements for the system are contained in this conceptual block diagram

THEORETICAL CONSIDERATIONS

The equalization speed of any random shaker control system is determined by two main factors:

1. The time it takes to attempt one equalization;

2. The number of equalization attempts necessary to achieve equalization.

A certain amount of trade-off can be exercised between these two points. If one attempt of equalization is based on data with low statistical confidence, the speed of one equalization attempt is high, but a higher number of attempts is necessary to achieve equalization; plus the fact that the resulting equalized spectrum will have a distributed mean which is very undesirable. The Random Shaker Control system minimizes the number of attempts; therefore, input data is needed with a high statistical confidence.

We know from various references the statistical accuracy of a PSD estimate is a function of the effective noise bandwidth of the analysis filter and the time over which the output of the filter is averaged. Mathematically, this can be expressed as:

$$\% \epsilon = \frac{1}{\sqrt{BT}} \times 100, \quad (1)$$

where B is the Noise Bandwidth of the analysis filter and T is the total averaging time in seconds.

Or,

$$\epsilon \text{ dB} = 20 \log \left(1 + \frac{1}{\sqrt{BT}}\right). \quad (2)$$

The above formula is valid for $\epsilon \leq \pm 20\%$.

Since we decided we wanted an ϵ of approximately 12% or ± 1 dB, we could use the above formula.

In the Random Shaker Control system, the Real Time Analyzer produces a 500-line PSD estimate of the accelerometer signal every 50 msec, or twenty 500-line estimates per second, independent of the rate at which the input signal is sampled; that is, independent of the bandwidth of analysis. The RTA samples the input signal at 1½ times the Nyquist rate (equal to 3 times the full scale frequency range); therefore, the 500-line PSD estimate is based on the 1500 sampled values. As long as it takes less than 50 msec to collect the 1500 sampled values (one Memory Period), the PSD estimates produced at 50 msec rate are independent of each other. However, in practical cases the memory period is longer than 50 msec. At 2 kHz for instance, the memory period is 250 msec, resulting in 5 PSD estimates per memory period or about 20% independence of successive PSD estimates. As each PSD estimate is produced, it is averaged with previous estimates. We have termed this redundant averaging.

Although redundant averaging does not contribute to the accuracy of the PSD estimate faster than non-redundant averaging, it does reduce the variance of the estimate faster by reducing the measurement noise due to instrument noise and the beating of nearby frequency components. The accuracy of the PSD estimates in the Random Shaker Control system can be further improved by choosing 1/2 or 1/4 of the measurement resolution for control resolution. In these cases the number of control filters is reduced by a factor of 2, or 4, by combining 2, or 4, PSD frequency components into one filter. The result is that the bandwidth of the control filters is effectively doubled or quadrupled.

Using Equation 2 for 125-line operation of the system, a bandwidth of 4 x noise bandwidth of the 500-line analysis is used since averaging 4 of the 500-line filters gives the reduced resolution of 125 lines. The effective noise bandwidth of the 500-line analysis is approximately equal to 1.5 x the filter spacing. On the 2000 Hz range, the filter spacing is

$$\frac{2000}{500} = 4 \text{ Hz}.$$

$\therefore$ BW = 1.5 x 4 = 6 Hz Noise Bandwidth.

Thus, when four filters are averaged, a BW for 125-line operation equal to 24 Hz is obtained.

Using the criterion of 12% accuracy of the PSD estimate, Equation 1 is used to determine the averaging time.

Solving for

$$T = \frac{1}{\epsilon^2 B} \times 10^4 = \frac{1}{3456} \times 10^4 = 2.9 \text{ sec}.$$

Since redundant averaging was used, or a spectrum is averaged every 0.050 seconds, the closest value to 2.9 sec that was a binary multiple of 0.05; i.e., 2 x 0.05, 4 x 0.05, etc., is chosen (64 x 0.05 = 3.2 seconds).

The reason for a binary multiple is for software simplicity in dividing the resultant averaged values by the number of averages. Thus, the resulting accuracy of the PSD estimate can be computed using Equation 2.

$$T = 64 \text{ avg.} \times 0.05 \text{ sec} = 3.2 \text{ sec.}$$

$$\pm \epsilon \text{ dB} = 20 \log \left(1 + \frac{1}{\sqrt{24 \times 3.2}} \right) = \pm 0.8 \text{ dB.}$$

Another expression of statistical confidence is the number of statistical degrees of freedom based on a Chi Square distribution; or,

$$N = 2BT = \qquad (3)$$

$$2 \times 2^4 \times 3.2 = 154 \text{ statistical degrees of freedom.}$$

It has been generally accepted in the field that 128 degrees of freedom will usually provide accuracy of ± 1 dB in a PSD estimate.

Thus for 125-line operation, the PSD estimate takes 3.2 seconds. The PSD estimate takes 6.4 seconds for 250 lines and for 500 lines takes 12.8 seconds, maintaining in all cases the same PSD statistical accuracy.

The loop time, or the period of one equalization, is defined as the total time that the system takes to:

a) Make the PSD measurement;

b) Compare against the reference spectrum with limit checks;

c) Generate a new drive spectrum; and

d) Inverse FFT to create new drive time function.

This is kept as short as possible so that the PSD measurement will be the major factor controlling speed.

Another design decision made was that once equalization is achieved within ± 1 dB a new drive spectrum or output record is no longer created; thus, removing a large portion of the major overhead in computation and approaching more closely the averaging time as the controlling loop time consideration.

Also decided was that each equalization attempted would correct 100% of the error between the measured response and the reference response. Thus, the following equation is used:

$$\text{New Drive Spectrum} = \frac{\text{Reference Spectrum}}{\text{Response Spectrum}} \times \text{Old Drive Spectrum} \qquad (4)$$

This computation is carried out point by point on the spectra involved, Figure 7. With a perfect PSD measurement and a linear mechanical system, this would reduce the error between measured spectra and desired spectra to zero after only one loop time.

FINAL SYSTEM CONFIGURATION

Figure 8 shows the final system configuration with the display oscilloscope, the control panel, the Real Time Analyzer and the computer.

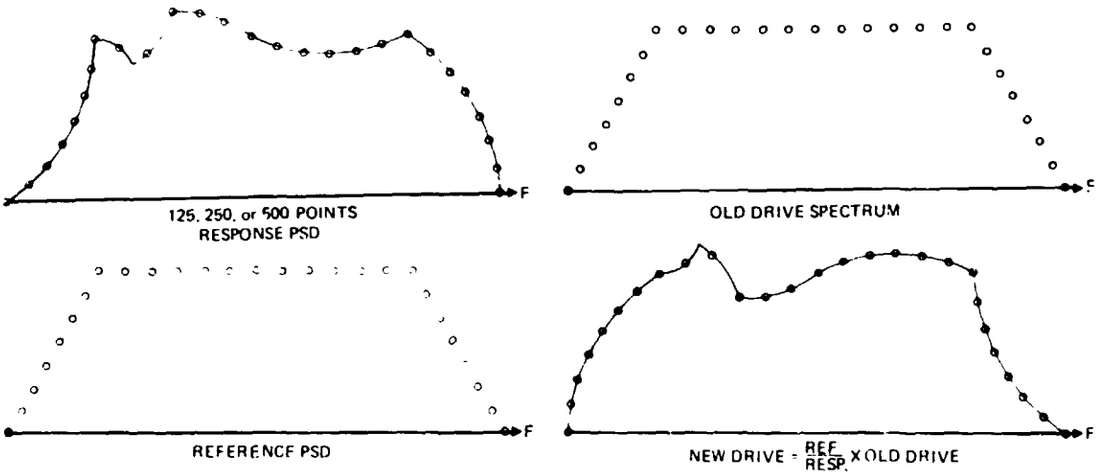

Figure 7. Error Correction for Measured Response

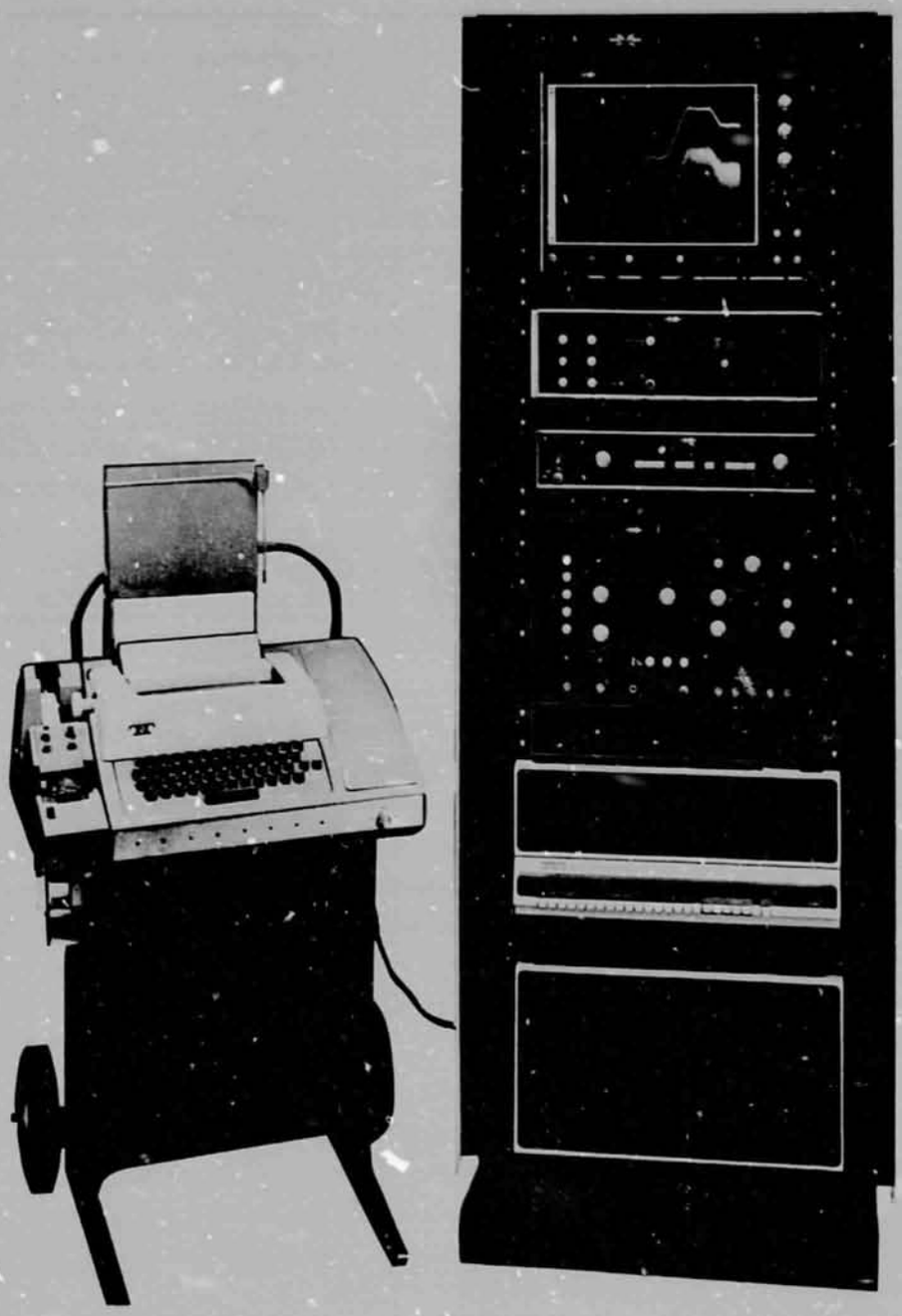

Figure 8. Final System Configuration

Figure 9 shows the data flow through the computer.

Figure 10 shows the system controls necessary to run a test after test profiles have been entered and stored.

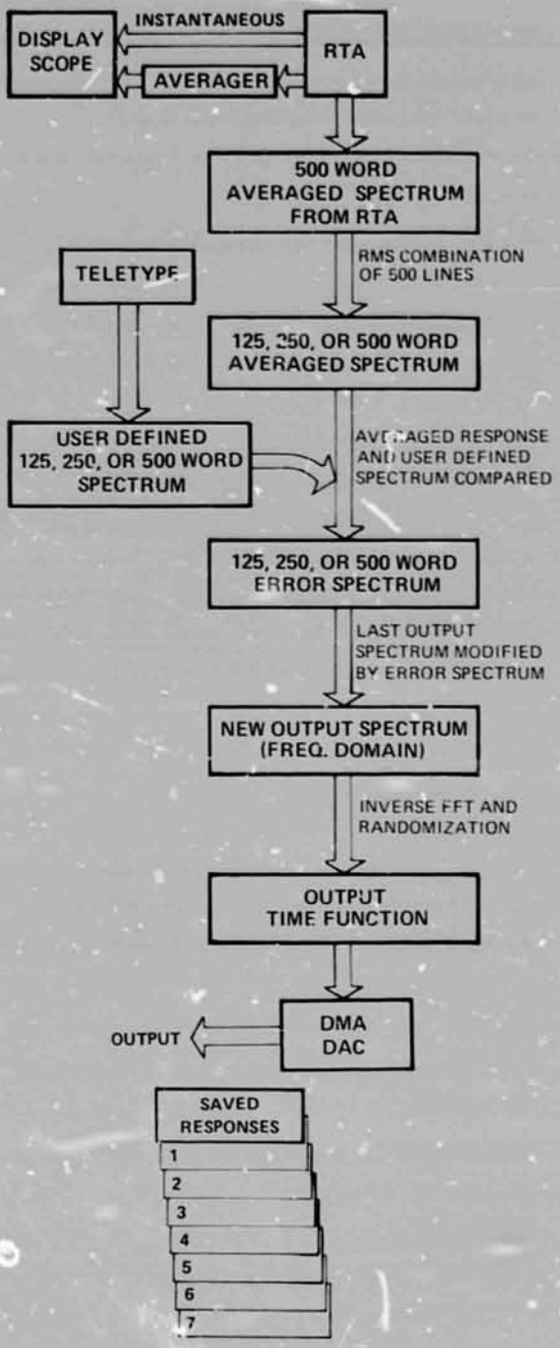

Figure 9. Data Flow Block Diagram

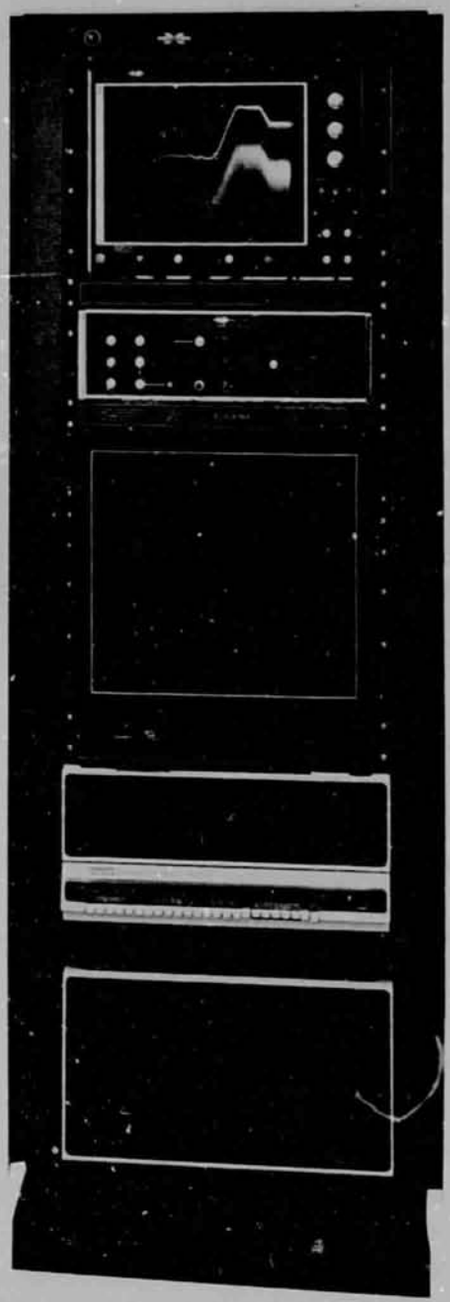

Figure 10. Essential Controls to Run a Test

Of significance is Figure 11 showing the display modes of the Real Time Analyzer with its cursor, dual or single display. Having the cursor eliminates the problem of putting calibrated graticules on the X axis of the scope and provides a rapid method to read the frequency of some point of interest.

Figure 12 shows a typical example of how a test specification can be presented to a system operator. The tolerance/abort and standard spectrum can be entered using discrete frequency and PSD points, or by initial slope and final slope plus discrete frequency and PSD points.

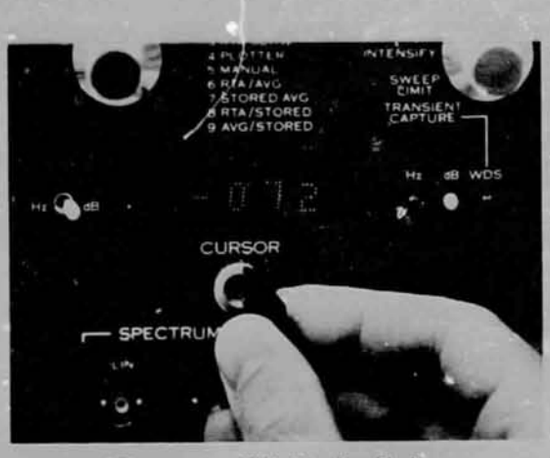

Figure 11. RTA Display Modes

Figure 13 shows the dialog required to enter a test. The example shown is for the specification given in Figure 12.

Once a test is entered, it can be verified by "listing" as shown in Figure 14. Additionally, if a mistake is noted or a modification is desired, the test can be edited as shown in Figure 15. A final listing is shown in Figure 16.

Referring to the test dialog shown in Figure 13, the first line of the dialog is the question, "Output Limit dB relative to 1 Volt?" This is a question that when answered, restricts the level of the output voltage to the power amplifier to a safe level in the event of no feedback from the response pickup.

During the startup phase of the system the system looks for one of two possible conditions to exist:

1) The system output will increase until an overload on the Real Time Analyzer is detected, indicating sufficient signal with which to operate; or,

2) It will simply increase the output level to a limit that is specified in this first question of the dialog.

Lines No. 2, 3, and 4 are self-explanatory. Line 5 asks Automatic mode "Yes" or "No"? In the Automatic mode, once the start button has been depressed, the system will automatically progress through the specified pretest levels. It will equalize at each level, failing to equalize at each level , it will make a preselected number

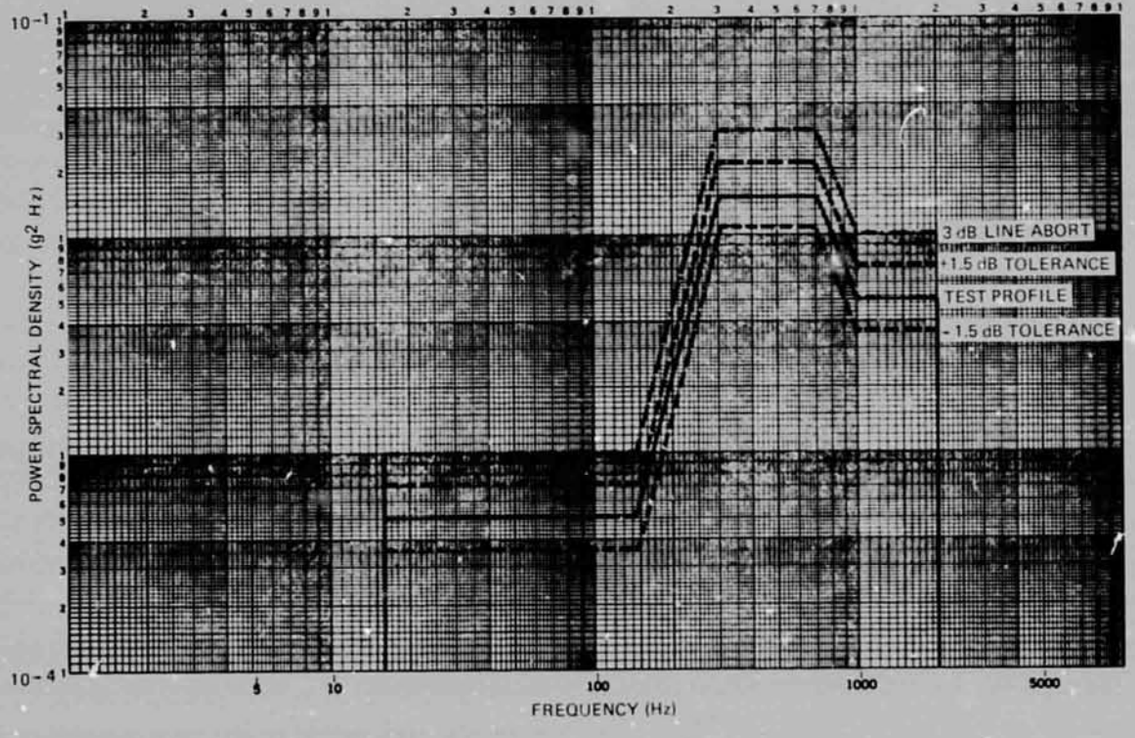

Figure 12. Typical Test Specification

of attempts at equalization at each level, then automatically progress to the next level. This process is continued until the full test level is reached. The test is then run until the timer has been satisfied, or the operator terminates the test.

```
TEST NUMBER:   0
DEFINE? (Y/N): Y
1. OUTPUT LIMIT (DB RE 1 VOLT): 20
2. TEST DURATION (SEC) (0=CONTINUOUS): 120
3. CONTROL RESOLUTION (LINES): 125
4. ACCELEROMETER SENSITIVITY (MV/G): 100
5. AUTOMATIC MODE: (Y/N): Y
6. ENABLE LOOP OPEN FUNCTION: (Y/N): Y
   ARE YOU SURE: (Y/N): Y
7. NUMBER OF PRETEST LEVELS: 2
 PRETEST LEVEL (DB): 6
 PRETEST LEVEL (DB): 3
8. RMS ABORT (DB): 2
9. TOLERANCE & ABORT PROFILE
 NUMBER OF BREAKPOINTS: 2

 BREAKPOINT (HZ): 16
 UPPER TOLERANCE (DB): 3
 LOWER TOLERANCE (DB): 3
 ABORT (DB): 6

 BREAKPOINT (HZ): 2000
 UPPER TOLERANCE (DB): 1.5
 LOWER TOLERANCE (DB): 1.5
 ABORT (DB): 3
10. STANDARD SPECTRUM
 INITIAL SLOPE (DB/OCT): 0
 NUMBER OF BREAKPOINTS: 6

 BREAKPOINT (HZ): 8
 AMPLITUDE (G*G/HZ): 0

 BREAKPOINT (HZ): 16
 AMPLITUDE (G*G/HZ): .0005

 BREAKPOINT (HZ): 150
 AMPLITUDE (G*G/HZ): .0005

 BREAKPOINT (HZ): 300
 AMPLITUDE (G*G/HZ): .015

 BREAKPOINT (HZ): 700
 AMPLITUDE (G*G/HZ): .015

 BREAKPOINT (HZ): 1000
 AMPLITUDE (G*G/HZ): .005
 FINAL   SLOPE (DB/OCT): 0
```

Figure 13. Initial Dialog

Line 6 asks whether or not to enable the Loop Open function. If the response to that is "Yes", it asks the question, "Are you sure?" At full test level, by pressing the Test button an additional time, the feedback loop can be opened and the system continue to output the last equalized drive spectrum into the package. This is particularly useful for doing fixture evaluation and looking at responses of other points on a package. The only danger in this is that all the software limit checking and protection is disabled; thus, the system has no software protection and if no hardware protector is present, then the system would be totally with out protection.

The Loop Open function is provided as a convenience for those who wish to do evaluations and look at responses from other points of a package. In essence, it completely frees the Real Time Analyzer for various other functions, even looking at responses on different frequency ranges. As a matter of fact during operation of the system, the Real Time Analyzer and the Averager have been disconnected and removed from the rack.

Line 7, Number of Pretest Levels, is used to define up to four different pretest levels, which can be defined at any level relative to full test level.

```
TEST NUMBER:   0
DEFINE? (Y/N):
LIST? (Y/N): Y
LIST ALL? (Y/N): Y



TEST NUMBER:   0

1. OUTPUT LIMIT (DB RE 1 VOLT): - 20
2. TEST DURATION (SEC) (0=CONTINUOUS):    120
3. CONTROL RESOLUTION (LINES):  125
4. ACCELEROMETER SENSITIVITY (MV/G):    100.00
5. AUTOMATIC MODE: YES
6. ENABLE LOOP OPEN FUNCTION: YES
7. PRETEST LEVELS (DB):
      - 6
      - 3
8. RMS ABORT (DB):   2.0
9. TOLERANCE & ABORT PROFILE
 BRKPT  +TOLER  -TOLER  +ABORT
   16     3.0    -3.0     6.0
 2000     1.5    -1.5     3.0
10. STANDARD SPECTRUM
 INITIAL SLOPE (DB/OCT):  0.00
 FINAL   SLOPE (DB/OCT):  0.00
 BRKPT (HZ)  AMPLT
      8       0.0000
     16       0.0005
    150       0.0005
    300       0.0150
    700       0.0150
   1000       0.0050
```

Figure 14. Initial Listing

Line 8, Ask for an RMS Abort in dB, if the test level is exceeded by x dB, the system will shut the test down. Undertest, however, is not protected except for loss of feed back.

Line 9 is fairly self-explanatory. The tolerance and abort profiles are entered, the same as a standard spectrum is entered. The upper and lower tolerance in dB is referred to the level of the standard spectrum. The abort level is an imaginary line that rides on the top of the upper tolerance profile and if any particular spectral line exceeds the specified dB relative to the standard, it will shut the test down.

Line 10 is the dialog used to enter the standard spectrum. It, once again, is self-explanatory.

```
TEST NUMBER:   0
DEFINE? (Y/N):
LIST? (Y/N):
EDIT? (Y/N): Y
LINE NUMBER: 3


3. CONTROL RESOLUTION (LINES): 250


LINE NUMBER: 7


7. NUMBER OF PRETEST LEVELS: 3
 PRETEST LEVEL (DB): 9
 PRETEST LEVEL (DB): 6
 PRETEST LEVEL (DB): 3


LINE NUMBER:
```

Figure 15. Editing

```
TEST NUMBER:   0
DEFINE? (Y/N):
LIST? (Y/N): Y
LIST ALL? (Y/N): Y


TEST NUMBER:   0

1. OUTPUT LIMIT (DB RE 1 VOLT): - 20
2. TEST DURATION (SEC) (0=CONTINUOUS):   120
3. CONTROL RESOLUTION (LINES):  250
4. ACCELEROMETER SENSITIVITY (MV/G):   100.00
5. AUTOMATIC MODE: YES
6. ENABLE LOOP OPEN FUNCTION: YES
7. PRETEST LEVELS (DB):
      - 9
      - 6
      - 3
8. RMS ABORT (DB):   2.0
9. TOLERANCE & ABORT PROFILE
 BRKPT  +TOLER  -TOLER  +ABORT
   16     3.0    -3.0     6.0
 2000     1.5    -1.5     3.0
10. STANDARD SPECTRUM
 INITIAL SLOPE (DB/OCT):  0.00
 FINAL   SLOPE (DB/OCT):  0.00
 BRKPT (HZ)  AMPLT
      8      0.0000
     16      0.0005
    130      0.0005
    300      0.0150
    700      0.0150
   1000      0.0050
```

Figure 16. Final Listing

Put yourself in the place of an operator and take a look at Figure 17. How do you run a test?

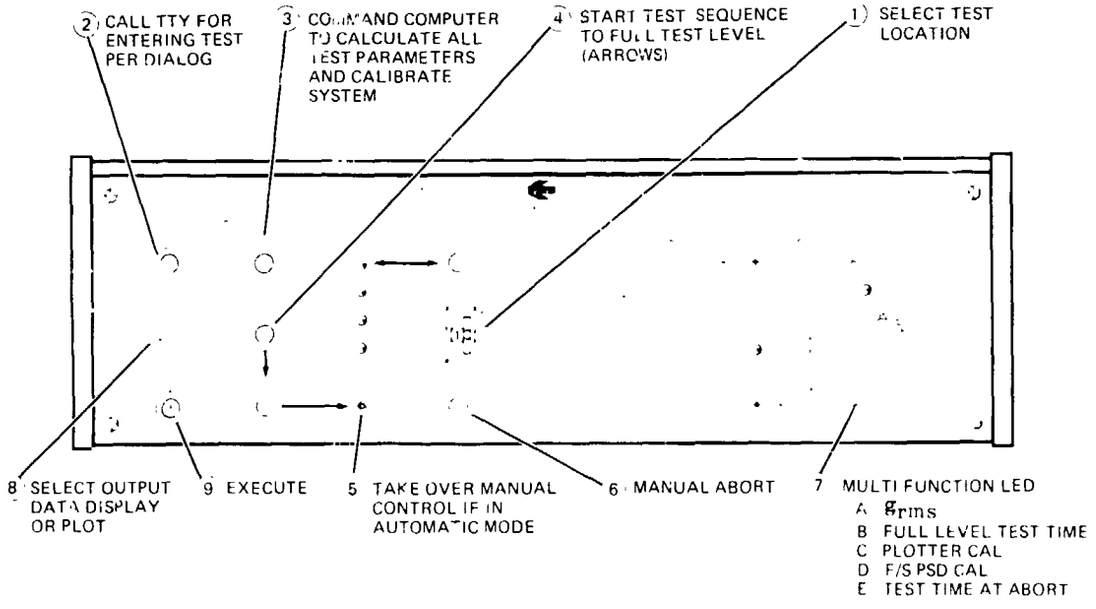

Figure 17. Typical Test Sequence

First, assume that a test profile has been defined and assigned the test number 5. Dial "5" into the TEST NUMBER switch and press START. If a system calibration is necessary, the CAL light turns on, and the system does a full calibration and functional check. When this is complete, the STOP light comes on. Now, pressing the START button turns on the START lamp and starts the full test sequence. Note that the system will not allow the test to proceed until a proper calibration is performed. If the same test is run repeatedly, a CAL is necessary only for the first run. This is the type of operational "interlocks" built into the system software to insure safe operation.

If the Automatic mode in the TTY dialog is specified for test 5, the operator simply sits back and watches. The system now equalizes at each of the pre-defined pretest levels. As equalization is accomplished, or with a preselected number of tries to equalize (if equalization is not achieved within the test tolerances), the system steps to the next pretest level and again attempts to equalize. Following the last pretest level, the system increases the drive level to full test level, and turns on the TEST lamp.

From the operator's standpoint, he must keep in mind only two rules:

1. He can never start a test without intentionally pressing START;

2. He can stop a test at any time by pressing STOP.

If the test is to be timed, the system automatically shuts off at the end of the test time and indicates an 05 in the numeric indicator. If the system should abort, the numeric indicator shows the operator the reason:

01 External Abort #1

02 External Abort #2

03 External Abort #3

04 External Abort #4

The External Abort signals are simply contact closures which are connected to the system through the control panel. Each pair of contact lines may be jumpered for Normally Open or Normally Closed operation. These signals would typically indicate system "status" lines such as shaker overtravel, power amplifier overheating, or hand-held push button switches held by test observers.

06 RMS Abort (the rms level has exceeded the abort limit)

07 Line Abort (one or more spectrum amplitudes have exceeded the abort limit)

08 Loss of input signal

During the test, the operator is informed about what the system is doing through the Real Time Spectrum display and the system front panel. The oscilloscope display gives a continuous look at the actual power spectrum achieved at the control accelerometer. The LED numeric readout on the system panel shows the g_{rms} level at the accelerometer. If the operator wishes, he can press the TIME button, and momentarily override the g_{rms} display and show the elapsed time for the test. Releasing this button again shows the g_{rms} level.

Three indicators tell the operator how accurately the system is achieving equalization. If the yellow GAIN light is on, the system (including the system power amplifier) needs more gain to reach full test level. This light is active during all startup modes (START and PRETEST) as well as in the TEST mode, to alert the operator to increase the system gain, either with the control panel OUTPUT GAIN control, or with the power amplifier gain control.

The green TOLERANCE light tells the operator that the system is not equalized to within the specifications called out in the input dialog. The red ABORT light signals any premature interruption of the test.

During the test, the operator may choose to store PSD spectra at any time for plotting at the conclusion of the test. He does this by pressing the POST TEST DATA button. The spectrum thus stored is assigned a number which appears momentarily in the numeric indicator. The POST TEST rotary switch can then be used at the test conclusion to reference and plot these spectra.

Since the test verification is really the "final product" of any vibration test, considerable attention has been paid to producing calibrated hard copy plots of the accelerometer PSD. Since the computer is in control of the system gain settings at all times, the calibration of each plot is done automatically, and the operator is alerted as to the full scale value of each plot via the numeric indicator on the control panel.

EXPANSION CAPABILITIES

Shock Synthesis And Analysis

Expansion of the system for shock work on shakers is accomplished by simply substituting either the standard Model SD320 or SD321 Extended Memory Shock Spectrum Analyzer for the Real Time Analyzer in the Random System and loading new software into the PDP-11 Computer. The system has three decades of frequency coverage, 10 to 10,000 Hz, 1 to 1,000 Hz and by using the Extended Memory, 0.1 to 100 Hz for seismic and transportation work. Specially designed phase equalized aliasing filters are used to preserve integrity of the input transient. A sampling rate of four times the upper frequency limit is used to permit optimum rolloff and rejection by the aliasing filter.

Block Diagram Figure 6 illustrates the simplicity of the interchange of the independent analyzers in the system.

Figure 18 shows the Extended Memory Shock Spectrum Analyzer mounted in a companion rack for mating with the Random System.

Analysis

The Shock Spectrum Analyzer consists of a digital input memory, an analog section for high speed analysis and both digital and analog outputs. When not in use for closed loop system operation, the analyzer can be used as a stand-alone unit.

Analysis speed depends upon the amount of data stored in input memory. Functionally, data is analyzed at a rate of 4,000 words in two seconds. Primarily for seismic work, the Extended Memory version of the analyzer permits selection of up to 40,000 words of data in 4,000 word increments. Maximum analysis time under this condition would be 20 seconds.

The analyzer's performance in the system provides extremely fast feedback information for the computer to permit rapid re-definition of an input time history to the vibration shock testing system. The transient stored in Memory or the shock response spectrum may be viewed on an oscilloscope. See Figure 18.

Synthesis

The Wavelet Amplitude Equalization (WAE) technique is employed for shock synthesis in the system. The technique has been well described in technical literature and will not be expanded upon in this paper. Shock synthesis can be performed on either 1/3, or 1/6, octave spacing as defined by the operator. A simple dialog sequence is performed by the operator to select resolution on either a 1/3, or 1/6, octave spacing together with the number (up to 4) of pre-test excitation levels to be used in coming up to full test. The operator selects the frequency and amplitude breakpoints of the desired response spectrum profile, or individually defines each wavelet's amplitude and delay. When the spectrum profile approach is used, the computer calculates the least energy required to meet the desired spectrum amplitude and automatically adjusts each wavelet accordingly. As in the Random System, 10 test profiles may be stored and recalled by front panel control selection.

Response data from the package is fed into the input of the analyzer where analysis is performed on 1/3, 1/6 or 1/12 octave basis at whatever damping has been selected for the test. Data can be directly output to an X-Y plotter at this point. The digitally stored response spectra information is automatically fed back to the computer where a new output waveform series can be generated for output to the system if desired.

Sine Testing

Originally, it was inconceivable to SDC designers that anyone would use an expensive system of the type described above to do sine testing. We already make several relatively inexpensive analog sine controllers that are simple to operate. Lately, we are finding that more of our customers are interested in sine control expansion. We have plans to add this capability in the future.

FINAL SYSTEM PERFORMANCE SUMMARY

Frequency Ranges:

Standard - 2 kHz
Highest Range - 5 kHz
Other Ranges - Optional

Control Resolution:

125, 250, or 500 filter elements

Core Requirements: 16k per 125 lines operation, 24k for 250 and 500 lines.

Dynamic Range:

Standard Spec. cannot exceed 30 dB.

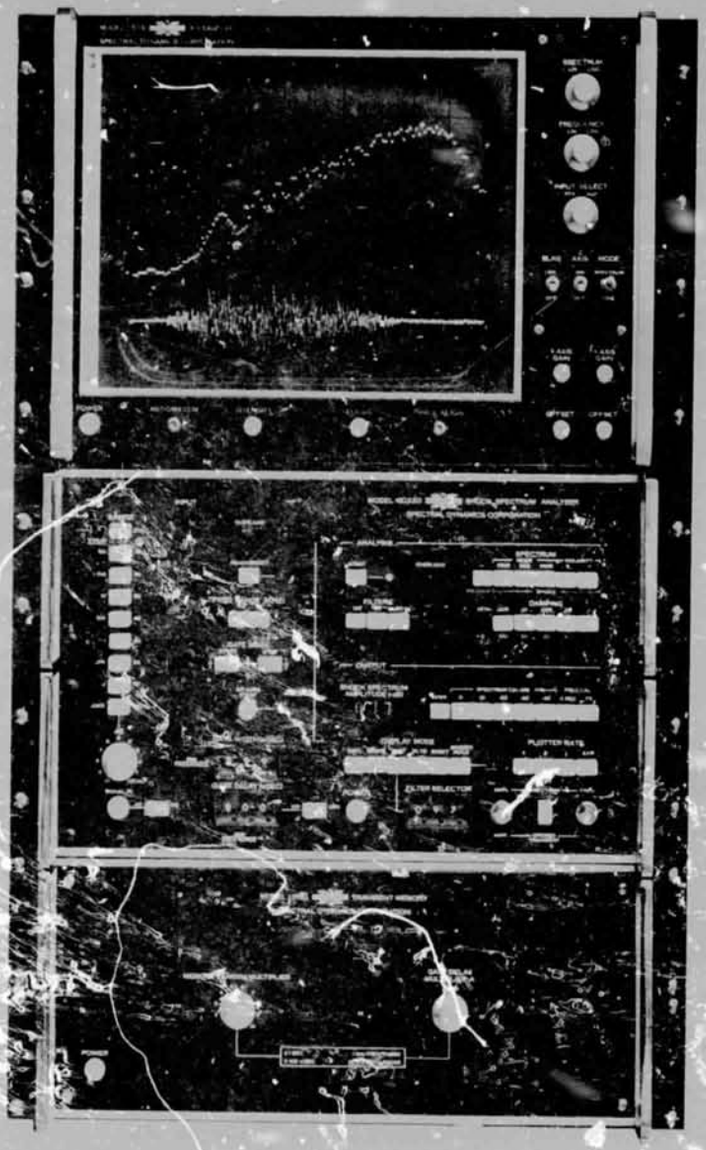

Figure 18. Extended Memory Shock Spectrum Analysis System

Output Drive Spectrum: Greater than 60 dB.

Equalization Speed.

125 lines - 4.65 seconds
250 lines - 8.6 seconds
500 lines - 16.5 seconds

Max. Output Level: 20 V peak-to-peak

Statistical Confidence of PSD estimates:

Program adjustable - ± 0.8 dB standard.

Output Waveform: Gaussian Random Noise or Psudeo Random Noise with Three Sigma peak limiting.

Dialog: Entering a test requires answering ten questions - Standard and tolerance/abort spectra can be entered as discrete frequency and amplitude points, or by initial and final slopes plus discrete frequency and amplitude points. Points are joined together so as to straight lines on a log frequency, log amplitude scale.

Automatic Mode. Brings system up automatically and proceeds automatically through the pretest levels up to full test level.

Loop Open: System continues to output last equalized random spectrum. Analyzer can be used independently in Loop Open mode.

Response Records: At any time during test or pretest operation, a record of the response accelerometer can be saved. Three records can be saved in the 16k system. Up to seven records can be made in the 24k system except when using 500-line resolution, only five can be saved.

Limit Checks and Aborts: Standard spectrum is compared with the response spectrum; then the profile tolerance comparison is done on a relative "shape" basis. Abort levels are checked on an "absolute level" basis. No input signal,or loss of input signal is an abort check.

Software: System comes loaded with FOCAL interpreter and all software required for Random Control. Diagnostic software is also supplied.

CONCLUSIONS

By beginning with specific guidelines for a system configuration, the evolution of a simple-to-operate automatic control system with built-in safety protection has been shown. Sample software routines have been given to show the ease with which test routines can be established and modified. By using the Real Time Analyzer for basic PSD computation, not only has test visibility been greatly increased, but analysis flexibility has been increased through overlapped processing, and system costs kept to a minimum using proven, off-the-shelf hardware.

Michael K. Stauffer

TECHNIQUES FOR NARROWBAND RANDOM OR SINE ON WIDEBAND RANDOM VIBRATION TESTING WITH A DIGITAL CONTROL SYSTEM

Michael K. Stauffer
Time/Data Corporation
Palo Alto, California

Random Sine, and Shock vibration control and testing programs were previously implemented in Digital Control Systems using the same basic hardware. To take full advantage of this existing digital control hardware, new programs are being developed for testing other environments which have been limited to analog hardware. Two of these programs now available are "Swept Narrowband on Broadband Random Vibration Control" and "Swept Sine on Random Vibration Control". Although these programs use the same hardware as the basic Digital Control Systems, their unique environments required special techniques to achieve the test criteria. The techniques for implementing these new programs are described here in two parts.

PART I. DIGITAL SWEPT NARROW BAND ON BROADBAND RANDOM VIBRATION CONTROL SYSTEM

INTRODUCTION TO PART I

Part I of this paper describes a digital narrowband on broadband random vibration control system. The system has been implemented by modifying a standard digital vibration control system such that the reference spectrum is the superposition of a static broadband spectrum and a sweeping narrowband spectrum. Depending upon test philosophy, superposition is defined in at least two ways:

1. The sum of the narrow and broad spectrum amplitudes at each frequency.
2. The maximum amplitude of the narrow or broadband spectrum (that is, whichever is greater) at each frequency.

In the case of summing the two spectrums, overall GRMS level is constant as the narrowband spectrum sweeps. For the case of controlling to the maximum, the GRMS level varies as the narrowband spectrum sweeps. Controlling to the sum is obviously a more severe test than controlling to the maximum. The system described here allows for control to either the sum or the maximum of the narrowband and broadband reference spectrums.

GENERAL DESCRIPTION

The control system shown in Fig. 1, is built around a standard minicomputer and a 200 kHz data acquisition system that serve as the heart of a family of signal analysis and shock and vibration products (1-5). The hardware configuration is identical to that of a standard random vibration control system as shown in Fig. 2. Narrowband on broadband vibration control is obtained by executing the appropriate software in the minicomputer. A single output channel of shaped random Gaussian noise is generated to drive a shaker system, and a single channel is sampled and controlled.

Operator interaction with the system occurs in two ways. A switch control panel, shown in Fig. 3, is used to select system functions and to execute control commands, while an alphanumeric keyboard is used to enter test parameters.

IMPLEMENTATION

A functional block diagram of the control strategy is shown in Fig. 4. Basically, the system attempts to control the amplitude of a designated control signal to match the amplitude of an operator-specified swept narrowband on broadband reference spectrum by continuously adjusting the random noise drive signal at each frequency. This drive adjustment compensates for nulls and resonances in the shaker system transfer function. The control strategy is identical to that

Fig. 1. Random Vibration Control System Hardware

used in the standard random vibration control system described by Norin[3].

Instead of a single reference spectrum, three reference spectrums are maintained in computer memory. These are the broadband, narrowband, and superimposed spectra. The broadband and narrowband spectra are specified by a conversational setup routine and, once generated, remain static throughout a test. The superimposed spectrum is the sum or the maximum value of the broad and sweeping narrowband spectra. The narrowband spectrum is swept across the broadband spectrum by updating an index variable (INDX) which denotes the relative position of the narrowband and broadband spectra origins in terms of spectral lines. The data values representing the narrowband spectrum never actually shift position in memory. Whenever INDX changes a new total reference spectrum is generated by combining the broadband and the "shifted" narrowband spectra. The narrowband spectrum is extended into an extra buffer to maintain continuity in the combined spectrum when the narrowband spectra sweeps toward lower frequencies.

SWEEP TIMING AND FREQUENCY UPDATE

Sweep timing is obtained from the end-of-frame interrupts generated by the data acquisition and output hardware. Given the desired sweep rate, the sampling rate, and the number of samples per output frame, a frequency change per interrupt is calculated. This frequency change is positive for increasing fre-

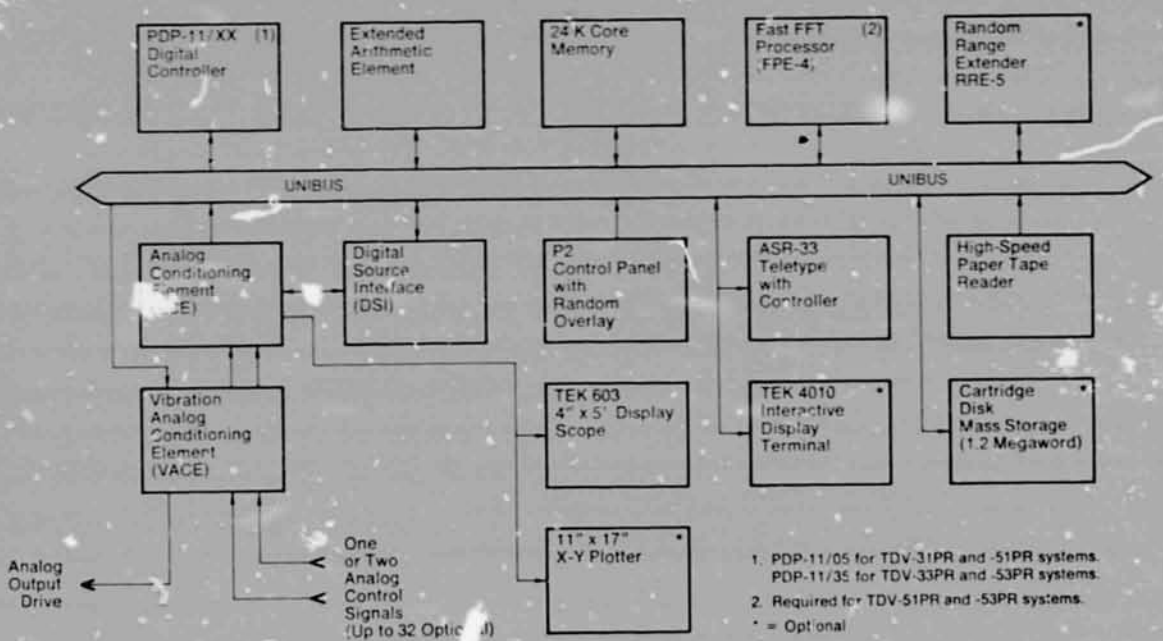

Fig. 2. Block Diagram of Hardware Configuration

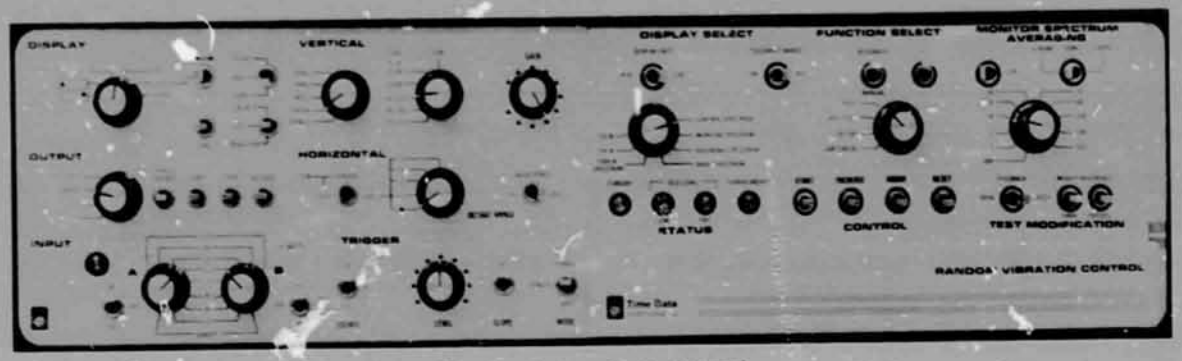

Fig. 3. System Control Panel

quency sweeps and negative for decreasing frequency sweeps. The sign of this frequency change is complemented each time a sweep limit is reached.

The flow chart in Fig. 5 shows how the sweep operates. Interrupts are accumulated in a counter variable. Once each loop time a frequency accumulator representing the present frequency of the right-most narrowband spectrum breakpoint is updated by a value equal to the number of interrupts times the frequency change per interrupt. The interrupt accumulator is then reset to zero. An integer variable (NEWINL) is updated by:

$$\text{NEWIND} = \frac{\text{Right-most narrow breakpoint frequency}}{\text{Frequency change per spectral line}}$$

If NEWIND changes, so must the superimposed spectra, and the shifted narrow spectrum is combined with the broadband spectrum to generate a new superimposed reference spectra. The variable INDX discussed previously is also updated whenever NEWIND changes.

When sweeping towards higher frequencies, the frequency at the highest narrowband spectrum breakpoint is compared to the operator-specified upper sweep limit. If it equals or exceeds this limit, the sweep direction is reversed. When sweeping toward lower frequencies, the frequency of the lowest narrowband spectrum breakpoint is compared to the lower sweep limit. If it is less than or equal to this limit, sweep direction is reversed.

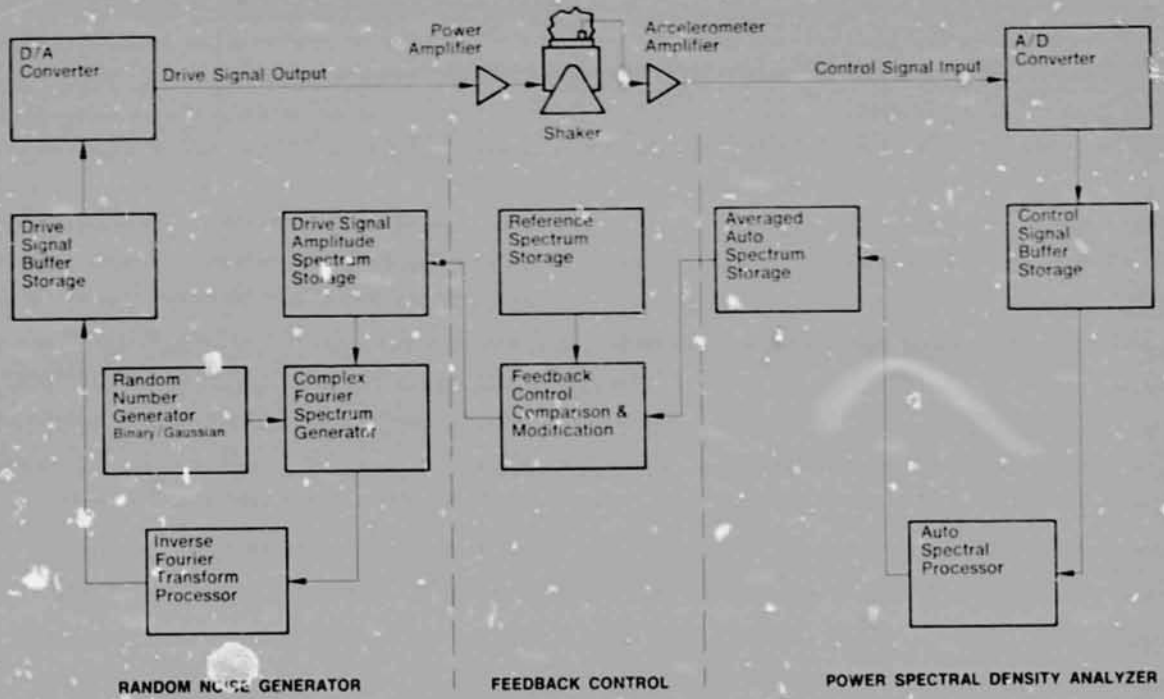

Fig. 4. Functional Block Diagram

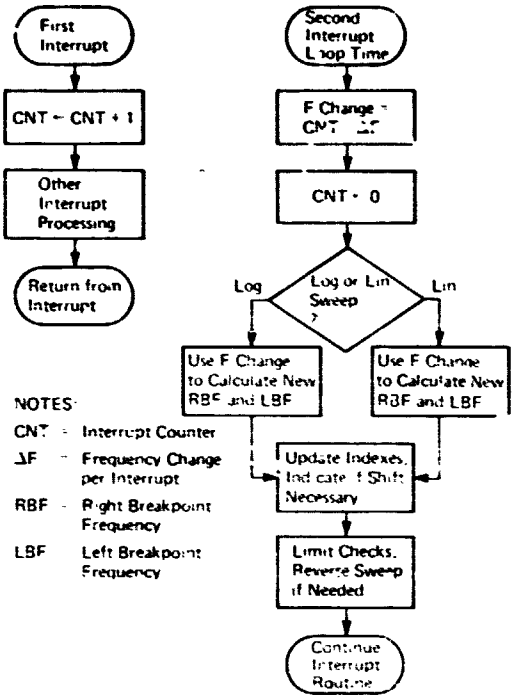

Fig. 5. Narrowband on Broadband Flow Chart of Sweep Frequency Updating

TYPICAL SYSTEM OPERATION

Parameters of a typical swept narrowband on broadband random vibration control test are shown in Fig. 6. Note that specification of the narrowband spectrum is similar to broadband spectrum setup with the exception of alarm limits. Note also the superposition option of SUM or MAX and the LOG/LINEAR sweep and INITIAL DIRECTION options under SWEEP PARAMETERS.

Displays of the combined reference spectrum at various times throughout a test are shown in Fig. 7. The control spectrum follows this reference spectrum rather closely during the test. How closely depends on the spectrum shapes and the sweep rate.

SUMMARY OF PART I

Part I of this paper discussed one implementation of a digital swept narrowband on broadband random vibration control system. By utilizing the same hardware as a series of other basic vibration testing programs (random, shock, sine), this software is a flexible and economic supplement to the basic capabilities of the testing laboratory.

PART II. DIGITAL SWEPT SINE ON RANDOM VIBRATION CONTROL SYSTEM

INTRODUCTION TO PART II

Part II of this paper explores several techniques for the implementation of a digital swept sine on random vibration control system. These techniques differ primarily in the cost-performance tradeoffs associated with the sine frequency generation method and the sine control strategy. Discussion begins with the least expensive and lowest performance method and proceeds through the increasingly expensive and higher performance methods. The limitations and reasons for the limitations of each method are also discussed.

METHOD I

This method is the least expensive in terms of add-on hardware to the basic system hardware required for a flexible vibration control system. The hardware configuration, shown in Fig. 1, is that of a standard vibration control system (1-5).

The block diagram in Fig. 8 outlines the basic control strategy. An estimate of the shaker system transfer function is obtained from the input and output power spectral densities using the method described by Norin[3]. This transfer function estimate is used in the random control algorithm exactly as explained by Norin[3]. The sine control algorithm uses this same transfer function estimate in a similar manner, but it is otherwise independent of the random control strategy.

An estimate of the sine control value is obtained as follows:

$$\text{SINE CONTROL} = H(f_s) \cdot \text{SINE DRIVE}$$

where SINE DRIVE was the amplitude of the sine drive output while $H(f_s)$, the transfer function estimate at the sine frequency, was calculated.

The sine control estimate is compared to a sine reference value which remains constant in amplitude but varies in frequency according to the type and rate of sweep. The error between the control and reference indicates how to update the sine drive value to compensate for the shaker transfer function.

This technique has the advantage that no bandpass filter is required to extract the sine energy from the sine plus random control signal. The reason for this is that the sine control is calculated from the product of the known sine drive and the transfer function estimate. Because of the way it is calculated, the transfer function estimate is the same whether or not a

```
ENTER PARAMETERS 1=YES 0=NO: 0

CORRECTIONS 1=YES 0=NO: 0

LIST 1=YES 0=NO: 1

1 TEST ID: PARAMS

2 HEADING: TEST 1

3 BANDWIDTH: 2048.

4 RESOLUTION 64/128/256/512: 128.0
FREQUENCY INCREMENT: 16.00

BROADBAND REFERENCE SPECTRUM:
5 INITIAL SLOPE, DB/OCT: 0.000
   ALARM LIMIT DB : 6.000

6 FREQUENCY     HZ.: 384.0
   LEVEL  GSQR/HZ.: 1.000
   ALARM LIMIT DB : 6.000

7 FREQUENCY     HZ.: 496.0
   LEVEL  GSQR/HZ.: 1.000
   ALARM LIMIT DB : 6.000

8 FREQUENCY     HZ.: 640.0
   LEVEL  GSQR/HZ.: .1000
   ALARM LIMIT DB : 6.000

9 FREQUENCY     HZ.: 1376.
   LEVEL  GSQR/HZ.: .1000
   ALARM LIMIT DB : 6.000

10 FREQUENCY    HZ.: 1600.
   LEVEL  GSQR/HZ.: 1.000
   ALARM LIMIT DB : 6.000

11 FREQUENCY    HZ.: 1792.
   LEVEL  GSQR/HZ.: 1.000
   ALARM LIMIT DB : 6.000

12 FINAL SLOPE, DB/OCT: -48.00

BROAD GRMS : 27.43
```

NOTE: Frequencies were automatically adjusted by program to an integral multiple of the frequency increment.

```
13 SUM OR MAX OF BRD/NRW 1=MAX,0=SUM: 0

NARROWBAND REFERENCE SPECTRUM:
14 INITIAL SLOPE, DB/OCT: 64.00

15 FREQUENCY    HZ.: 992.0
   LEVEL  GSQR/HZ.: 1.000

16 FREQUENCY    HZ.: 1200.
   LEVEL  GSQR/HZ.: 1.000

17 FINAL SLOPE, DB/OCT: -64.00

NARROW GRMS : 17.67
TOTAL GRMS : 32.63

18 SWEEP PARAMETERS:
 MODE 1=LOG,2=LIN: 0
 RATE, HZ./SEC:  6.000
 INITIAL DIRECTION  1=UP, 2=DOWN: 1

19 LOWER SWEEP LIMIT, HZ.: 400.0
20 UPPER SWEEP LIMIT, HZ.: 1500.
21 LOW LEVEL, -DB: -20.00
22 LEVEL INCREMENT, DB: 2.000
23 START-UP TIME SEC: .6251
24 SHUT-DOWN TIME SEC: .9377
25 TEST TIME HRS, MIN, SEC: 0,4,0
26 CONTROL CHANNELS: 1
27 ACCEL SENS MV/G: 10.00
28 DRIVE CLIPPING 1=YES,0=NO: 0
29 ABORT LEVEL GRMS: 60.00
30 ALARM LINES: 1,3,5
31 ABORT LINES: 14,16

CORRECTIONS 1=YES 0=NO: 0

LIST 1=YES 0=NO: 0

SAVE 1=YES 0=NO: 0
```

Fig. 6. Listing of Setup Parameters for Narrowband on Broadband

sine is superimposed on the random signal. This, of course, also means that the sine energy does not affect the random control signal since it is calculated in a similar manner.

In Method I the sine drive amplitude is adjusted on frequency data stored as a buffer of discrete, evenly spaced sine frequencies. The number of discrete sine frequencies is equal to the number of spectral lines in the random spectrum. The frequency difference, Δf, between adjacent sines is:

$$\Delta f = \frac{\text{random spectrum bandwidth}}{\text{resolution (number of spectral lines)}}$$

The inverse Fourier transform of this sine amplitude buffer is calculated to generate a buffer of time domain data representing the actual sinusoidal time waveform. This buffer is added to the random data buffer, and the sum is output through the digital-to-analog converter.

SWEEP MECHANISM

Sweep timing is obtained from end-of-frame interrupts generated by the data acquisition and output hardware. Given the desired sweep rate, the sampling rate, and the number of samples per frame, a frequency change

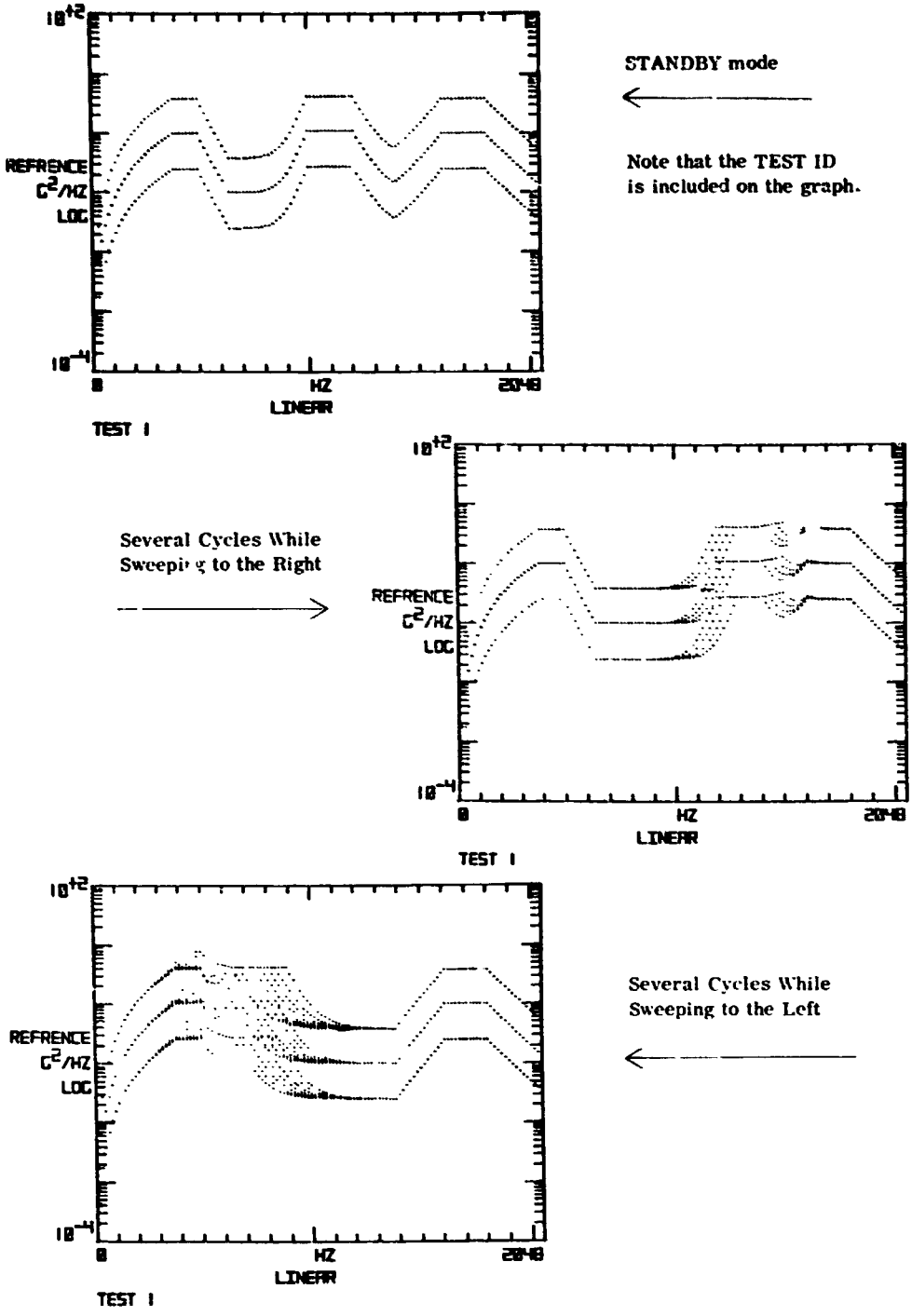

Fig. 7. Swept Narrowband on Broadband Reference Spectra

per interrupt is calculated. This frequency change is positive for increasing frequency sweeps and negative for decreasing frequency sweeps. The sign of this frequency change is complemented each time a sweep limit is reached. The flow chart in Fig. 9 shows how the sweep operates.

Interrupts are accumulated in a counter variable. Once each loop time a frequency accumulator for each sine is updated by a value equal to the number of interrupts times the frequency change per interrupt. The number-of-interrupts counter is then set to zero. Next a frequency index variable for each sine is cal-

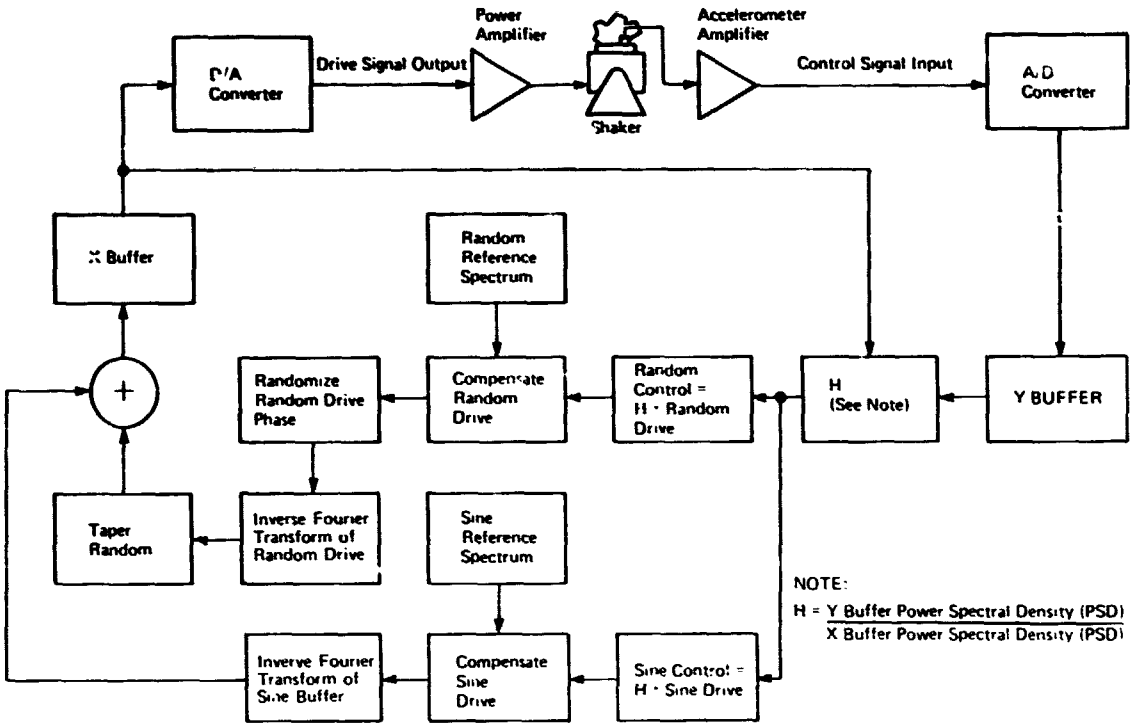

Fig. 8. Swept Sine on Random Basic Control Strategy Block Diagram

culated from:

$$\text{FREQ INDEX} = \frac{\text{FREQUENCY ACCUMULATOR}}{\text{FREQUENCY CHANGE PER SPECTRAL LINE } (\Delta f)}$$

This index is the new sine frequency (it may be unchanged).

When full test level is reached, the sine waves sweep synchronously up or down at a user-programmed rate (linear or logarithmic) until a limit frequency is reached by one of the sine waves. The sine waves then reverse direction, sweeping at the same rate until the opposite limit frequency is reached by one of the sine waves. The sine waves again reverse direction and continue sweeping back and forth in this manner until test time expires.

LIMITATIONS

Method I has some fundamental limitations on the basic sine resolution and the sweep resolution. As mentioned previously, the fundamental sine resolution is limited to Δf as calculated above because the time domain sine waveform is generated by an inverse Fourier transform. Also, since the sweeping sine frequencies are updated once each loop time, the sweep resolution (increment) is limited by the sweep rate and Δf (bandwidth/resolution). The relationship is:

$$\text{MAXIMUM SWEEP RATE FOR A SINE RESOLUTION OF } \Delta f = \Delta f \text{ LOOP TIME}$$

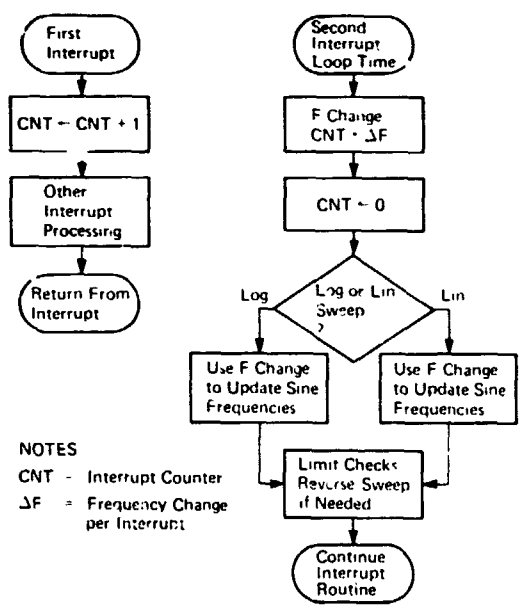

Fig. 9. Swept Sine on Random Flow Chart of Sweep Frequency Updating

If Δf is 16 Hz and the loop time is two seconds, then the maximum accurate sweep rate = 16 Hz/2 sec = 8 Hz/sec. That is, the sines will increment by one spectral line (16 Hz) each loop time. If a sweep rate of 32 Hz/sec were specified with a loop time of two seconds, the discrete sine frequencies would step in 64 Hz increments. Thus, the program provides better swept sine resolution at lower sweep rates.

The sine frequency is not updated more often than once per loop time because of the processing time required to perform the inverse Fourier transform.

HOW TO IMPROVE SINE RESOLUTION

At least two different sine generation methods can be used to obtain better sine frequency resolution; a software sine table lookup or a hardware sine synthesizer (Method II and Method III, respectively).

METHOD II

To obtain finer sine resolution without additional hardware, the sine values can be generated by a table look-up procedure, as is done in some hardware digital sine synthesizers[6]. Amplitude control is accomplished by multiplication of each sine point by the amplitude factor produced by a control strategy similar to that used in Method I. Sine values obtained from the look-up table are multiplied by the amplitude factor and added directly to the tapered random output buffer. This sum buffer is then output through the digital-to-analog converter. The sine generation procedure is continuous and oblivious to output buffer boundaries. Figure 10 shows how this procedure works.

In addition to having increased resolution, this technique does not require an inverse Fourier transform. However, a multiplication is required for each output point. The number of multiplications increases with the number of sines, thus placing limitations on bandwidth (bandwidth is related to how fast points can be output).

Control strategies for random and sine can be the same as in Method I, or modified as explained below.

METHOD III

Bandwidth limitations imposed by Method II can be overcome by adding a hardware sine synthesizer to the system described in Method I. Figure 11 is a block diagram of a single sine system of this type.

It is desirable to use strategies similar to the above methods for random and sine control. However,

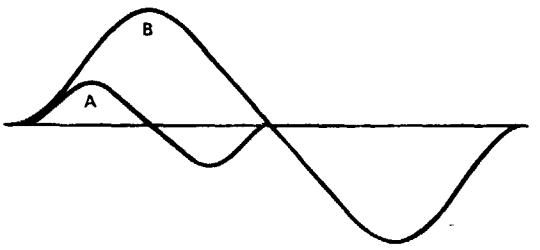

NOTES.
A = Inverse Fourier Transform (IFT) Generation
B = Table Lookup
B has twice the resolution of A and can get even better resolution

Fig. 10. Table-Lookup Buffer Overlap

since the sine is superimposed on the random in the analog domain, no digital information exists for this sum which is the input to the shaker system. Therefore, a second analog-to-digital conversion channel can be used to sample this analog sum simultaneously with the output of the shaker system. This sampled data is equivalent to the digital sum of the sine and random data output through the digital-to-analog converter in Method I.

Therefore, the techniques discussed in Method I can be applied to control the sine and random signals. A sine synthesizer is required for each sine to be generated and controlled.

CONTROL STRATEGIES AND SWEEP RESOLUTION IMPROVEMENT

The finer sine resolution of Methods II and III may necessitate changes in the sine control strategy. Sine control can be accomplished by several techniques. One method is to use the transfer function estimate calculated for random control to generate a control estimate as in Method I. This control estimate is then compared to the sine reference, and the sine drive is compensated accordingly through adjustment of the sine amplitude multiplier. As mentioned before, the advantage of this is that no tracking filter is required to extract the sine information. The disadvantage is that the transfer function estimate has much coarser frequency resolution than the actual sine. Thus, narrow resonances and nulls may not be discriminated very accurately.

Another method of control uses a tracking filter to extract the sine amplitude and phase information. This method is explained in greater detail by Norin[7].

Now that two options for improving the basic sine resolution and two basic control strategies have been presented, several methods for improving the sweep resolution will be discussed. Consider the sine con-

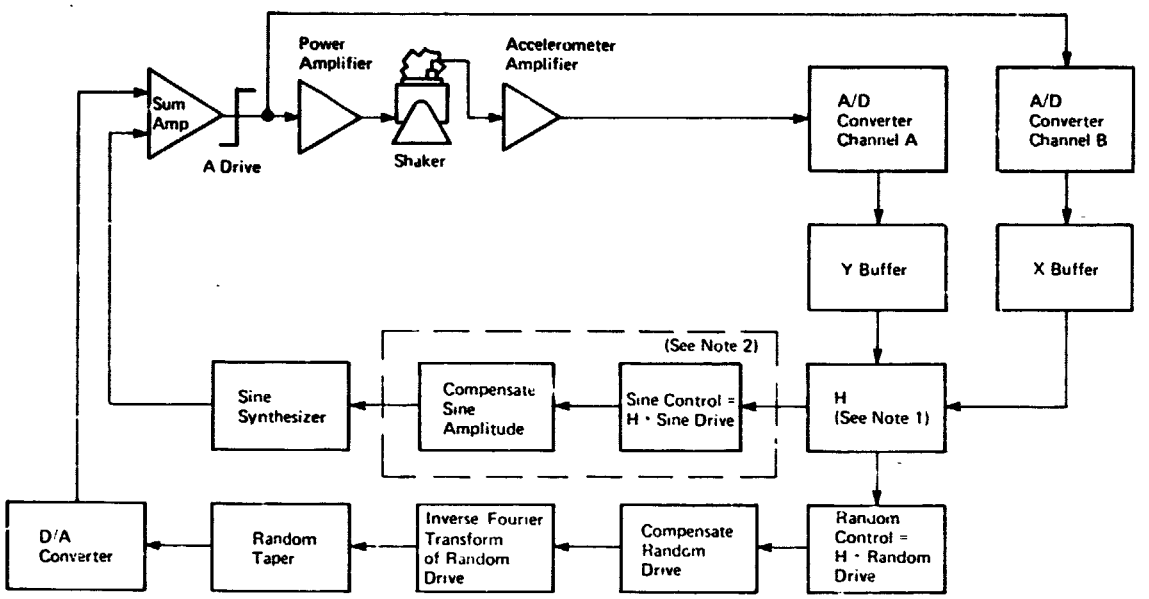

NOTES:

1. $H = \frac{\text{Y Buffer Power Spectral Density (PSD)}}{\text{X Buffer Power Spectral Density (PSD)}}$
2. Broken lines indicate operations which could be performed by a parallel microprocessor.

Fig. 11. Swept Sine on Random with Hardware Sine Synthesizer Block Diagram

trol strategy using the transfer function estimate technique. If the sine frequency is only updated once per random loop time (e.g., when the transfer function estimate has been updated), then the same sweep resolution exists as in Method I.

It is desirable to update the sine frequency as often as possible. Once every interrupt is the maximum rate. Updating the frequency at this rate is not difficult. The problem lies in the control strategy, whose calculations can take considerable time and, thus, increase the overall loop time. Several strategies can be used:

1. The control is updated each time the frequency is updated. This increases overall loop time and limits bandwidth, but it provides the best control possible with the most recent transfer function estimate. Note that the transfer function estimate is updated only once per loop time.
2. Control update occurs less frequently than frequency update. In effect, the sine sweeps part of the time without being tightly controlled. Thus, the sine control is not as good, but more time is available for random control which is consequently better. For example, the control could be updated once per loop time, but the frequency updated once per interrupt.
3. A mix of 1 and 2 is to "look ahead" at the transfer function where the sine will be sweeping to determine what sort of compensation will be required. If the transfer function is relatively flat, sine control can be done less frequently than if the transfer function contains resonances and/or nulls.

PERFORMANCE EXTENSIONS USING PARALLEL PROCESSORS

Since much of the sine control computation is independent of the random control computation, these two control calculations can proceed in parallel. The wide variety of low-cost microprocessors available makes multiprocessor systems economically viable. The sine control computations can be implemented with one or more microprocessors.

For example, consider the block diagram of Fig. 11. The parallel microprocessor would perform the processing functions enclosed by the dotted line. It would interrupt the main processor to get the transfer function, compute the control signal, compensate the drive, and update the sine synthesizer amplitude. This microprocessor would also update the sine synthesizer frequency using a real-time clock as a time reference. Memory requirements for the parallel processor would be minimal. One extra parallel processor should be able to handle four sine synthesizers efficiently.

Another variation on this approach is to have the microprocessor generate the sine from a lookup table as well as compute the control algorithm. This sine data could be transferred to the main processor and added to the random data before output to the DAC, or the sine data could be output through a separate DAC and summed with the random data in the analog domain. Reasonable performance might be possible with a single microprocessor generating and controlling four sines.

Use of a parallel processor makes control strategy number one viable. Since no random processing need be done, sine frequency update, control, and output are the only functions in the loop. This promises to provide the best control for reasonably fast, high-resolution sweep rates. The sweep resolution is limited by the sine control loop time. This time is greater if the microprocessor also generates the sine waveform as opposed to simply controlling a hardware sine synthesizer. Control strategies two and three can also be used if even faster sweep rates are desired. Note again that the transfer function estimate used in the sine control strategy is updated only once per random loop time.

IMPLEMENTATION OF METHOD I

The techniques described in Method I have been implemented into a working digital swept sine on broadband random vibration control system. A typical setup procedure is shown in Fig. 12, and results of a test with four swept sines are shown in Fig. 13. This implementation has all the features and limitations described in Method I.

SUMMARY OF PART II

Various techniques for implementing digital swept sine on broadband random vibration control systems have been presented. Several sine generation methods and sine control strategies have been proposed with indications of the expected relative cost-performance aspects of each. In particular, the use of parallel processors to improve system performance was discussed. Feasibility of a digital swept sine on random vibration control system has been demonstrated by an actual implementation.

```
1 TEST ID: SR31 RCT

2 HEADING: RECEIVING CHECKOUT TEST

3 BANDWIDTH: 2048.

4 RESOLUTION 64/128/256/512: 128.0
FREQUENCY INCREMENT: 16.00

REFERENCE SPECTRUM:
5 INITIAL SLOPE, DB/OCT: 12.00
   ALARM LIMIT DB : 6.000

6 FREQUENCY    HZ.: 16.00
   LEVEL  GSQR/HZ.: 1.000
   ALARM LIMIT DB : 6.000

7 FREQUENCY    HZ.: 2000.
   LEVEL  GSQR/HZ.: 1.000
   ALARM LIMIT DB : 6.000

8 FINAL SLOPE, DB/OCT: -48.00

RANDOM GRMS: 45.01


9 SINE FREQUENCY,HZ: 500.0
 SINE REFERENCE LEVEL, G'S: 5.000


10 SINE FREQUENCY,HZ: 800.0
 SINE REFERENCE LEVEL, G'S: 1.000


11 SINE FREQUENCY,HZ: 1000.
 SINE REFERENCE LEVEL, G'S: 10.00


12 SINE FREQUENCY,HZ: 1500.
 SINE REFERENCE LEVEL, G'S: 5.000

TOTAL GRMS: 45.84

13 SWEEP PARAMETERS:
 MODE, 1=LOG,0=LIN: 0
 RATE, HZ/SEC: 3.000
 INITIAL DIRECTION 1=UP,0=DOWN: 1

14 LOWER SWEEP LIMIT, HZ: 400.0
15 UPPER SWEEP LIMIT, HZ: 1600.

16 LOW LEVEL, -DB: -20.00
17 LEVEL INCREMENT, DB: 2.000
18 START-UP TIME SEC: 1.875
19 SHUT-DOWN TIME SEC: .9377
20 TEST TIME HRS, MIN, SEC: 0,4,0
21 CONTROL CHANNELS: 1
22 ACCEL SENS MV/G: 10.00
23 DRIVE CLIPPING 1=YES,0=NO: 0
24 ABORT LEVEL GRMS: 60.00
25 ALARM LINES:
26 ABORT LINES:
```

NOTE: Frequencies were automatically adjusted by program to an integral multiple of the frequency increment.

Fig. 12. Listing of Setup Parameters for Sine on Random

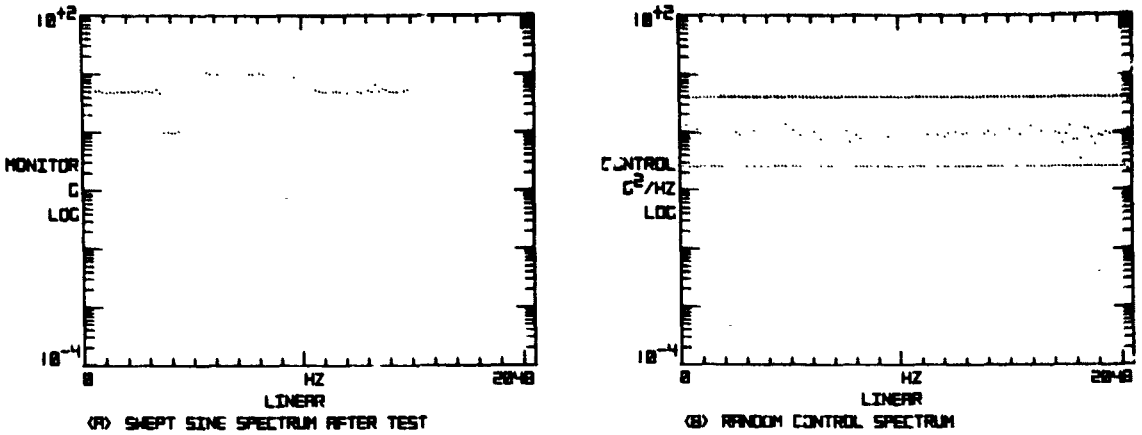

Fig. 13. Test Results with Four Swept Sines

REFERENCES

1. Heizman, C. L., "A High Performance Digital Vibration Control and Analysis System," Institute of Environmental Sciences, 1972 Proceedings, pp. 309-315.

2. Nelson, D. B., "Performance and Methodology of a Digital Random Vibration Control System," Institute of Environmental Sciences, 1973 Proceedings, pp. 187-192.

3. Norin, R. S., "Pseudo Random and Random Testing," Seminar on Understanding Digital Control and Analysis in Vibration Test Systems, 1975 Proceedings.

4. Barthmaier, J. P., "Shock Testing Under Minicomputer Control," Institute of Environmental Sciences, 1974 Proceedings.

5. Barthmaier, J. P., "Two Approaches to Computer-Controlled Shock Synthesis," The 20th International Instrumentation Symposium, 1974 Proceedings.

6. Cooper, H. W., "Why Complicate Frequency Synthesis?," Electronic Design, July 19, 1974, pp. 80-84.

7. Norin, R. S., "A Multi-Channel, Multi-Strategy Sinusoidal Vibration Control System," Institute of Environmental Sciences, 1974 Proceedings.

A REVIEW OF ENVIRONMENTAL TEST INNOVATIONS PERMITTED BY DIGITAL CONTROL SYSTEMS

W. Brian Keegan
NASA-Goddard Space Flight Center
Greenbelt, Maryland

This paper reviews the innovations of digital control systems from the perspective of one who establishes environmental test requirements for aerospace hardware to the dynamic environments of vibration and mechanical shock. It reviews the type of options that specifications might permit in those laboratories that possess digital control systems. The innovative tests mentioned consider only the capability of digital control systems and are not presented as formally approved changes to recommended test philosophy. They are intended simply to highlight the kinds of tests that, in the future, might be considered to constitute acceptable portions of the environmental test sequence of aerospace hardware.

Each of the environments of sinusoidal vibration, random vibration, and mechanical shock are addressed separately. In each area, potentially innovative test methods are discussed. The paper concludes with a warning to avoid the temptation to perform unnecessarily complex environmental tests simply because the capabilities of digital control permit them to be run.

INTRODUCTION

With the advent of digital control systems for performing environmental tests, simulation techniques previously impossible or at best tediously difficult with analog control systems have been made far more straightforward. Digital systems thus facilitate the use of more accurate simulation methods, enhancing the realism of the environments to which hardware is subjected prior to acceptance for service. This paper views the advantages of using digital control not from the perspective of the test equipment designer or operator, but rather from that of an environmentalist responsible for establishing test criteria for aerospace equipment which must survive the rigors of vibration, acoustic noise, and mechanical shock upon initiation of its service life. Simultaneously, it views the audience as being astutely aware of environmental facility design and operational capabilities, but not necessarily well grounded in environmental test philosophy for aerospace equipment.

When originally invited to present this paper, the suggested topic was "Test Specification Changes Required for Environmental Test Implementation Using Digital Test Systems." Upon consideration of the kind of material that could be presented, however, the word "required" seemed to be unnecessarily restrictive, thus sparking the change to the current title. In fact, no changes are necessitated by the change to digital control systems with the exception of some minor ones to test tolerances, as will be discussed later in this paper. Since analog control systems pre-existed digital ones by several years, the original design of digital systems of necessity had to possess all the capabilities of analog systems and then some in order to make them marketable items. Additionally, from the standpoint of maintaining specifications that are universally applicable to all

environmental test laboratories, it will be necessary for some time to come to consider those labs that still utilize analog control systems. Most tests on aerospace hardware are component level tests which are often performed by smaller labs that can logically be expected to be among the latter companies purchasing digital control systems.

Writing this paper was viewed more as an opportunity to describe how one might take advantage of the increased capabilities offered by digital control equipment. Thus the paper reviews the type of options that might be permitted for those laboratories that possess digital control systems in order to perform more realistic simulations of the environments of sinusoidal and random vibration and mechanical shock. For each of these three areas the problems that may be encountered with existing test tolerances brought about by the change to digital control will be discussed. Additionally, the increased test complexity facilitated by, as well as the innovative types of tests permitted by digital systems, will be reviewed. As such, the ensuing discussions are intended to highlight the kinds of tests that might in the future constitute acceptable portions of the environmental test sequence of aerospace hardware.

SINUSOIDAL VIBRATION

As implied in the previous section, it is not the purpose of this paper to address the problem of whether sinusoidal vibration testing should be performed. Rather, it starts with the ground rule that sine testing must be performed and considers how it might be done better using digital control equipment.

First, consider a typical sinusoidal test profile such as the one illustrated by the solid line in Figure 1, which has been extracted from the NASA-Goddard test specification for spacecraft. Such a profile of constant acceleration segments is a simplistic envelope of the illustrated flight data that has been analyzed by either narrow-band analysis or shock response spectrum techniques. In almost all instances such flight data could have been more closely enveloped had capability existed in the test equipment to easily run non-constant acceleration versus frequency profiles. It is known that capability has long existed in analog systems for controlling at the fixed positive slope values of +3 dB per octave and +6 dB per octave by controlling respectively to constant velocity or constant displacement but these are limited in frequency since the once or twice differentiated acceleration feedback signal rapidly becomes too small to accurately control. Moreover, it is known that analog curve followers exist that permit test profiles to contain any acceleration slope value at any frequency. These, however, are bulky peripheral units that are time consuming and tedious to set up and use.

Digital systems on the other hand are programmed such that the acceleration versus frequency profile can be subdivided into any reasonable number of straight-line segments simply by specifying the breakpoints. This drastically simplifies the process of running sinusoidal tests whose profiles are far more realistic such as that envisioned by the heavy dashed line in Figure 1.

There do exist times when a step change in acceleration is the desired way to define a sinusoidal test specification. One example of such an instance would be the simulation of the Pogo event of the Delta Launch Vehicle. Pogo, briefly described, is an oscillation of the launch vehicle and payload at its first longitudinal, "accordian", resonant mode that is induced near the end of first-stage burn by coupling between the launch vehicle primary structure and pressure oscillations in the propellant feed line. The amplitude of this oscillation has been measured on enough flights that it is amenable to statistical analysis. The frequency of occurrence is predictable to within a frequency band equal to the change in the first mode frequency over a few seconds flight time. As a result, there exists a narrow frequency band over which a relatively high sinusoidal acceleration test level is required. At frequencies outside this band, the flight data shows significantly lower levels and the data envelope is generated by events that occur at other flight times. Thus, a step increase and a step decrease, as illustrated in the lower frequency portion of Figure 1, are a desired portion of the test profile.

In such instances, digital control systems may not be able to complete the step change acceleration within the traditional frequency tolerances of two percent. The customary procedure

for performing such a change with an analog system is to terminate the sweep, change the input vibration level, and when control has stabilized at the new level, re-initiate the sweep. This process undoubtedly exposes the test item to more high-amplitude stress reversals than is realistically required. It is accepted practice though because it is felt to be the optimum trade-off between maintaining control and completing the level change within an acceptable frequency band. Digital systems, being more highly automated, do not stop sweeping but rather change levels as they sweep. Since control systems have finite compressor speeds, they require a finite length of time to change levels without losing control of the process. The bandwidth in which this stabilization to the new level can be completed is a function of the percentage change in level, the compressor speed, the sweep rate, and the frequency at which the change was initiated, as is defined in Ref. 1. There it is stated that:

$$\Delta f \approx f \left[\left(\frac{g_1}{g_2} \right)^{\left(\frac{.1N}{S} \right)} - 1 \right]$$

where

Δf = the bandwidth needed to accomplish the level change

f = the frequency at which the level change is initiated

g_1/g_2 = the amplitude ratio of the step change

N = the sweep rate, and

S = the compressor speed of the control system at f

The approximation error in the above equation is less than one percent.

As a specific example of the above, consider the Delta Pogo specification where at 17 Hz there is a step change from 1.5g to 4.5g while sweeping at 4 octaves per minute. Using, from Ref. 1, an average compressor speed of 4 dB per second for a digital control system at 17 Hz, it can be seen that it would take a 2 Hz band to complete the step change. This is considerably greater than the currently acceptable 2 percent frequency band in which such step changes in level must be accomplished.

The digital control algorithms must, of course, be written to run safe tests and the permissible test tolerances must be broadened to permit operation of the test equipment that does not jeopardize the integrity of the test item. Of more potential significance, however, is the fact that the test engineer must be made aware of how the control algorithm is written so that he can anticipate the response of the item under test. Suppose, for example, a spacecraft had a fundamental resonance just below or just above the frequency band of Figure 1 in which the input levels are the highest. If, in order to meet the input amplitude requirements in that band, the test level began to change well below the beginning of the band and was not fully reduced until well after the band, the possibility would exist of exciting the structure at its resonant mode to unrealistically high levels, significantly high enough such that special provisions should have been made for limiting the response of the structure. Thus, it can be seen that the problem goes well beyond the operational one of meeting specification tolerances and becomes one of assuring that pertinent information regarding system performance capabilities has been disseminated to the proper individuals who must utilize it for proper test planning.

This brings us logically then to perhaps the most significant advancement in using digital control systems to perform sinusoidal vibration tests: the ability to automatically limit the response of many points to some predetermined response value, thereby precluding inadvertant overtests due to unanticipated high amplifications. For several years now, analog systems have had limited capability to transfer control to some response point when a predetermined limit was reached or to initiate a controlled shutdown if some abort limit was exceeded. These features are mandatory on systems that are required to control the various environments to which today's complex, multi-million dollar spacecraft are tested. In analog systems, these features were contained in peripheral hardware that took up precious space in the control room and was often difficult and time consuming to check out, calibrate and set up. More importantly, limitations on equipment availability usually placed severe constraint on the number of response points that could be so monitored, often necessitating a compromise between the level of sophistication one desired to have in a test and the level one was able to have.

With digital control systems, however, such limiting and control of responses other than the primary control point is contained in the control algorithm where it requires no additional hardware space and can be set up easily through the ...letype interface. Additionally, such capability exists in great amounts allowing many response points to be limited, thereby permitting far more complex tests to be run than are currently possible in laboratories with analog control equipment. A word of caution may be in order, however, in that one should not run unnecessarily complex tests simply because the control system has unused capability. Sound engineering judgement must still temper the complexity of environmental tests since the likelihood of a setup error increases with test complexity no matter how simple the control system may be to use.

The final point of discussion regarding sinusoidal testing concerns the use of variable sweep rates during the vibration profile in the control algorithms of some manufacturers of digital equipment. This feature reduces the sweep rate at frequencies at which the system transfer function is rapidly changing in order to more accurately control the applied vibration level to that desired. This approach is felt to have some distinct disadvantages and the potential problems associated with its logic will be drawn out in the following example cited from a test on the Orbiting Astronomical Observatory (OAO) at the Goddard Space Flight Center.

Using an analog control system and a fixed sweep rate it was desired to perform a base excited sinusoidal vibration test of the 5000 pound Spacecraft at a constant acceleration level of 0.25g while sweeping at a rate of 4 octaves per minute from 5 to 15 Hz. The actual control acceleration profile measured at the base of the spacecraft was as shown in Figure 2a. As can be readily seen there, the input varied by a considerable amount from the desired in the vicinity of the 9 Hertz first cantilevered bending mode of the spacecraft. The explanation for this occurrence is that as one approaches the fixed-base resonant frequency of such a large test item, the apparent mass, and hence the driving force required to be supplied by the shaker armature to maintain a constant acceleration level, changes more rapidly than the compressor of the control system can compensate for it (See Figure 2b). Thus, the input acceleration falls below the desired level and continues to fall further below until the slope of the apparent mass decreases to the point that the compressor can begin to compensate and adjust the input to the desired level. After the resonant frequency is passed, the inverse action occurs in that as the required force decreases more rapidly than the compressor can react, the input rises above the desired level until such time as the slope of the apparent mass levels off and the compressor is again able to provide acceptable control.

Although the above problem was described in the frequency domain, it is in fact a problem of the time domain, in that the main cause is the relatively slow compressor speed. Increasing the compressor speed is an unacceptable solution to the problem since it may cause servo loop instabilities thereby losing control completely as it attempts to correct too rapidly for changes in the system transfer function. Decreasing the sweep rate, however, effectively increases the compressor speed without creating potential instabilities by reducing the time rate of change of the system transfer function thereby allowing the compressor more time to respond and enabling it to significantly lessen the deviations of the actual vibration level from the desired.

From a test operations viewpoint then, this automatic reduction of the sweep rate below the specified level at frequencies at which the system transfer function is changing rapidly is an ideal solution. It permits running more precise tests and is most likely the reason why some manufacturers have included it in their sinusoidal vibration control algorithm. There are, however, considerations that should be made when performing tests over and above that of maintaining precise control of the input level.

The prime consideration during vibration testing is that the proper load be applied for the desired duration. Variations from the desired level as severe as those illustrated in Figure 2 occur only at the fundamental cantilevered resonances of very massive test items. It is at these frequencies that the Goddard test philosophy permits a reduction of the input vibration level below the specification value so as to limit the response of the test article to the maximum predicted by analysis to occur in flight. Thus, while in the

W. Brian Keegan

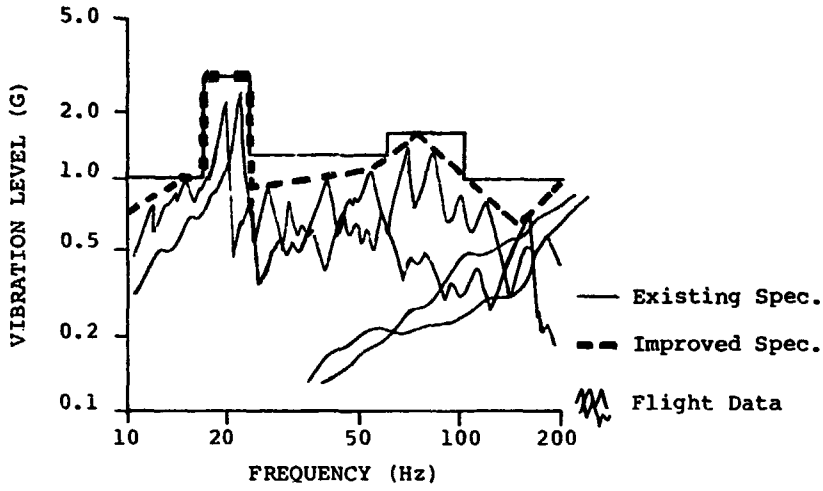

Figure 1: Comparisons of Sinusoidal Vibration Profiles

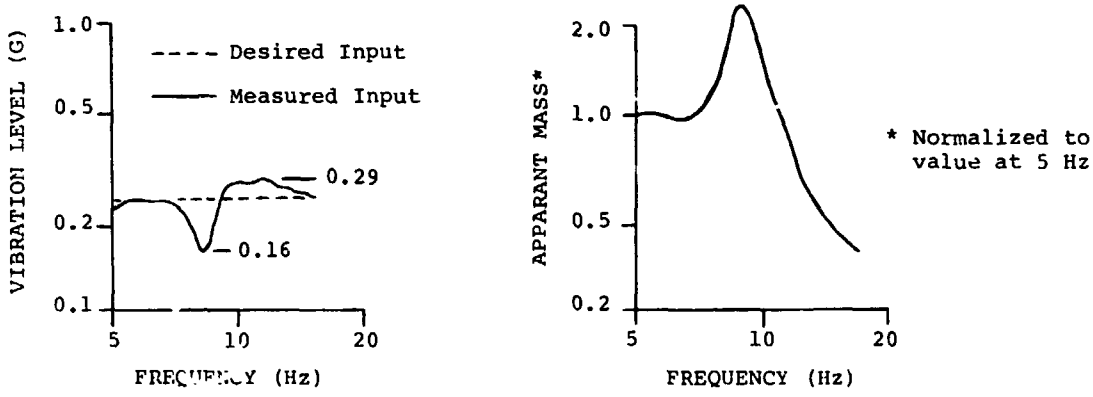

(a) Input Acceleration (b) Apparant Mass

Figure 2: Results of OAO Sinusoidal Vibration Test

cited example the input acceleration was the control parameter, it was not a specified acceleration level but rather some nominal acceleration predicted by the results of a low-level survey to be the one needed to develop the desired response load in the critical areas of the spacecraft structure. So long as the percentage deviation of the control acceleration from the desired was the same for both the full level run and the low level run that had been used as the basis for the extrapolation, then the full level run would develop the desired responses. By slowing down the sweep rate in the vicinity of test item resonances, one would still need to employ some technique that limited the responses of the test to those desired. Thus, the same peak load would be developed. But by slowing down the sweep rate, the number of cycles for which the peak load was applied could increase drastically. When sweeping at the constant rate of 4 octaves per minute, the OAO Spacecraft saw a load greater than 90 percent of maximum for 19 cycles in the vicinity of the 9 Hertz resonance. This was already considerably in excess of the number of cycles for which the load was predicted to last by the flight dynamics loads analysis. To significantly increase this number of applied load cycles even further in order to provide improved control accuracy by slowing down the sweep rate seems unreasonable.

The fact that fatigue damage is not usually a problem with aerospace hardware is not an acceptable argument since one of the basic tenets of environmental testing as envisioned by the Goddard Space Flight Center is to expose hardware to as realistic a simulation of the service environment as is practicable. It is felt that the reduced sweep rate feature loses sight of this objective and for this reason it is recommended that it be excluded from the sinusoidal vibration control algorithm of digital control equipment.

RANDOM VIBRATION

For the control of random vibration inputs, digital control systems offer significant improvements over analog systems for reasons of both shorter equalization time and finer spectral resolution. Using a digital system, the bandwidth of the vibration profile can be subdivided into 400 or more filters. Assuming 400 filters are used, then a profile over the traditional bandwidth of 10 to 2000 Hertz could be equalized with an approximately 5 Hertz resolution. This compares with existing analog systems that have 80 filters varying from 12 to 50 Hertz.

It is this improved resolution that is felt to be a potential problem area not from the standpoint of being not as good a test but from the standpoint of meeting existing specification tolerances. These traditional tolerances require that in any single filter bandwidth the power spectral density (PSD) be controlled to within 3 dB of the desired value. This is not a serious problem with wider filters because it is really the average PSD value in the band that is being controlled within the specified tolerances. As the filters become very narrow, the average PSD value in a single filter bandwidth is radically affected by narrow band, high amplification resonances in the test item. Although no actual data was available to the author, the case can be envisioned in which the digital control system was unable to compensate sufficiently for such a resonance because of its finite dynamic range. If such cases were encountered regularly, then specification tolerances would have to be broadened to permit greater than 3 dB variations from the desired level over a certain percentage of the narrow band filters. It must be emphasized, however, that this is not a case of digital systems being unable to control as well as existing analog systems. It is rather a case of digital control systems being sensitive enough to detect far more sophisticated problems than analog systems can and thus requiring a change to test specification tolerances in order to take into account this increased level of sophistication.

As far as random vibration control techniques are concerned, there is one area which the control algorithms do not currently address that is particulary amenable to the capabilities of a digital system. That is the ability to control vibration responses generated in one frequency band by energy input in another frequency band. One example of such a case would be a resonance excited by input energy in the skirts of the filters adjacent to one in which the resonance lies. Another would be the excitation of response at one frequency generated by energy input at eigher a harmonic or sub-harmonic of that frequency. To the author's knowledge, existing control techniques utilize the measured

response of the control point in the filter band to regulate the input force in only that same band so that the measured response equals that desired. In the cases mentioned above, such a control algorithm would have no effect on the equalization of the PSD at the control point.

When such a case is encountered using analog control systems, the operator begins a process of manual equalization by adjusting the various sliders to see if equalization can be accomplished. This can be a time consuming process and often results in a decision to run the test with one filter knowingly outside the tolerance limit simply because one does not wish to take the extensive time required to adjust each filter until proper equalization is achieved.

Although such instances may not be encountered frequently, it would seem worthwhile to have provisions for them incorporated into the random vibration control algorithms of digital systems. Such provisions would consist of sequentially changing the input energy in each filter band and checking to see if the response in the unequalized band was affected. In such a manner the filter generating the response could be located and a secondary control loop established whereby its output energy was controlled by the response in the unequalized band. When such an equalization problem was encountered, this supplemental portion of the control algorithm could be activated by a simple teletype input in order to provide capability of conducting a good environmental test even when the test item possesses such unusual dynamic characteristics.

The final topic for discussion under this heading of random vibration concerns extension of the existing control algorithms to a new area. Current practice calls for random vibration tests to be run for some specified time at some overall RMS acceleration level. When one speculates as to how they might improve the realism of random simulation, the idea of a time varying RMS acceleration level, similar to the profile illustrated in Figure 3, comes to mind. This profile shows the RMS acceleration level measured at the interface of a spacecraft with the Delta Launch Vehicle from lift-off through the regions of transonic flight and maximum aerodynamic pressure. While no firm test requirements for such a profile yet exist, it seems reasonable to think that such a profile may some day be a requirement. Moreover, it seems that implementation of such a requirement could be easily added to the random vibration control algorithm of digital systems. When room for potential improvements exists, requirements have the demonstrated ability of growing to meet such potential. The writer feels that such will be the case for the time varying RMS random vibration profile discussed here.

MECHANICAL SHOCK

The area of mechanical shock is the one in which digital control systems have provided the greatest improvement. They offer two distinct methods of environmental simulation: shock response spectrum matching, in which the potential simulation accuracy has been significantly improved over that of analog systems through increased resolution, and transient waveform control, a completely new test capability that is not environmental simulation at all but rather environmental duplication. Prior to a discussion about either of these methods, let us depict the environment that we are trying to simulate. Depicted in Figure 4a is a shock transient measured on the primary structure of a typical spacecraft during a pyrotechnic event such as separation from the launch vehicle. It is a high-G multi-frequency oscillation characteristic of such events. Figure 4b meanwhile presents the acceleration shock response spectrum of the transient for a critical damping ratio of 0.05. Both of these are representations of the same environment, one being a description of structural motion and the other a prediction of the amount that single degree of freedom systems with the defined damping would respond to that structural motion. If one wished to simulate the event, then he has the freedom to work in either the time domain or the frequency domain.

Recent past practice with analog systems has been to simulate the desired shock spectrum by synthesizing a time history whose shock spectrum matched, for the specified damping value and within the allowable tolerances, the desired shock spectrum. This was done by summing several discrete frequency wavelets into a single complex time history with the amplitude of each frequency component individually adjusted to control the resultant shock spectrum at its own frequency. The frequency spacing, or

resolution, of these frequency components was usually one-third octave, but it must be understood that such shock spectrum synthesis techniques do not utilize filters that control the spectrum over the entire one-third octave band. True control of the shock spectrum magnitude exists only at the one-third octave center frequencies. Because of the shape of the shock spectrum of each wavelet the shock spectrum magnitude falls below the desired value at all frequencies between adjacent one-third octave center frequencies. As a result, for test items whose predominant response frequencies lie between one-third octave center frequencies, an undertest may result.

The concept of shock spectrum synthesis is the same for both analog and digital systems. The use of digital systems does offer improved simulation, however, by providing increased resolution, such as one-sixth or one-twelfth octave, thereby providing exact matching of the desired spectrum magnitude at a greater number of frequencies that are also closer together. Thereby, the amount of inaccuracy in spectral values at frequencies between two adjacent control frequencies is also significantly reduced.

One serious deficiency of any method of shock spectrum matching is that it is good for only one value of damping. If the damping coefficient of the particular item under test does not equal that for which the shock spectrum was matched or if the item is sufficiently complex that its behavior is not at all predictable by the single-degree-of-freedom analogy upon which the shock spectrum concept is based, then the response induced in the test item by the test environment will not be the same as that induced by the service environment and the test will not have accomplished its objective. This is so for a given time history because the variation in shock spectrum magnitude as a function of the analysis damping coefficient is dependent upon the number of cycles for which the time history lasts. This is illustrated in Figure 5 where the variation of peak shock spectrum magnitude with damping has been plotted for several types of time history. As can be seen, if the test item has a lower damping value than that for which the shock spectrum was computed, as is often the case because many subsystems have high-Q resonances and most specifications are defined for Q equal to 10, and a typical shock spectrum synthesis technique is employed, then the simulated environment will produce an overtest.

One method of controlling the amount of overtest or undertest so induced is to control the number of cycles in each individual wavelet of the simulated environment such that the variation in spectral magnitude as a function of damping approximates that seem in the real environment. It is understood that certain digital shock spectrum synthesis control algorithms possess such capability, and it would seem advisable for test laboratories to have such capability if possible. This does not, however, provide a universal solution because the ratio between peak shock spectrum magnitude and peak magnitude of the input time history is reduced as the number of cycles in each wavelet is reduced thereby lowering the upper magnitude of the shock spectrum that can be so synthesized due to shaker and amplifier force limitations.

One final shortcoming of the shock spectrum matching technique is that, even if excited to the proper response levels, the test item experiences peak stresses for a greater number of cycles because the simulated environment usually lasts longer than the service environment. The way of avoiding the problems of spectral matching completely is to utilize the transient waveform control capability of digital systems. With this technique, accurate duplication of the measured service environment can be achieved. Evaluating the responses induced in the test item by this method in terms of the foregoing shock spectrum matching discussion, then, there are no frequencies at which the spectrum magnitude of the test environment varies from the desired spectrum value. In addition, the variation in shock spectrum magnitude as a function of the analysis damping coefficient is precisely the same for both the test environment and the service environment. Thus the necessity of knowing the damping coefficient of the test item in advance in order to assure a realistic test is eliminated. Finally, the number of peak stress cycles is precisely duplicated since the duration of both the test and service environments are exactly the same. Transient waveform control therefore is a significantly improved shock test method offered by digital control systems that should be adopted whenever possible.

Prior to implementation of such a test method for other than development testing, however, an approved specification must exist and a method for generating a specification that provides

W Brian Keegan

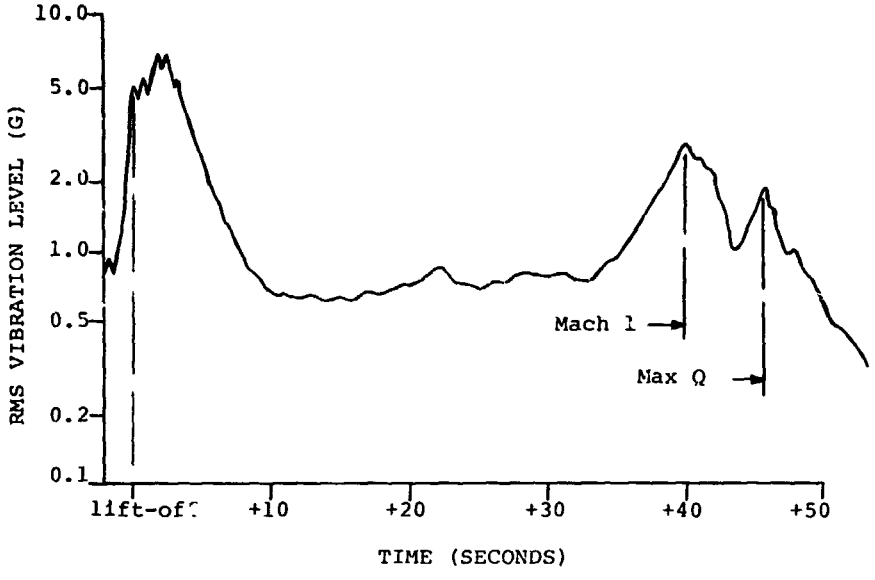

Figure 3: Typical RMS Time History of Overall Random Vibration level Measured at Spacecraft/Launch Vehicle Interface

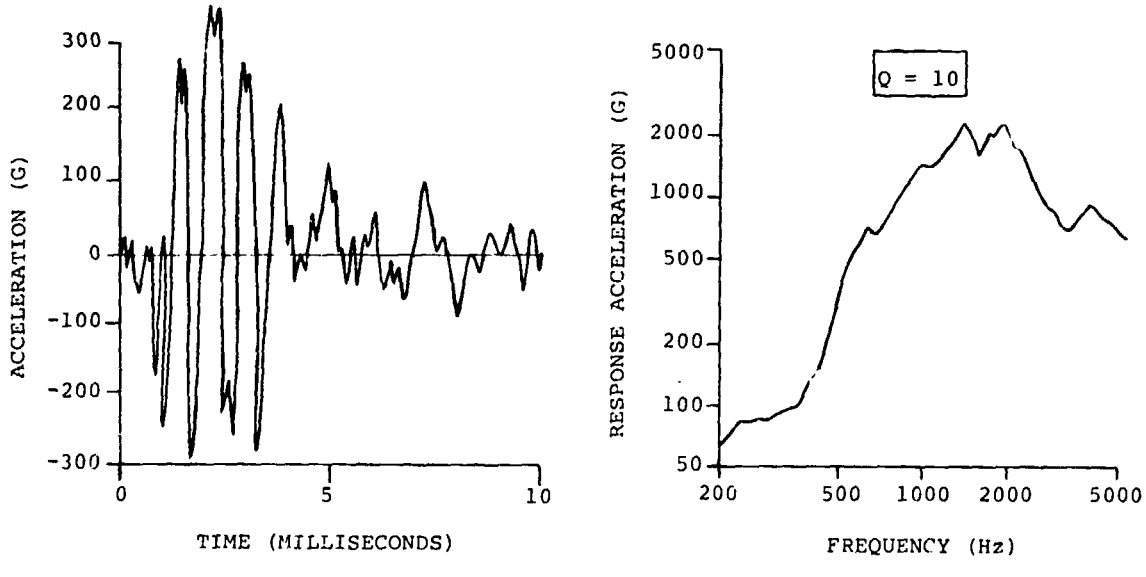

(a) Time History (b) Shock Response Spectrum

Figure 4: Typical Aerospace Pyrotechnic Shock Environment

a qualification time history is not straightforward. In the case of developing a shock spectrum specification, one needs to do a shock spectrum analysis for some defined damping coefficient over the frequency range of interest of all flight data deemed appropriate for inclusion into the particular specification being developed. A test specification can then be constructed by either enveloping the composite spectra encountered in service or if sufficient data samples exist, by performing a statistical analysis to determine some desired environmental probability level of occurrence. Combination of the various data samples is thus easily achieved when developing a shock spectrum specification.

Still in terms of the shock spectrum, let us now consider the development of a qualification time history. Seldom if ever does a single time history generate the worst case shock spectrum at all frequencies. Thus, there will probably never exist a single time history that can be uniquely defined as the worst case for a particular specification. Moreover, because the shock spectrum is not a reversible process, one cannot take a composite envelope shock spectrum of several time histories and generate a unique time history for definition in a test specification. The most likely time-history specification that would be developed then would be a set of such time histories, each of which would generate the worst case test item responses over a portion of the frequency range for which the specification was defined. Such specifications should begin to be defined in the near future.

One of the expected advantages of performing mechanical shock tests under the control of digital systems is the ability to improve the accuracy to which the desired responses can be controlled. Current tolerances on shock spectrum tests are +50%, -10%, a large band in which test amplitudes may fall and still be termed acceptable. The usually quoted accuracies on transient waveform control are ±10%. This, however, assumes that no non-linearities are encountered between the equalization level and the full level test. When equalization is conducted 6 dB or more below full level, as is usually recommended, non-linearities well in excess of 10% can be expected, as is illustrated in Ref. 3. When this occurs, even perfect equalization will not result in tests that meet the stated capabilities of ±10%.

The writer feels that significantly improved mechanical shock test accuracy could be achieved if both the shock spectrum and transient waveform digital control algorithms were expanded to include measurement of and compensation for the non-linearities inherent in the test item. One suggested method for accomplishing this would be to first equalize initially at the -12 dB level (25%), and next perform a run at the -6 dB level (50%). The differences between the predicted inputs for the -6 dB run, based on a linear extrapolation of the - 12 dB run, and the actual inputs could serve as a measure of the non-linearities encountered in the transfer function of the test item when subjected to a 6 dB increase in excitation level. This non-linearity measurement could then serve not only to re-equalize at the -6 dB level, but more importantly to anticipate the additional non-linearities now expected to be encountered between the -6 dB and the 0 dB (100%) runs. Thus, there would exist a technique for at least attempting to compensate for test item non-linearities. The Goddard Shock Test Handbook (Ref. 4) currently recommends such a procedure be followed for manually equalizing shock spectrum tests using the analog synthesizer. Incorporation of this technique into the digital control algorithms would improve an already good test method.

Even with the vast improvements in shaker shock test methods facilitated by digital control systems, there still exists room for argument that any form of on-the-shaker test induces much greater responses throughout the test item than are seen if one exposes the same test item to the actual pyrotechnic event. One possible explanation of this is that on the shaker the input is coherent at all mounting points of the test item, whereas if one measures the time history at the various mounting points of a test item during an actual pyrotechnic event, he will see that they are not exactly the same. This topic, however, does not warrant further discussion in this paper, but is undoubtly one that will receive much attention in the near future.

SUMMATION

Thus, the capabilities of digital control systems have been reviewed as they interface with environmental test specifications. They provide vastly increased capabilities in some areas, and in others offer test methods previously impossible. They do not, however, eliminate the need for constant

care on the part of the test engineer to verify that the objective of realistic environmental simulation is being met.

Finally, then, it is felt that a warning must be sounded. Avoid the temptation to perform unnecessarily complex environmental tests simply because the extensive capabilities of digital control systems to automatically monitor large numbers of parameters permit them to be run. Sound engineering judgment must continue to be the hallmark that identifies cost effective test programs that have properly balanced test complexity against the ramifications of inducing an unrealistic failure because of an improperly conducted test.

REFERENCES

1. Digital Vibration Control Techniques by P. Chapman and B. K. Kim; Jet Propulsion Laboratory Report; Pasadena, California; September 1974.

2. The Effect of "Q" Variations in Shock Spectrum Analysis by M. B. McGrath and W. F. Bangs; Proceedings of 42nd Shock and Vibration Symposium; Washington, D.C.; January 1972.

3. Capabilities of Electrodynamic Shakers When Used for Mechanical Shock Testing by W. B. Keegan; Goddard Space Flight Center Report; Greenbelt, Md.; July 1973.

4. Handbook for Conducting Mechanical Shock Tests Using an Electrodynamic Vibration Exciter by W. B. Keegan; Goddard Space Flight Center Report; Greenbelt, Md.; June 1973.

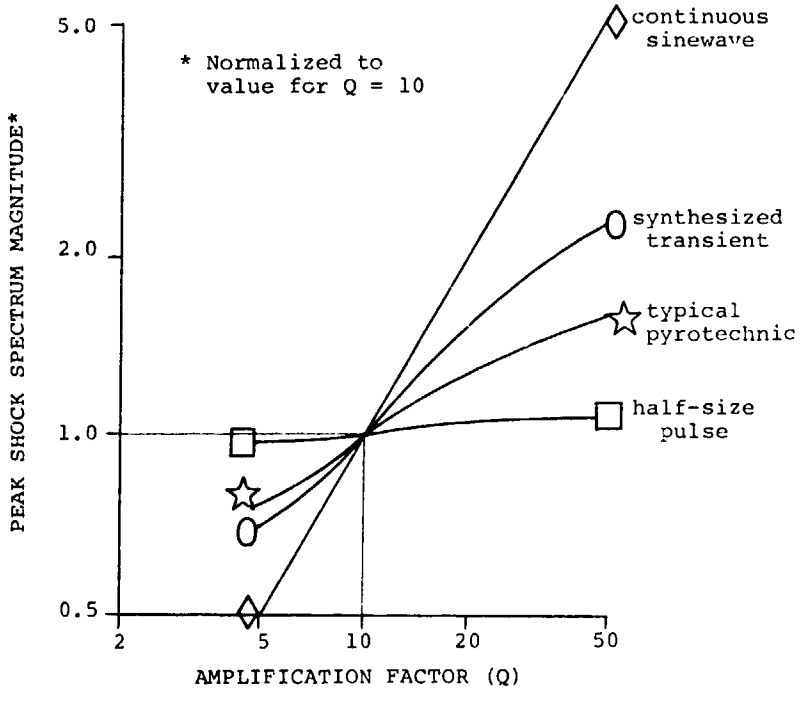

Figure 5: Variation of Peak Shock Spectrum Magnitude with Damping for Various Waveforms (partially extracted from Ref. 2)

SAFETY PROTECTION OF TEST ARTICLES USING DIGITAL CONTROL SYSTEMS

R. A. Dorian
NASA, Goddard Space Flight Center
Greenbelt, Maryland

Safety protection of test articles is a primary concern in aerospace vibration testing. Digital control systems have greatly enhanced the protection of test articles because of the speed and repetition with which they can perform monotonous tasks. Because of this, the greatest source of error, operator error, has been extensively reduced. Alarm and abort tolerances of individual spectral lines are monitored and compared to the operator's predefined values, and an orderly shutdown of the system is initiated if the alarm and abort strategy is violated. The systems also initiate corrective action, if required, by monitoring primary power source levels, control signal integrity and peripheral equipment environmental requirements. However, "exciter dumps," which are due to unwanted transients generated at the output stages of the control system or the power amplifier, are corrected by a separate system. In this case, a system external to the control system must monitor displacement, velocity, or acceleration of the exciter system and generate a controlled deceleration shutdown which prevents damage to the test article caused by the transients.

INTRODUCTION

One of the most undesirable occurrences during a vibration test is a shutdown due to the firing of an armature protector because of operator error, equipment malfunction, or power outage.

Present armature protectors are designed to protect the moving element (armature) of the shaker by preventing it from hitting the mechanical stops. Unfortunately, the sudden dynamic braking generates large accelerations which have caused the spacecraft or test article to be subjected to excessive levels and possible damage. The firing of an armature protector or "exciter dump" is particularly important since in most cases these exciter dumps are due to operator error rather than equipment malfunction or power outage.

To this end equipment manufacturer's have dealt effectively in solving "specimen protection" problems. The computer has been especially helpful since its speed and versatility allow it to perform a number of operations such as:

I. Checking operator error during the test set-up phase.

II. Monitoring test levels through various control strategies and warning the operator of impending problems.

III. Housekeeping operations - monitoring pertinent peripheral equipment parameters during a test.

It would seem logical to draw the conclusion that with all of the above capability a digital control system would circumvent any potential "exciter dumps." However, this is not necessarily true. A transient occurring within the power amplifier circuitry or at the output stages of the control system could not necessarily be controlled by the computer and therefore would pass to the exciter and test article. There are protective circuits, however, which

can decelerate the exciter in an orderly fashion without harming the test article.

DETAILED DISCUSSION

I DIGITAL CONTROLLER PROTECTION

A. Checking Operator Errors During Test Setup Phase

All digital control systems utilize what is commonly called a "conversational language" between the operator and the computer. During this conversation, the communication between the two takes place via teletypewriter or a CRT/keyborad operation. The operator responds to the question by typing an answer which is examined by the computer and either accepted if correct, or restated, if incorrect. Many tedious operations, which are handled by the computer, are certainly monotonous and consequenty prone to error, if performed by the operator. For example, the computer checks gain switches, performs calibration calculations, reference amplitude spectrum values, error spectrum, calculations, etc. and at a much faster rate than an operator.

A typical test set-up "conversational routine" is shown in Table 1, "Random Test Setup." As one can see, a number of parameters must be satisfied in order to ensure a successful test.

The operator specifies such items as transducer sensitivities, G^2/Hz at a specific frequency, overall G rms level, etc. The system automatically controls the signal conditioners, analog to digital converter, switches, etc., thus relieving the operator of these tasks. After the setup is completed and before any full level vibration test proceeds, the system provides a self-checking operation of the entire vibration system, including power amplifier, exciter and transducer channels, to ensure proper system connections, calibrations, and switch settings. As an example, the system may discover that the transducer sensitivity is too high for the test spectrum requested, in which case, the computer notifies the operator of such a condition.

B. Monitoring Test Levels Through Various Control Strategies And Warning the Operator of Impending Problems

Besides the self-checking procedure used by digital control systems prior to the test, these systems use various other techniques to protect the test specimen.

1. Control Strategies

Digital control can be accomplished through various techniques in order to protect the test specimen as much as possible. The following is an example of control techniques:

a. Control on the average of multiple selected channels.

b. Control against specified limits on specified signals.

c. Control on the highest or lowest of selected signals. (sine sweep)

d. Control on filtered or unfiltered (peak or rms) signals. (sine sweep)

The operator selects the desired control strategy and thereafter the system performs all the monitoring and corrective action. There are limitations as pointed out in an article by Dr. A. G. Ratz (2) in which he states the following:

> If a system has N inputs, each of which should be monitored and used in the control scheme, a problem can arise if only M of these inputs (N>M) can be analyzed each control cycle. For a typical gain control iteration, the CPU samples as many of the inputs as is practicable. This is done during the gathering time (t_o to (t_o+T_f)): if there are too many inputs to be handled in any one gathering time, the CPU commutates through the inputs, handling a different set of inputs each control iteration until all inputs are covered. Thus, if these are N inputs, only M of which can be handled during any one control iteration, it takes (N/M) control iterations to update all inputs. Data for non-sampled inputs must be stored and used from previous control iterations, to compute averages, external selections, etc.

The above obviously leads one to understand that even digital control systems have limited corrective capability when the number of response channel measurements exceed the monitoring capability of the control system for each control cycle.

2. Pretest Levels

In Table 1, line number 9, notice

TABLE 1 Random Test Setup

```
                    RANDOM EXECUTION READY

 1  READ TEST TAPE ?
 2  ENTER TEST IDENTITY  (1Ø CHARACTERS)
 3  ENTER TEST DATE (8 CHARACTERS)
 4  ENTER OPERATOR IDENTITY (1Ø CHARACTERS)
 5  ENTER OTHER DESCRIPTORS IF ANY (1Ø CHARACTERS)
 6  ENTER TRANSDUCER SENSITIVITY MV/G
 7  ENTER NO. OF CONTROL CHANNELS
    ENTER NO. OF SCANS
    ENTER 1 ST  CONTROL CHANNEL
    ENTER MONITOR CHANNEL
    ENTER TYPE OF MULTICHANNEL CONTROL
    1. AVERAGE  2. PEAK  3. EXTREMAL
    IS EXTERNAL REFERENCE DESIRED ? ?
 8  ENTER TOTAL TEST TIME IN MINUTES
 9  PRETEST LEVELS AVAILABLE =
      1.     -Ø dB
      2.     -6 dB
      3.    -12 dB
      4.    -18 dB
      5.    -28 dB
      6.    -3Ø dB
      ENTER 1., 2., 3., 4., 5., OR 6. FOR SELECTION
1Ø  CHANGE REFERENCE DESIRED ? ?
    BANDWIDTHS AVAILABLE =
      1.    1ØØ HZ
      2.    2ØØ HZ
      3.    3ØØ HZ
      4.    5ØØ HZ
      5.   1ØØØ HZ
      6.   2ØØØ HZ
      7.   3ØØØ HZ
      8.   5ØØØ HZ
      9.  1ØØØØ HZ
      ENTER 1., 2., 3., . . . 9. FOR SELECTION
    RESOLUTIONS AVAILABLE
      1.    W/2ØØ
      2.    W/1ØØ
      3.    W/5Ø
      4.    W/25
      ENTER 1., 2., 3., OR 4. FOR SELECTION
    ENTER NUMBER OF SPECTRUM BREAKPOINTS
    ENTER FREQS. AND PSDS. ALTERNATELY
      ENTER NEXT FREQ.
      ENTER NEXT PSD
      PROGRAMMED RMS LEVEL = x,xxy
      CHANGE IN RMS DESIRED ? ?
11  ENTER ALARM LEVEL IN DB
12  ENTER ABORT LEVEL IN DB
13  WRITE TEST TAPE ?
14  EXECUTE ?
    ENTER COMMAND
```

that the control system allows the operator to specify to what level (in dB) less than full scale the operator would like to initiate a test. During this time the control system does a self checking operation to ensure that the entire system is within desired tolerance levels. After the system has accepted the level, it then increments itself in approximately +6 dB steps until it comes up to full test level. In the event any abnormal responses occur, the system will warn the operator of such conditions and shut down if necessary.

3. Warning and Abort Valve Selection for Each Spectral Line of the Reference Spectrum

Generation of the reference spectrum (Random Vibration Test) for a digital control system is similar to an analog system in that amplitude values are chosen as a function of frequency. However, the analog values are selected through a slide wire mechanism, whereas the values are typed in for a digital system. One major advantage which a digital system has over an analog system is that at each spectral line, Alarm and Abort values can be specified and the system will constantly monitor these values and control to them.

The alarm check makes the operator aware of test conditions which are outside of the acceptable levels. The abort checks will cause a system to shut down. (See figure 1). Each segment of the spectral profile is automatically monitored to the specified tolerances where the tolerances are programmed in dB. Alarm tolerances generally cause a data report to be printed if the control amplitude exceeds the specified limit. The abort tolerance will cause a controlled shutdown and a message will be printed out.

Alarm and Abort limits are generally provided from approximately ±2 dB to ± ∞ dB in adjustable steps. These limits are applied to the smooth PSD and not the "instantaneous" PSD, X_o. To eliminate false alarms or false shutdowns, the alarm and abort signals are applied as follows:

a. A running count n, is to be kept for each line ($0 < N$), separate for alarm, and for abort.

b. Each time (each iteration of the control) the alarm/abort level is exceeded, n is increased by one count.

c. Each iteration of the control when the relevant limit level is not exceeded, n is decremented by one count.

d. n can never go negative.

e. When n reaches the value $n = N_o$, the relevant level is considered to be exceeded, and the alarm or abort action is initiated.

f. A suitable value for N_o is three. N_o should be adjustable for special considerations, however. (Ref. (3) Application Bulletin 440 by Dr. A. G. Ratz; 1/23/74).

From the above one can see that a fair amount of sophistication has been incorporated into digital alarm and abort specimen protection.

4. Gross Level Abort

The gross level abort is an operator selectable parameter that sets an overall RMS acceleration level which cannot be exceeded without terminating the test. Gross level aborts are used to protect both the system and test specimen against runaway conditions. A loose accelerometer or inadvertently increasing a manual gain control causes the gross level abort to shut down the test in an orderly manner.

5. Loop Integrity

In the event an open loop occurs in the response channel(s), catastrophic results could obviously come about. For single channel control, the system automatically detects the loss of control signal at any level and initiates an abort. When multiple channels are used for control, generally each channel is checked for loss of signal at -3 dB of full scale and the system aborts if any loss of signal is detected (Random Testing).

This check is made on control channel once every control loop cycle. These checks are made on input data prior to including the data in the control calculations. Therefore, the output level will not change (increase) when a control signal is lost; only the abort action is allowed to change the output level to zero in a smooth manner.

6. Power Fail Restart

Most control systems have an automatic power fail system. The system constantly monitors the line voltage.

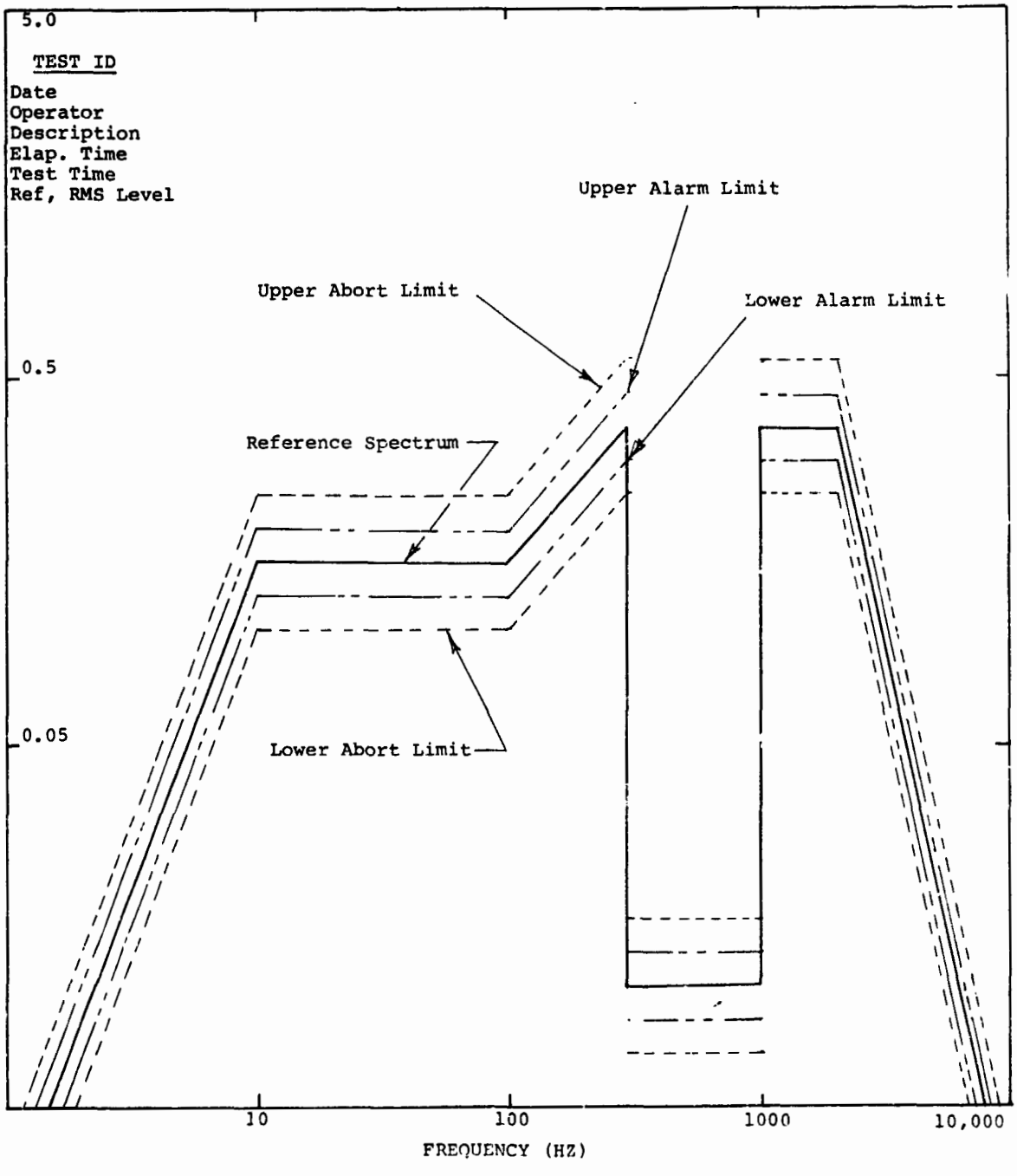

Figure 1 Power Spectral Density Plot of Reference Spectrum with Alarm and Abort Limits

and when the line voltage goes out of a preset tolerance band, the system systematically and smoothly shuts down. The more sophisticated systems continue to monitor the voltage and bring the system back on line once the problem clears up.

C. Housekeeping Operations - Monitoring Pertinent Equipment Parameters During a Test

The items discussed consume, with drive signal updating, much of the control system's time. However, there are still functions that a control system monitors. These functions or parameters are near static or DC values and consequently can easily be monitored by the system. A typical list might include the following:

- Amplifier door status
- Exciter overtravel status
- Exciter coolant flow status
- Exciter armature temperature
- Exciter field temperature
- Power amplifier coolant flow status
- Power amplifier heat sink temperature
- Field supply
- Amplifier overload
  1. overcurrent
  2. overvoltage
  3. overpower
- Loss of power supplies
- Power amplifier low water warning

If any of these parameters go out of tolerance, a printout occurs stating the problem and shuts the system down if designated by the operator through software.

II CONTROLLED DECELERATION SPECIMEN PROTECTION SYSTEMS

As previously stated in the introduction, there are conditions in which the digital control system has limited ability to protect a test specimen. A condition of this nature occurs when a transient is generated within the power amplifier or output stages of the control system and is directly transmitted to the exciter and the test article. To this author's knowledge there is no digital control scheme which can sense amplifier transients fast enough to initiate positive action to prevent the transient from being transmitted to the test article. The standard method used by amplifier/exciter manufacturer's to handle such transients has been to use the following technique. A concept known as "Armature Protection" is used in which the energy stored in the amplifier is discharged and the armature is short circuited. The purpose of this device is to protect the exciter and not the test article, in fact, when the protector is initiated, the deceleration levels generated are significantly high to cause possible damage to the test article. Goddard has consequently had two manufacturer's develop two Controlled Deceleration Specimen Protection Systems.

The existing systems effect controlled deceleration by automatically sensing displacement, acceleration, or velocity for excessive levels, and when triggered, insert variable damping resistors across the armature circuit to effect the desired deceleration shutdown.

CONCLUSION

The safety protection of a test specimen has certainly been enhanced through the use of digital control systems. The primary problem areas have been due to operator errors. To this end, the digital control system has been most successful, however, there are still areas of concern, namely, the "exciter dump" caused by transients out of the power amplifier or control system. This problem requires a system which can guarantee a controlled deceleration shutdown to prevent damage to expensive test articles when triggered by such transients.

REFERENCES

1. Cook, Lawrence L.; Shock and Vibration Bulletin 39, February 1969.

2. Engineering Specification (No. 701301) Ling Electronics, August 15, 1973.

3. Ratz, D. A. G., Application Bulletin 440 (Unpublished), January 23, 1974, Ling Electronics, Anaheim, California.

4. Engineering Reports (Unpublished), March 1975, Hewlett-Packard, Palo Alto, California.

5. Engineering Reports (Unpublished), August 1973, Time Data Corporation, Palo Alto, California.